LANGLEY RESEARCH CENTER
3 1176 00500 4826

NATIONAL ADVISORY COMMITTEE FOR AERONAUTICS

C-4

WARTIME REPORT

ORIGINALLY ISSUED
March 1945 as
Memorandum Report L5C07

CHARACTERISTICS OF SEVERAL SINGLE- AND DUAL-ROTATING PROPELLERS IN NEGATIVE THRUST

By W. H. Gray and Jean Gilman, Jr.

Langley Memorial Aeronautical Laboratory
Langley Field, Va.

NACA

WASHINGTON

NACA WARTIME REPORTS are reprints of papers originally issued to provide rapid distribution of advance research results to an authorized group requiring them for the war effort. They were previously held under a security status but are now unclassified. Some of these reports were not technically edited. All have been reproduced without change in order to expedite general distribution.

MR No. L5C07

NATIONAL ADVISORY COMMITTEE FOR AERONAUTICS

MEMORANDUM REPORT

for the

Army Air Forces, Air Technical Service Command

CHARACTERISTICS OF SEVERAL SINGLE- AND DUAL-ROTATING PROPELLERS IN NEGATIVE THRUST

By W. H. Gray and Jean Gilman, Jr.

SUMMARY

Thrust and power characteristics of several single- and dual-rotating propellers differing in blade width and number of blades are presented for the region of negative-thrust operation from -45° to 145° blade angle. The tests herein reported are an extension of previous single- and dual-rotating propeller tests utilizing blades of Hamilton Standard 3155-6 (Clark Y section) design.

The tests indicated that within reasonable accuracy it is possible to predict for a given propeller design characteristics in the negative-thrust range from known characteristics at a different activity factor.

Adequate negative thrusts were indicated for extremely high positive as well as negative blade angles.

For the particular selection of blade angles used in these tests, single rotation gave higher negative-thrust coefficients than dual rotation at low values of J, but at values of J higher than about 1.5, dual rotation produced higher coefficients.

INTRODUCTION

At the request of the Army Air Forces, Air Technical Service Command, tests of single- and dual-rotating propellers operating in the negative-thrust range were conducted in the Langley propeller-research tunnel. The blades selected for these tests were the Hamilton Standard

3155 design, which previously have been the subject of a rather broad test program in the positive-thrust range. (See reference 1.)

Negative thrust has a number of potential uses among which are reduction of landing run, reduction of terminal velocity in diving flight, tactical maneuvering of fighters, maneuvering of multiengine seaplanes on water, and mooring lighter-than-air ships.

At present the normal range for operation in negative thrust is at small blade angles, partly since the angle change necessary is smaller than that required by a change to the extremely high positive angles, and partly because operation at high positive angles might result in operation below the minimum engine-rotational speed. The use of negative blade angles necessitates passing through a minimum torque region with the danger of overspeeding the engine, whereas high positive angles require operation at very high power and very low engine speeds. Previous negative-thrust investigations (references 2 and 3) are limited in range of blade angles, solidity, and type of rotation. The tests reported herein were made over a blade-angle range from -45° to 145°, using single-rotating propellers having three and four blades and dual-rotating propellers having four, six, and eight blades.

COEFFICIENTS AND SYMBOLS

The results are presented in nondimensional forms of thrust coefficient, power coefficient, and torque coefficient.

$$C_T = \frac{\text{effective thrust}}{\rho n^2 D^4}$$

$$C_P = \frac{P}{\rho n^3 D^5}$$ negative when power is delivered to engine by propeller

$$Q_n = \frac{Q/n}{\rho V D^4} = \frac{C_P}{2\pi J}$$

The effective thrust is the measured thrust of the propeller-body combination plus drag of the body measured without a propeller (positive in the direction of flight).

The symbols used are defined as follows:

P	power absorbed by propeller, foot-pounds per second
Q	aerodynamic torque, foot-pounds
n	propeller rotational speed, rps
D	propeller diameter, feet
ρ	mass density of the air, slugs per cubic foot
V	free-stream velocity, feet per second
β, β_F, β_R	blade angle at 0.75 R, degrees

Subscripts F and R refer to front and rear components of dual-rotating propellers

J	advance ratio, V/nD
TAF	total activity factor $= \dfrac{B \times 100000}{16} \displaystyle\int_{0.2}^{1.0} \frac{b}{D}\left(\frac{r}{R}\right)^3 d\left(\frac{r}{R}\right)$
B	number of blades
b	blade width at station (r/R)
r	radius to station
R	radius to tip

EQUIPMENT AND PROCEDURE

A complete description of the equipment used in conducting these tests will be found in reference 4. Some features of the test setup, however, are repeated herein. The test setup, with wing, was mounted in the wind tunnel as shown in figure 1. Dimensions of the nacelle and symmetrical airfoil wing are given in figure 2. Power was supplied by two 25-horsepower electric induction motors which drove propellers on concentric shafts. Negative as well as positive torque was measured with spring-selsyn dynamometer equipment. Propeller rotational speed was determined by means of electric tachometers. Thrust was measured as negative drag on the regular wind-tunnel balance.

The 10-foot-diameter propellers, Hamilton Standard blade design 3155-6 (right-hand) and 3156-6 (left-hand) of activity factor 89.7, as well as the wide blades, Hamilton Standard 3155-6-1.5 (right-hand) and 3156-6-1.5 (left-hand) of activity factor 134.4, were those used in previous investigations. (See reference 1.) These propellers for which plan- and blade-form curves are given in figure 3 incorporate Clark Y airfoil sections.

In general, propellers at positive blade-angle setting between $\beta = 15^{\circ}$ and $\beta = 65^{\circ}$ were tested from the J for zero thrust to the highest attainable J. At all other blade angles, tests were made over the maximum J range attainable. High values of J were obtained in some cases by operating at propeller rotational speeds as low as 40 rpm. For dual-rotating propellers with values of β_F from 25° to 65°, it was deemed advisable to maintain the same differential between front and rear blade angles as that employed in previous tests of these propellers. (See references 1 and 4.) From β_F equals 15° to -45°, the front and rear blade settings were equal and from β_F equals 75° to 145°, the blades were set to maintain the difference used at the 75° blade angle. Figure 4 is a plot of the difference in front and rear blade settings. The rotational speeds of the front and rear components were equal throughout the tests.

Three- and four-blade single-rotating propellers were tested in the rear hub, while the blades of the four-, six-, and eight-blade dual-rotating propellers were equally divided between two hubs in tandem, with a hub spacing of 15 inches.

Because of the low power and speed of the electric motors, propeller rotational speeds were such that the tip Mach number was always lower than 0.3. The highest Reynolds number based on the chord at the 0.75 R was about 1,000,000. The effect of Reynolds number was not critical within the range of the tests as the effect of changes between one-half million and one million could not be measured.

RESULTS AND DISCUSSION

Negative-thrust characteristics are presented in figures 5 through 24. Figure 5 presents thrust coefficient, C_T for the three-blade propeller, plotted against J on rectangular coordinate paper and also plots of corresponding curves with a tangent scale which enables coverage of the full range of results on a reasonably sized figure. Corresponding values of power coefficient C_P are shown in figure 6. Figures 7 through 24 present thrust and power coefficients in the same order for other propeller configurations, as itemized in table I.

An idea of the testing accuracy may be obtained from the fact that the faired curves obscure the test points; there is generally no more scatter than the width of the faired line.

An important point that may be made following an inspection of these figures is that a blade angle of 145° gave almost as great a negative-thrust coefficient as -15°. The magnitude of the difference depends on the value of J at which the comparison is made.

In figure 25, for a wide range of front blade angles, data have been reduced to a common basis (activity factor 100). The points indicated on this figure are necessarily from faired data and are not test points. Values in the positive thrust range were obtained from reference 1. At each blade angle, the scatter of points indicates the accuracy. For single rotation, apparently, a simple allowance for activity factor would suffice to enable the negative-thrust characteristics of a propeller of any solidity to be predicted, provided the characteristics for a similar propeller of any other solidity were known. The accuracy of this adjustment for dual rotation, figures 25(c) and 25(d), is not as good as for single rotation. For the range of blade angles shown the scatter varies between 0 and 30 percent depending on J and β ; the greater negative or positive is β , the greater is the scatter. The scatter also increases at low values of J.

Figure 25 emphasizes points not so apparent in the preceding figures of which it is a composite. The negative blade angle for maximum negative thrust varies from -30 to -15 as J varies from 1 to 4 for single rotation, and from -40 to -25 for the same values of J for dual rotation.

As stated previously these dual-rotation tests had been run at equal front and rear blade angles for all negative blade-angle tests. It might have been possible to obtain the maximum negative thrust at front blade angles comparable to those for single rotation by a readjustment of blade-angle difference between the front and rear components. In a practical installation it would be possible to install stops for operation in negative thrust at the unequal front and rear blade angles thus necessitated. Some consideration should, however, be given the time required to shift blade angle; it would be desirable to start from or approach the same front and rear blade angle at negative thrust.

It is also more apparent from figure 25 than from the previous figures that little difference exists between the negative-thrust coefficient available at -15° and at 145° for a wide range of J's. As noted in the Introduction, the possibility exists for operation in negative thrust at high positive blade angles and the data bear out at least the feasibility of obtaining negative-thrust coefficients equal to those obtained at negative blade angles.

Some comparison may also be afforded for single and dual rotation from the two parts of figure 25. For low and negative blade angles larger values of thrust and power coefficient are indicated in the case of single rotation below a value of J of 2 than for dual rotation. Above a value of J of 2 the reverse is true. This condition is true, of course, only for the particular selection of blade angles used in these tests. At very high angles the value of J for equal thrust was approximately 1.5. At smaller values of J the negative-thrust coefficients were larger for single than for dual rotation. At values of J larger than 1.5 the coefficients were smaller. At high blade angles power coefficients for single rotation were appreciably smaller at all values of J than those for dual rotation.

Many applications of negative-thrust data are possible; the form of presentation best suited for any given application depends, of course, on the variables involved. References 5 and 6 present methods of approach to the problem of reducing speed on an overtaking airplane to increase firing time. Reference 6 also presents methods of solving problems of landing deceleration and reduced dive speed. These methods are based on standard coefficients as used in the present report. However, the use of special coefficients and/or methods of plotting may facilitate the solution of problems such as determination of the rate of pitch change necessary to limit overspeeding to a reasonable value. The question of overspeeding is of major importance when the blade-angle changes involved are from high positive values to negative angles. Methods of approach to this as well as to other problems employing special coefficients and plotting methods are outlined in reference 7.

Subsequent to the original test program additional tests were run with the three-blade 3155-6 design propeller to obtain characteristics for each degree of blade angle between -5° and 5°. These additional results are presented in figure 26 with the results of the original tests at 5° superimposed. The curves for -5° and 5° were not duplicated within several percent, not only because the original tests included a wing in the propeller wake whereas the tests at 1° increments were made without a wing but also because the magnitudes of the thrust in relation to tare drag and power were extremely small.

The primary reason for the additional program of blade angles was to check results which indicated three equilibrium rotational speeds (and consequently three thrusts) at a given forward velocity in the blade angle region between 3° and -4°.

Figure 27, which is a plot showing the variation of Q_n with J of the three-blade 3155-6 propeller at several blade angles, illustrates the characteristics in this doubtful range. For a given value of Q_n, V, and D, it would be reasonable to expect a unique value of J, and consequently, n. The results presented in figure 27, however, indicate as many as three possible values of J for a given Q_n. Similar curves obtained from 5868-R6 propeller results in reference 3 show only one value of J in the same range of blade angles.

An attempt to explain these peculiar results by theory was not conclusive because of the lack of adequate section data for the high negative angles of attack experienced.

CONCLUSIONS

The following conclusions are based on propeller test results free of compressibility effects.

1. For similar propeller blade designs, characteristics may be predicted in the negative-thrust range to a limited degree of accuracy for any activity factor, provided the propeller characteristics are known for one value of activity factor.

2. Adequate negative thrusts may be possible at extremely high positive as well as negative blade angles.

3. At low values of J, single rotation produced higher negative-thrust coefficients than dual rotation, but at values of J higher than about 1.5, dual rotation gave higher coefficients.

Langley Memorial Aeronautical Laboratory
National Advisory Committee for Aeronautics
Langley Field, Va.

REFERENCES

1. Gray, W. H., and Mastrocola, Nicholas: Representative Operating Charts of Propellers Tested in the NACA 20-Foot Propeller-Research Tunnel. NACA ARR No. 3I25, 1943.

2. Hartman, Edwin P.: Negative Thrust and Torque Characteristics of an Adjustable-Pitch Metal Propeller. NACA Rep. No. 464, 1933.

3. Hartman, Edwin P., and Biermann, David: The Negative Thrust and Torque of Several Full-Scale Propellers and Their Application to Various Flight Problems. NACA Rep. No. 641, 1938.

4. Biermann, David, and Hartman, Edwin P.: Wind-Tunnel Tests of Four- and Six-Blade Single- and Dual-Rotating Tractor Propellers. NACA Rep. No. 747, 1942.

5. Pearson, H. A., and Anderson, R. F.: A Brief Study of the Speed Reduction of Overtaking Airplanes by Means of Air Brakes. NACA ACR, May 1942.

6. Hedrick, William S., and Douglass, William M.: An Experimental Investigation of the Thrust and Torque Produced by Propellers Used as Aerodynamic Brakes. NACA ARR No. 4H26, 1944.

7. Brooks, M.: Negative Thrust and Torque Data and Sample Problems, Including Calculations of Necessary Pitch Change Rates. Eng. Rep. No. 64, Aeroproducts Div., General Motors Corp., Aug. 6, 1942.

TABLE I

LIST OF FIGURES

Figure	Number of blades	Rotation	Type of curve
5-6	3 narrow	Single	Characteristic
7-8	4 narrow	--do--	Do.
9-10	4 narrow	Dual	Do.
11-12	6 narrow	--do--	Do.
13-14	8 narrow	--do--	Do.
15-16	3 wide	Single	Do.
17-18	4 wide	--do--	Do.
19-20	4 wide	Dual	Do.
21-22	6 wide	--do--	Do.
23-24	8 wide	--do--	Do.
25	3 narrow to 8 wide (inc.)	Single and dual	Comparison
26	3 narrow	Single	Characteristic and comparison
27	3 narrow	--do--	Do.

NATIONAL ADVISORY
COMMITTEE FOR AERONAUTICS

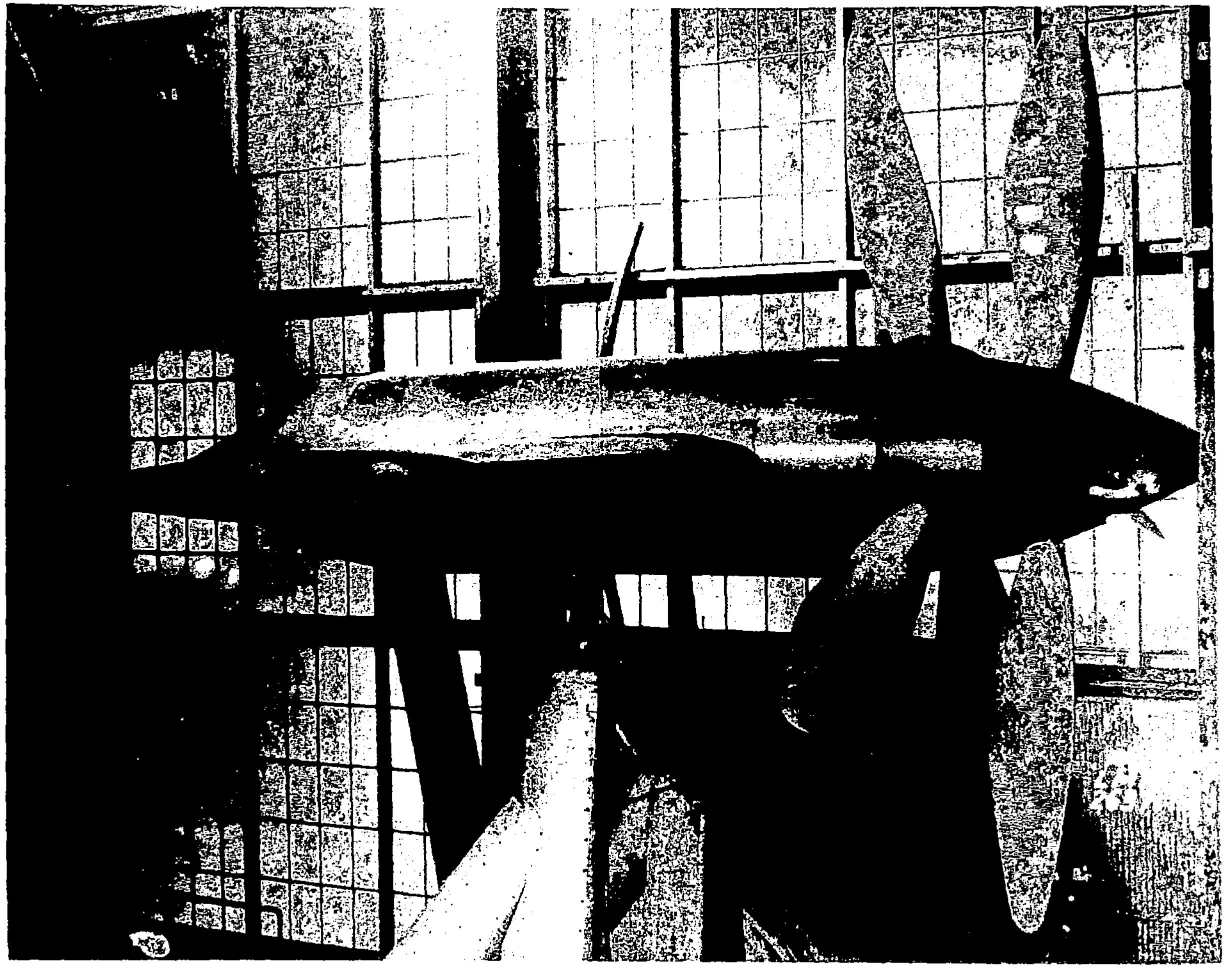

Figure 1.- Eight wide blade dual-rotating propeller on test setup.

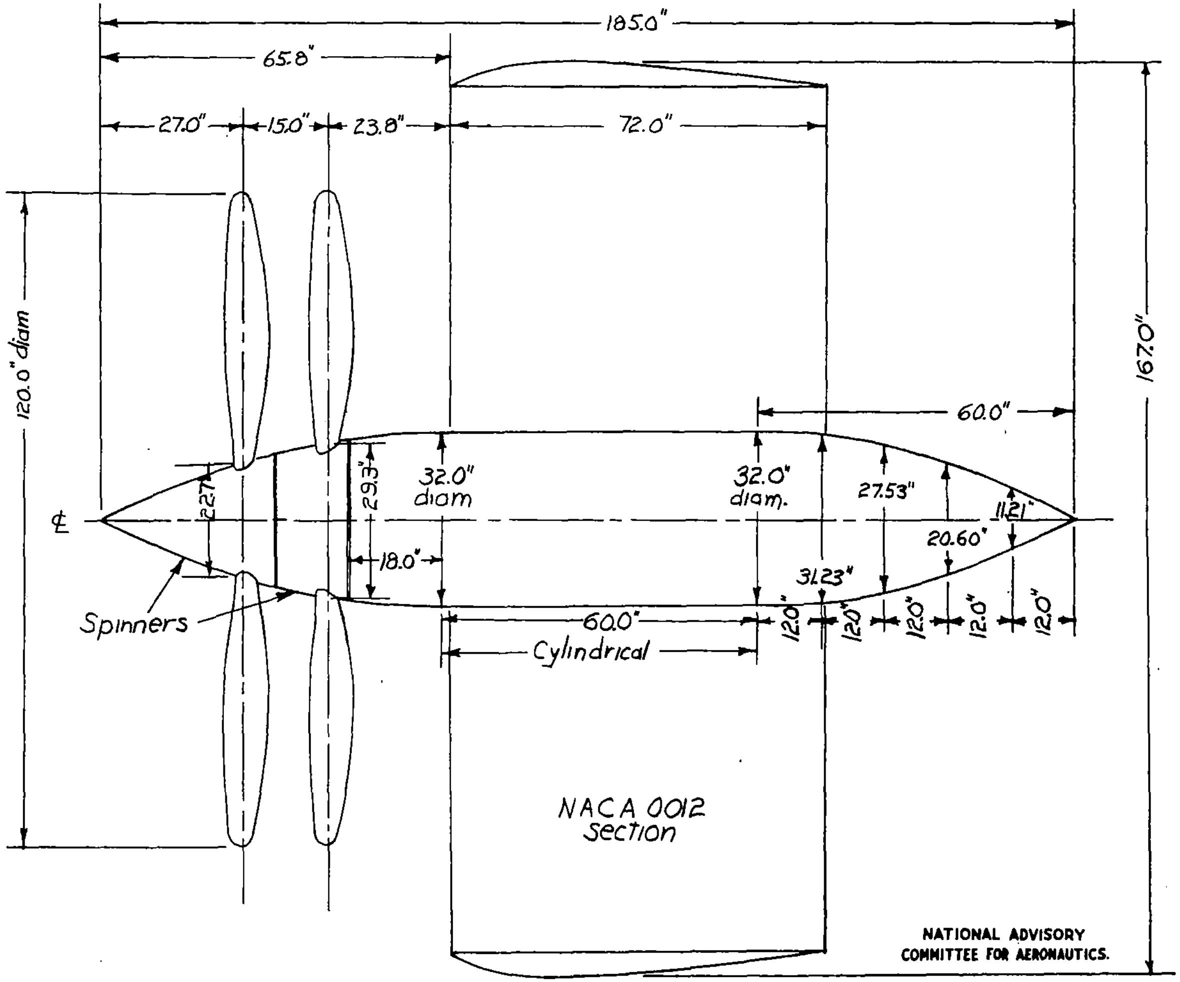

Figure 2.- Plan view showing dimensional details of wing and nacelle.

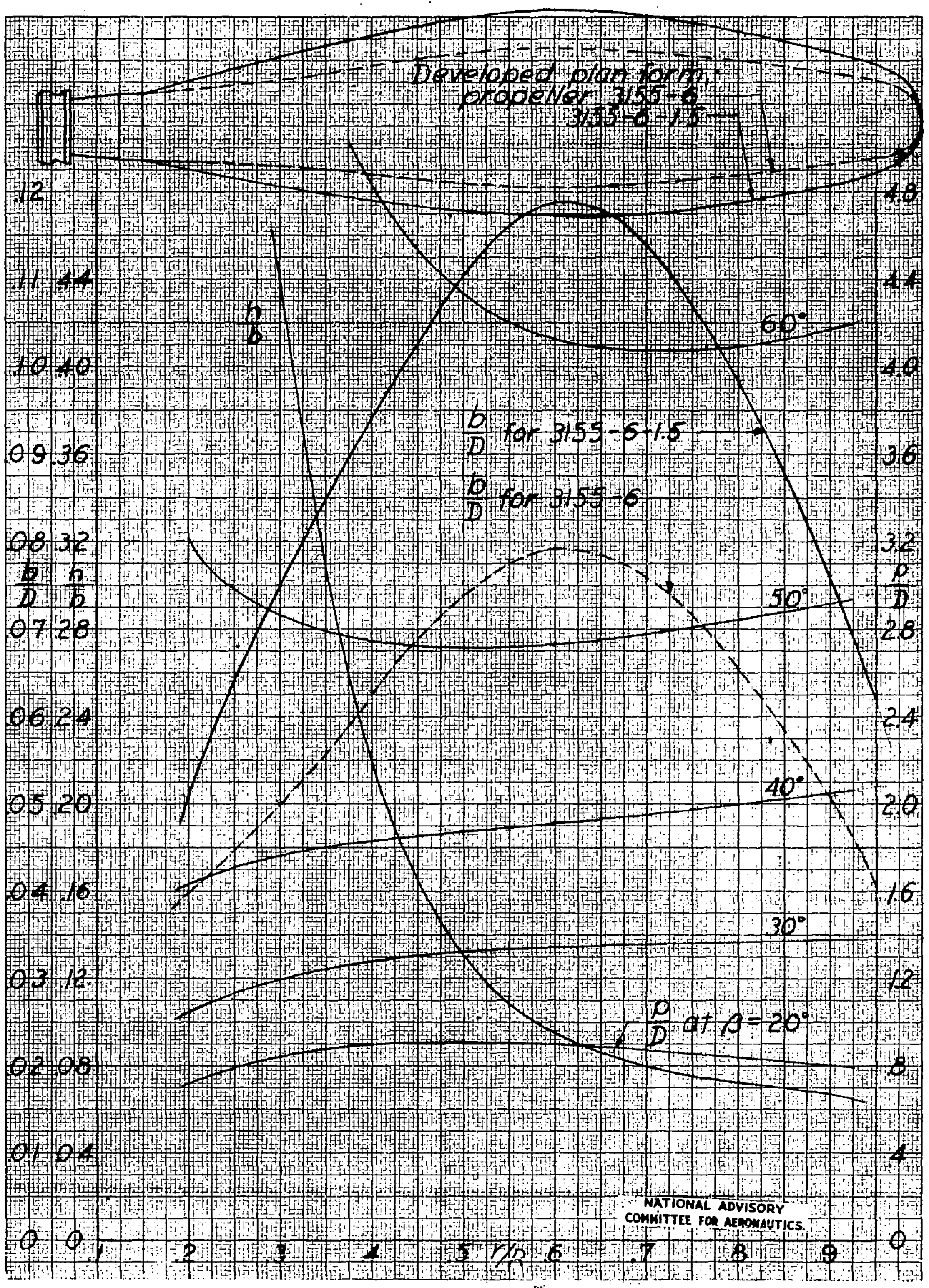

Figure 3.- Plan form and blade-form curves for propellers 3155-6 and 3155-6-1.5. Blade-form curves, except b/D, are identical for the two propellers. D, diameter; R, radius; r, station radius; b, section chord; h, section thickness; p, geometric pitch.

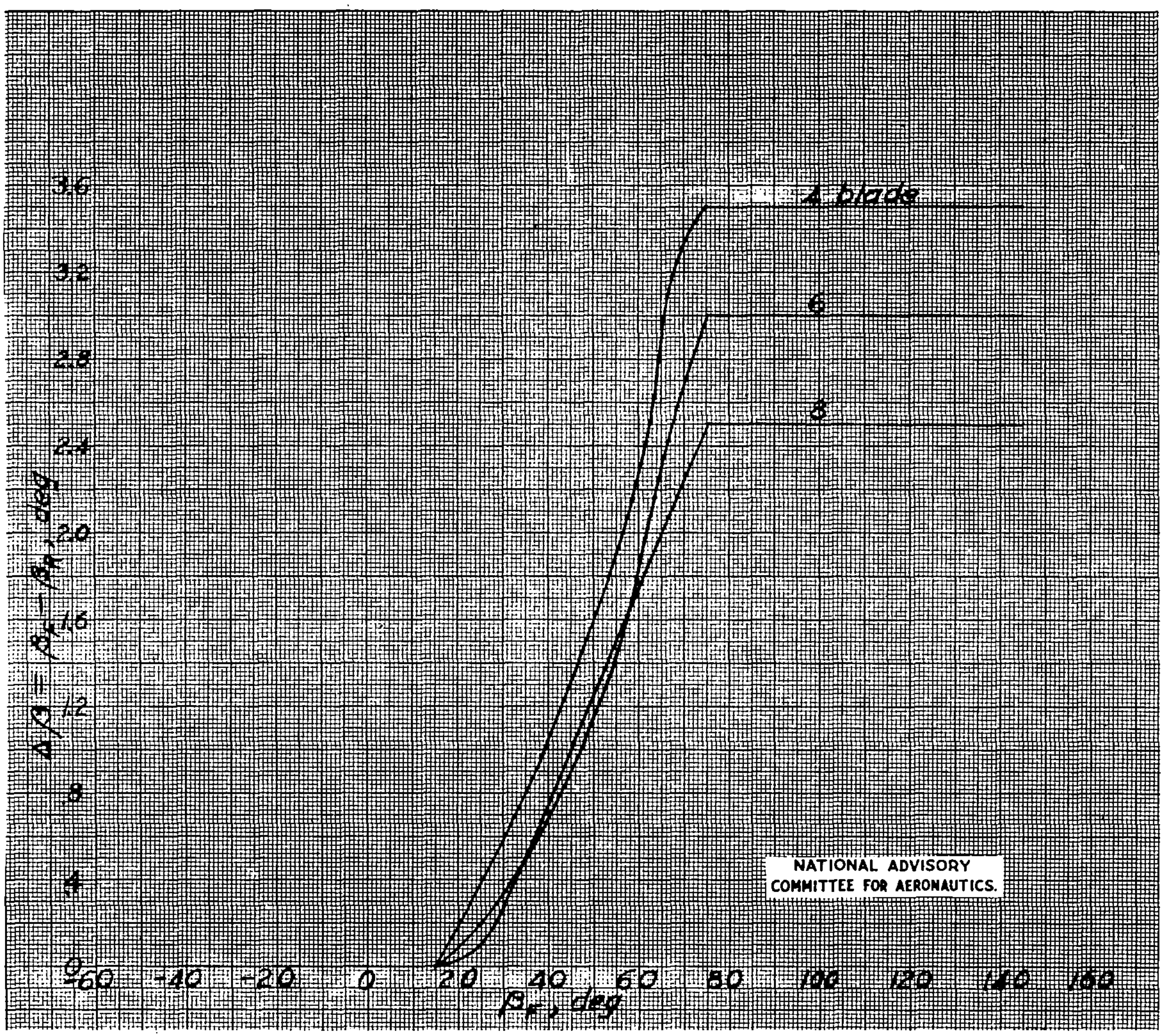

Figure 4.- Difference in blade angle of front and rear components, dual-rotating propeller.

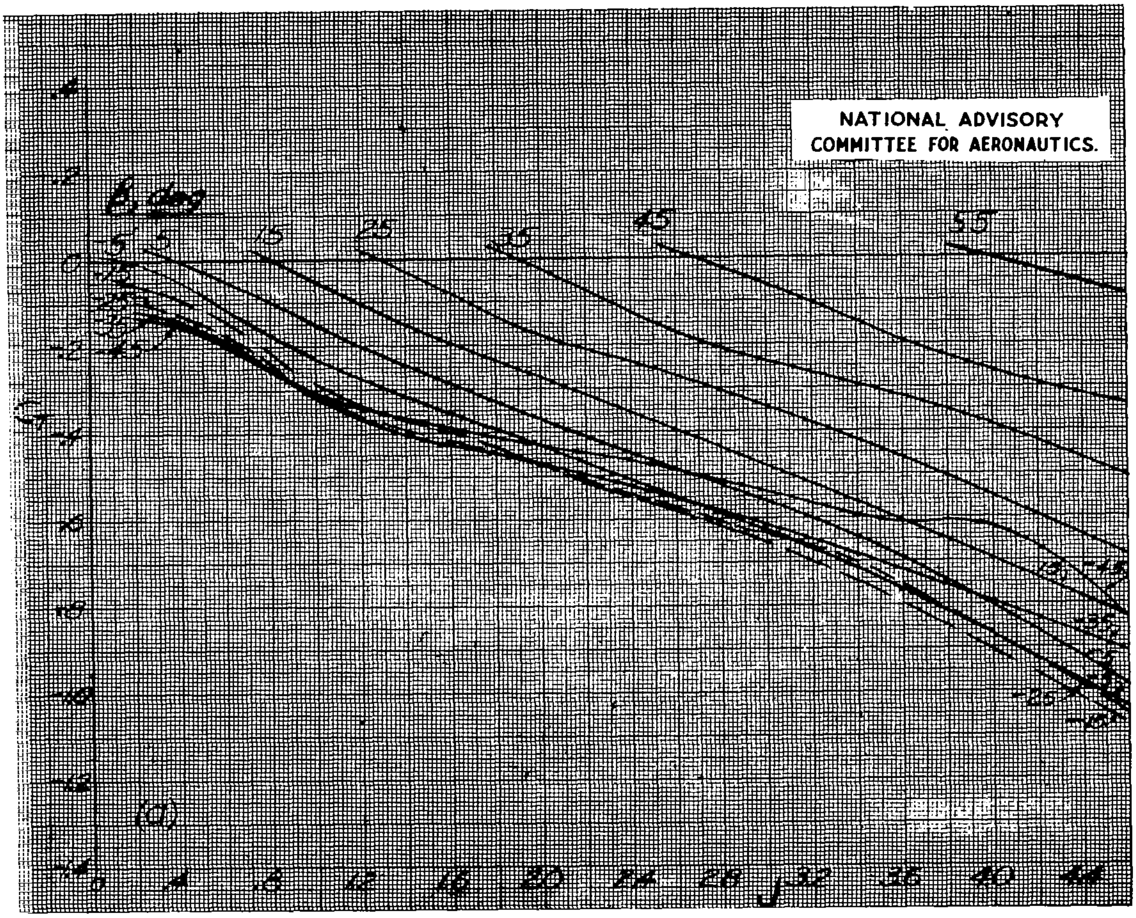

Figure 5.- Variation of thrust coefficient with advance ratio, three narrow blades.

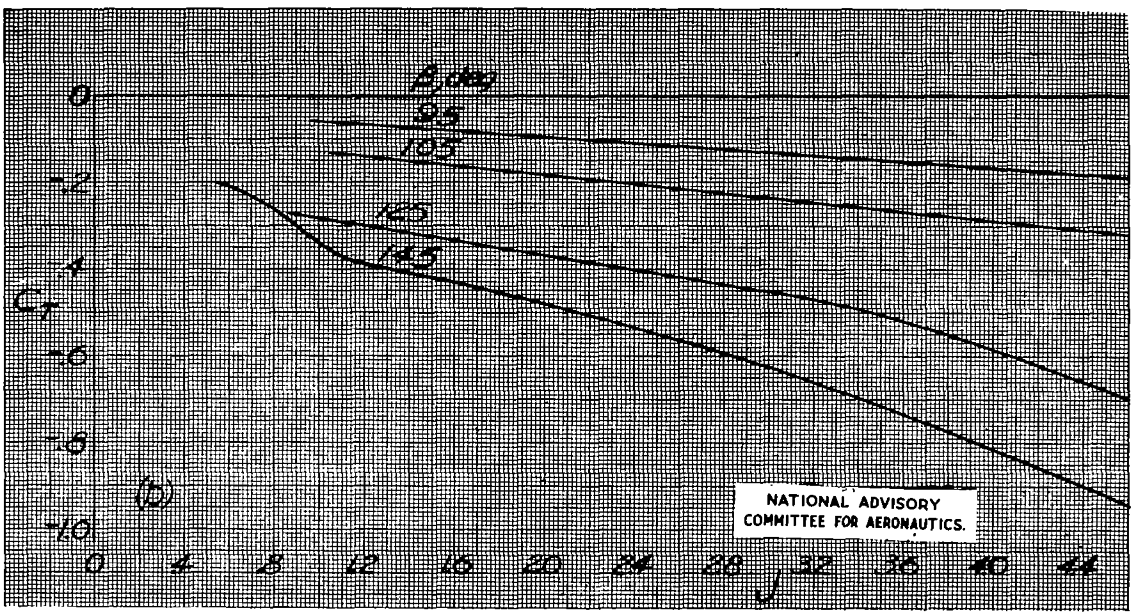

Figure 5.- Continued.

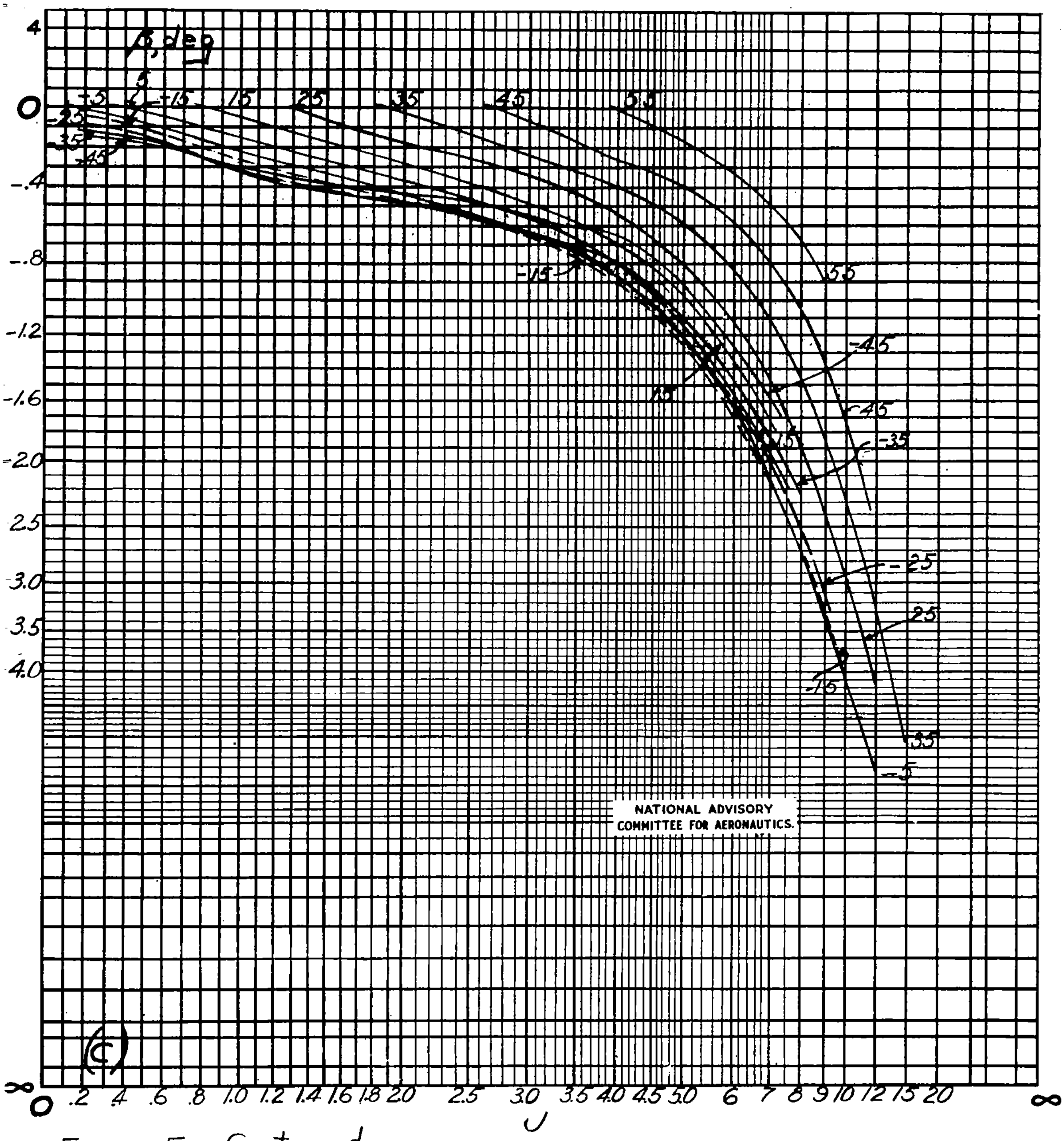

Figure 5.- Continued

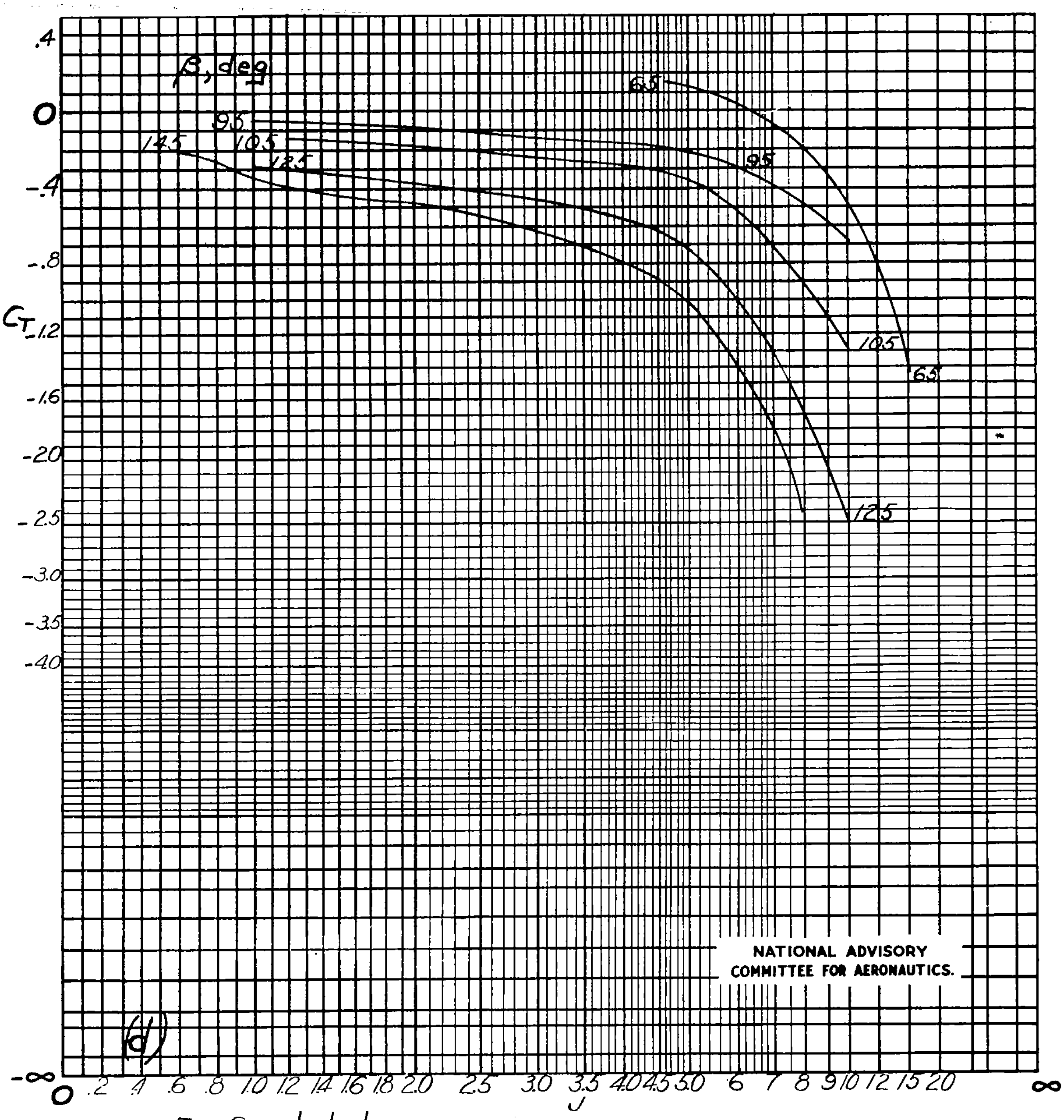

Figure 5.- Concluded

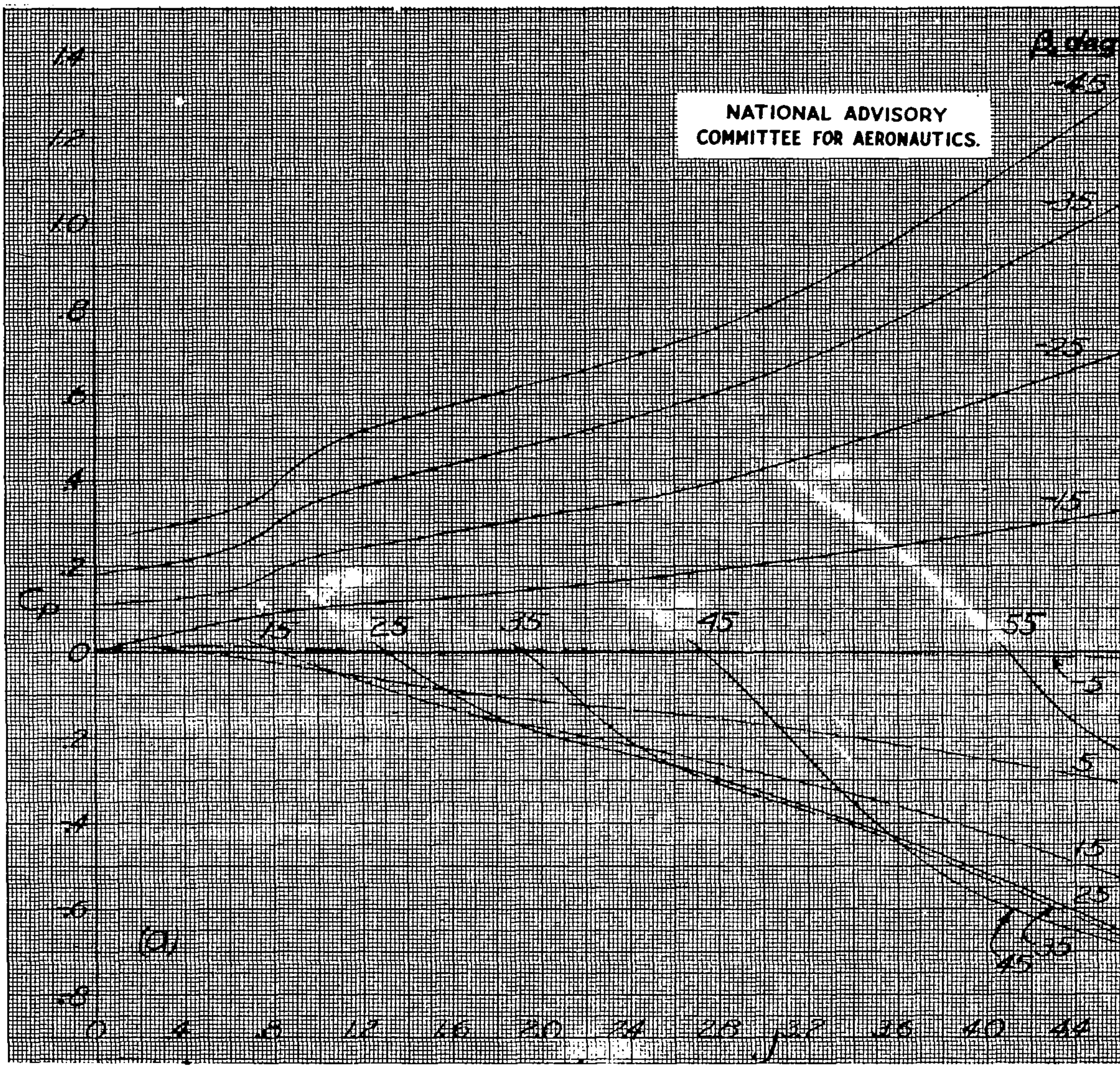

Figure 6.- Variation of power coefficient with advance ratio, three narrow blades.

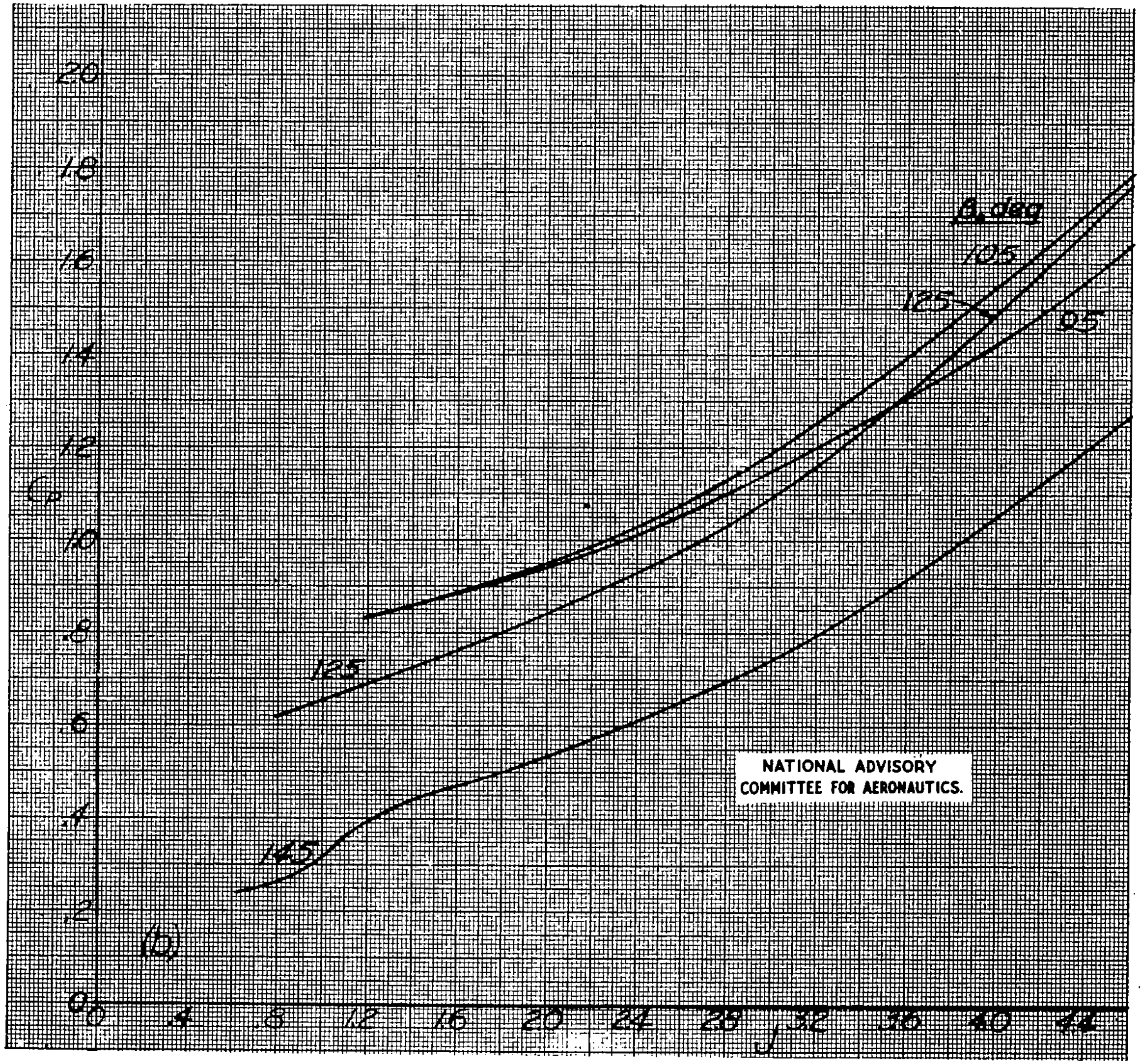

Figure 6.- Continued.

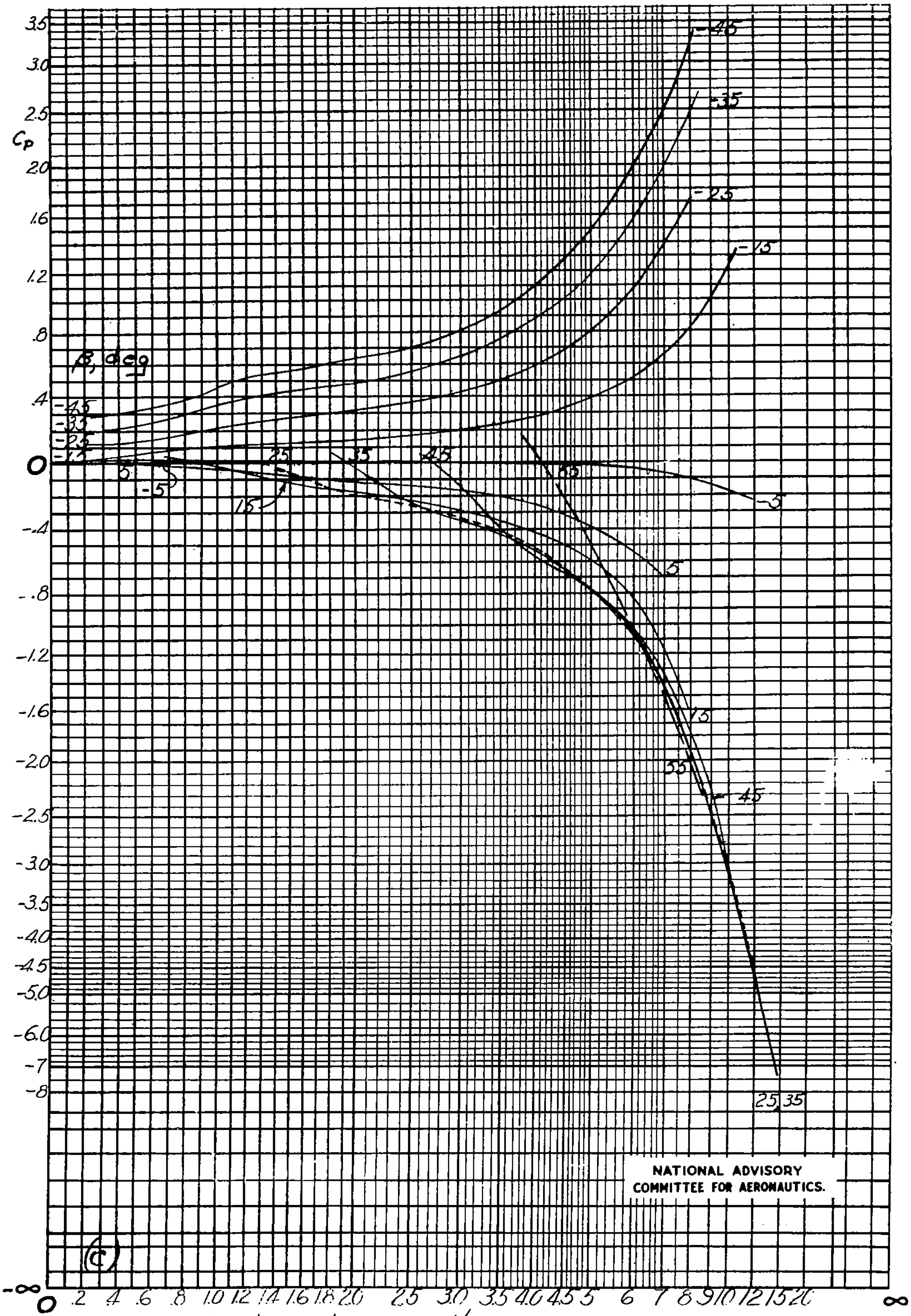

Figure 6.– Continued

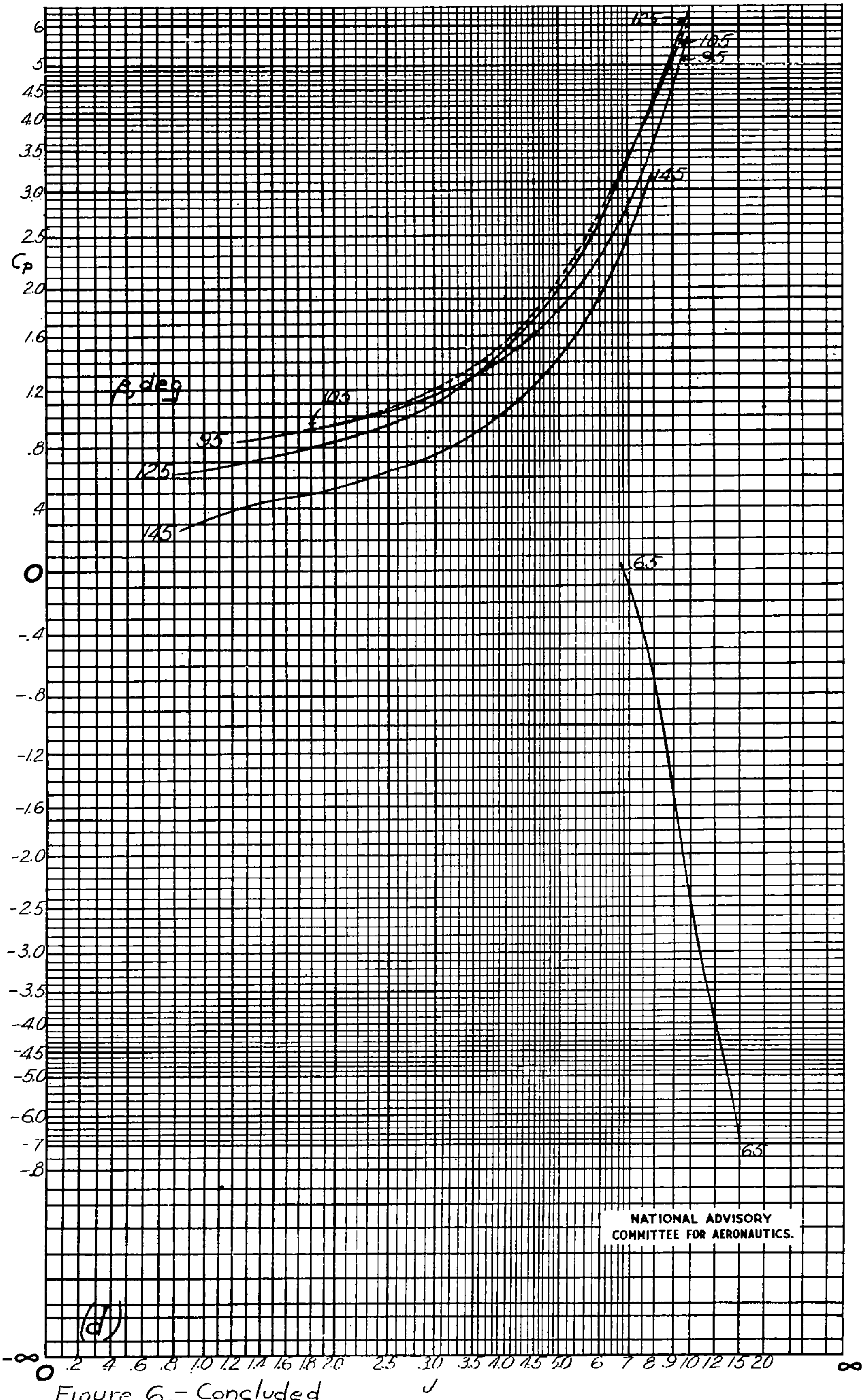

Figure 6.- Concluded

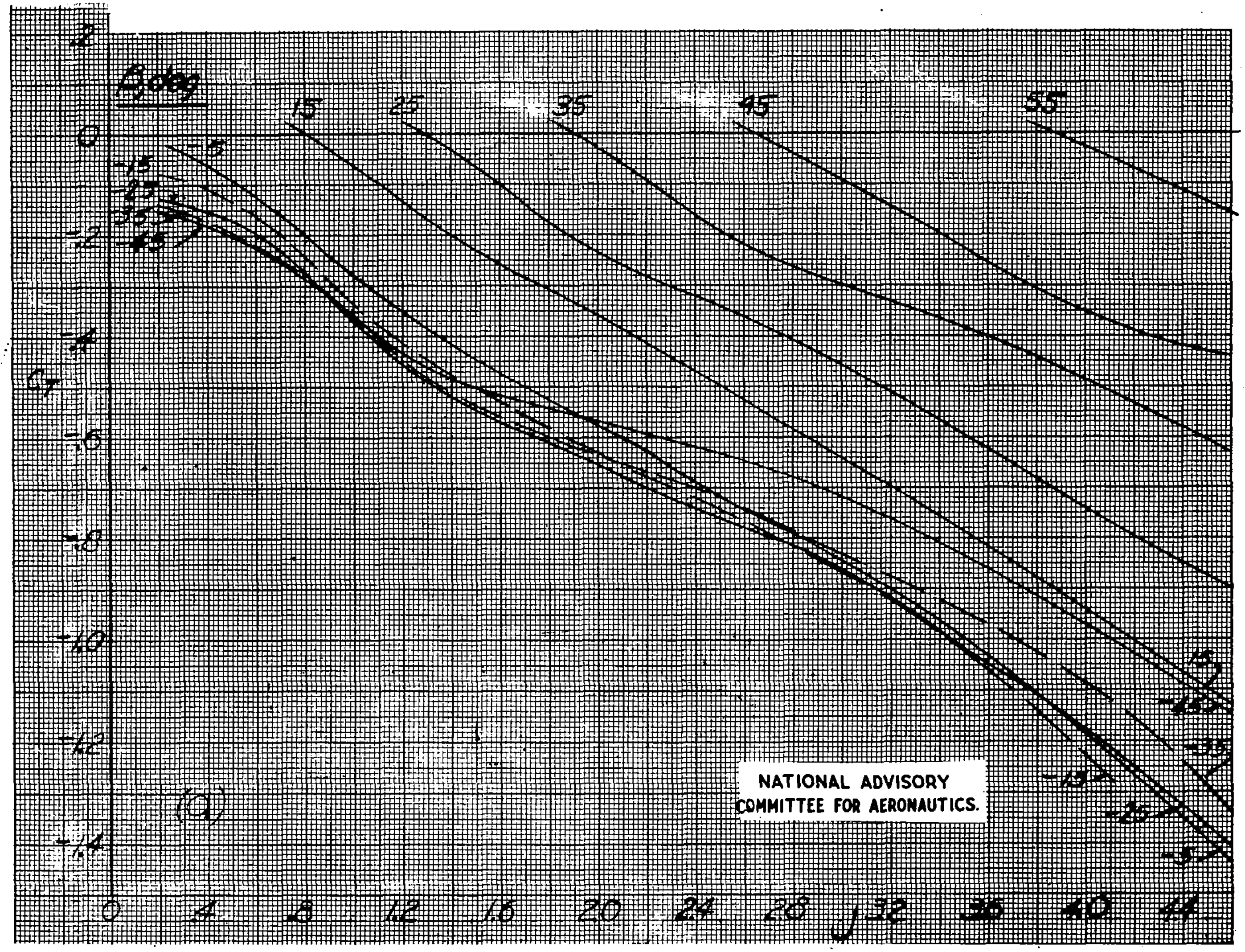

Figure 7.- Variation of thrust coefficient with advance ratio, four narrow blades, single rotation.

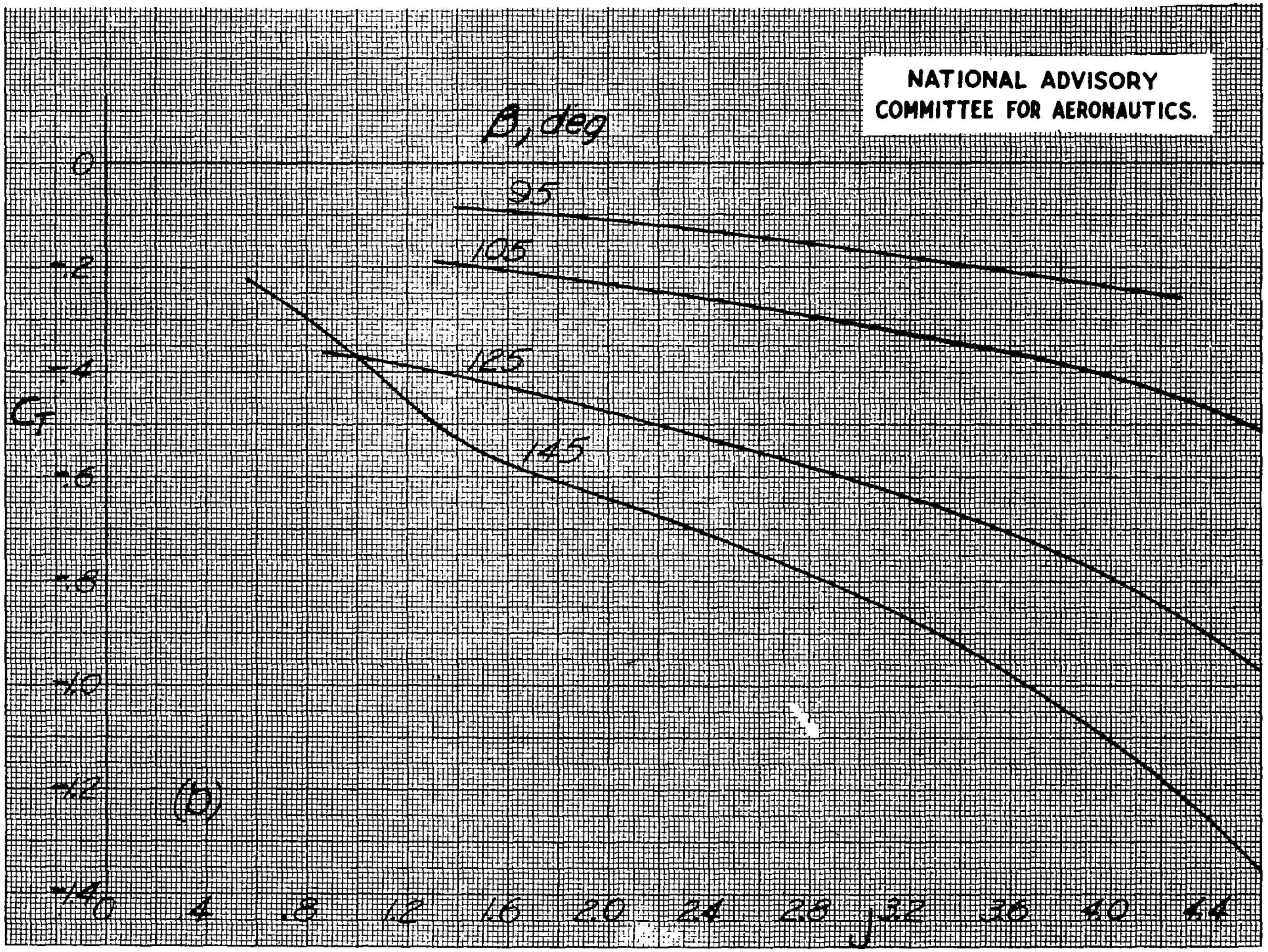

Figure 7.- Continued.

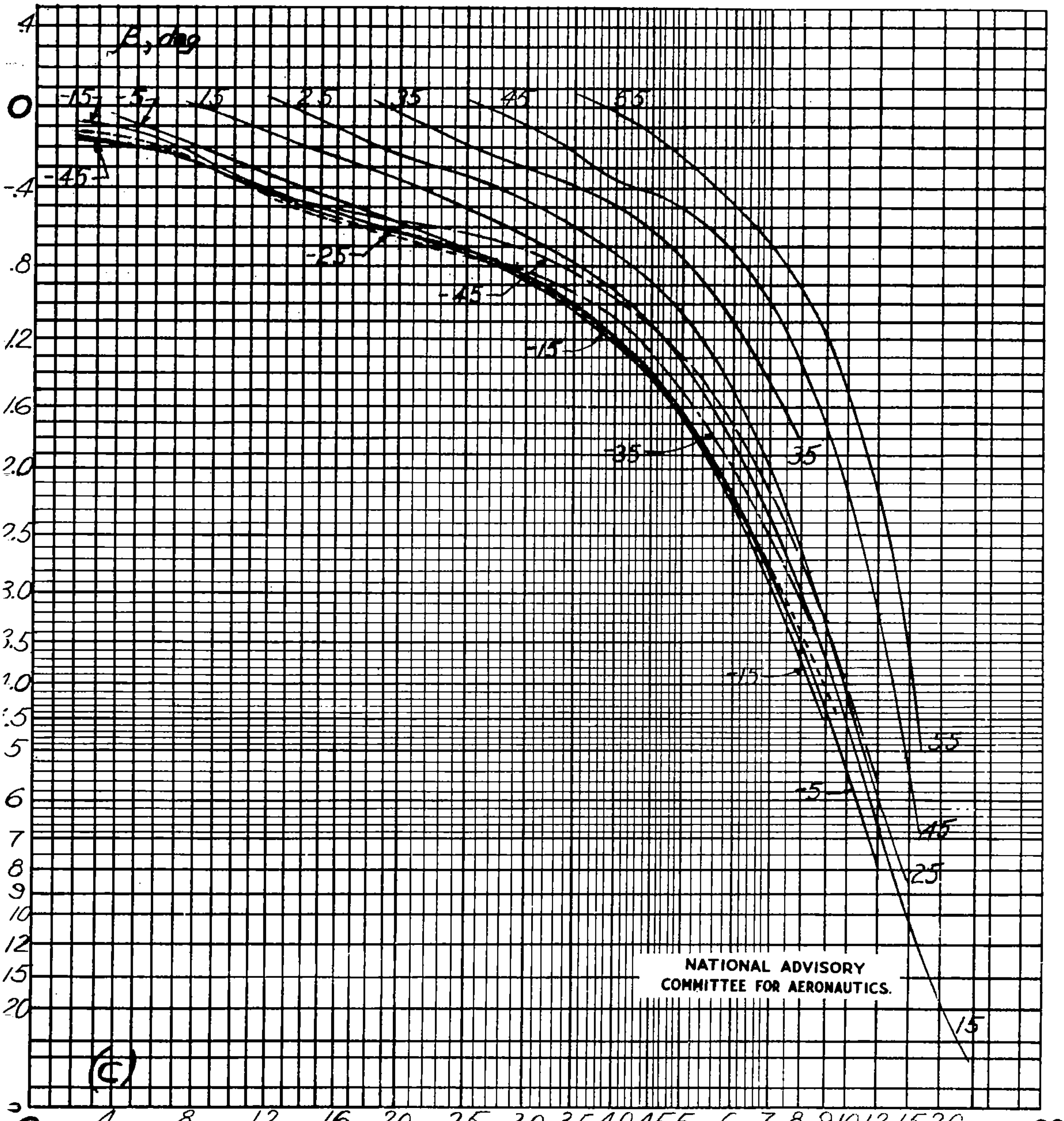

Figure 7.- Continued

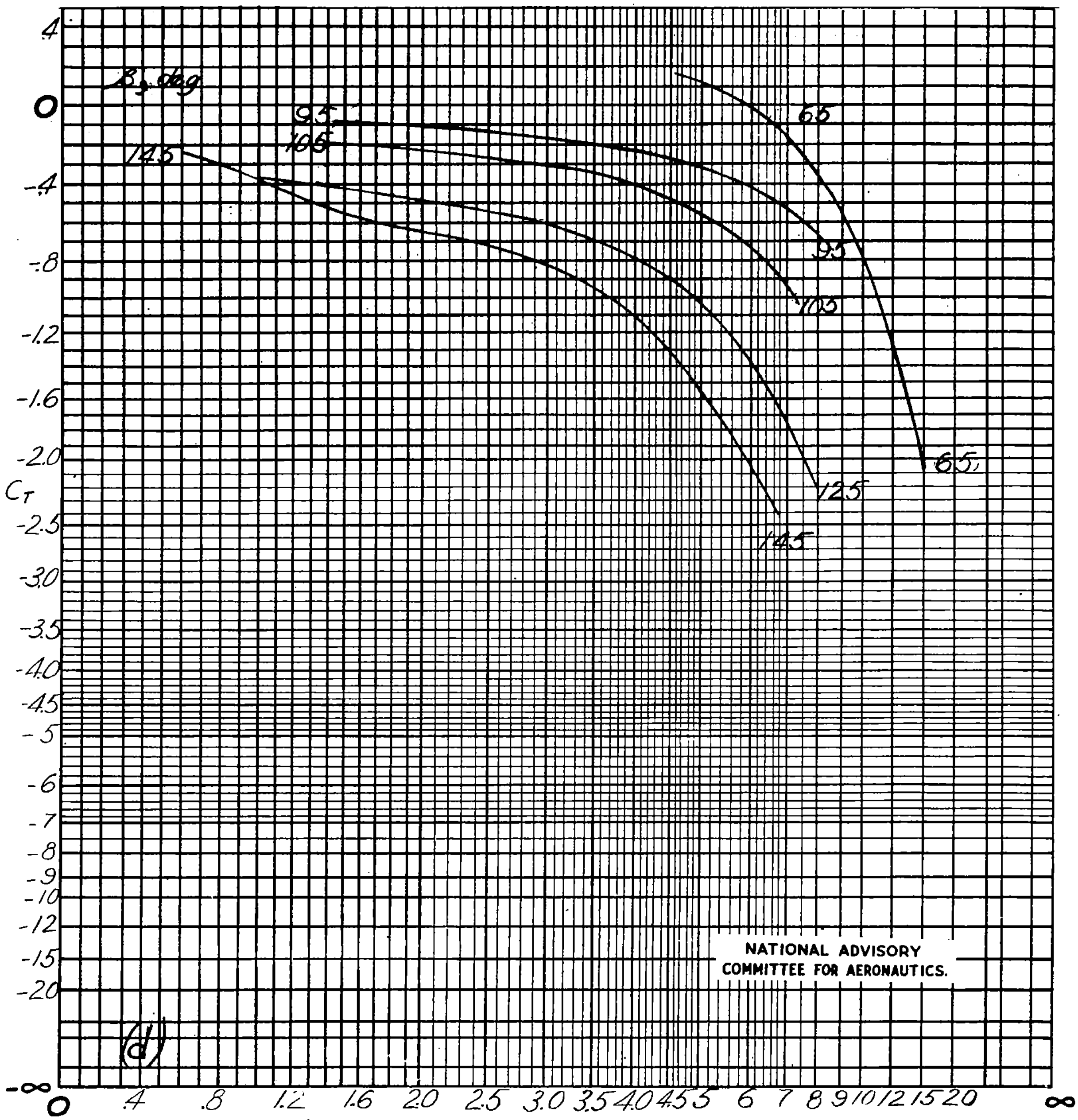

Figure 7.- Concluded

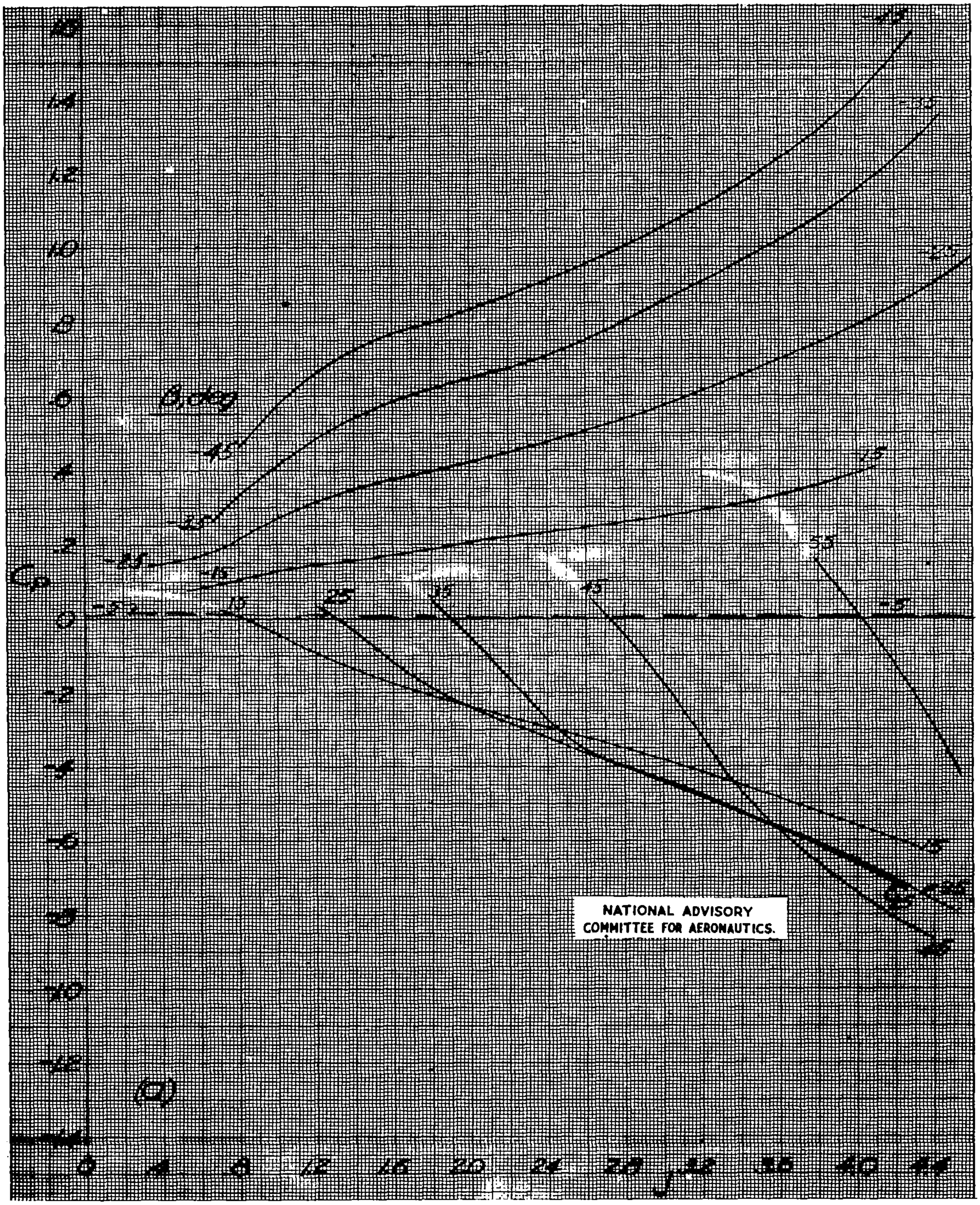

Figure 8.- Variation of power coefficient with advance ratio, four narrow blades, single rotation.

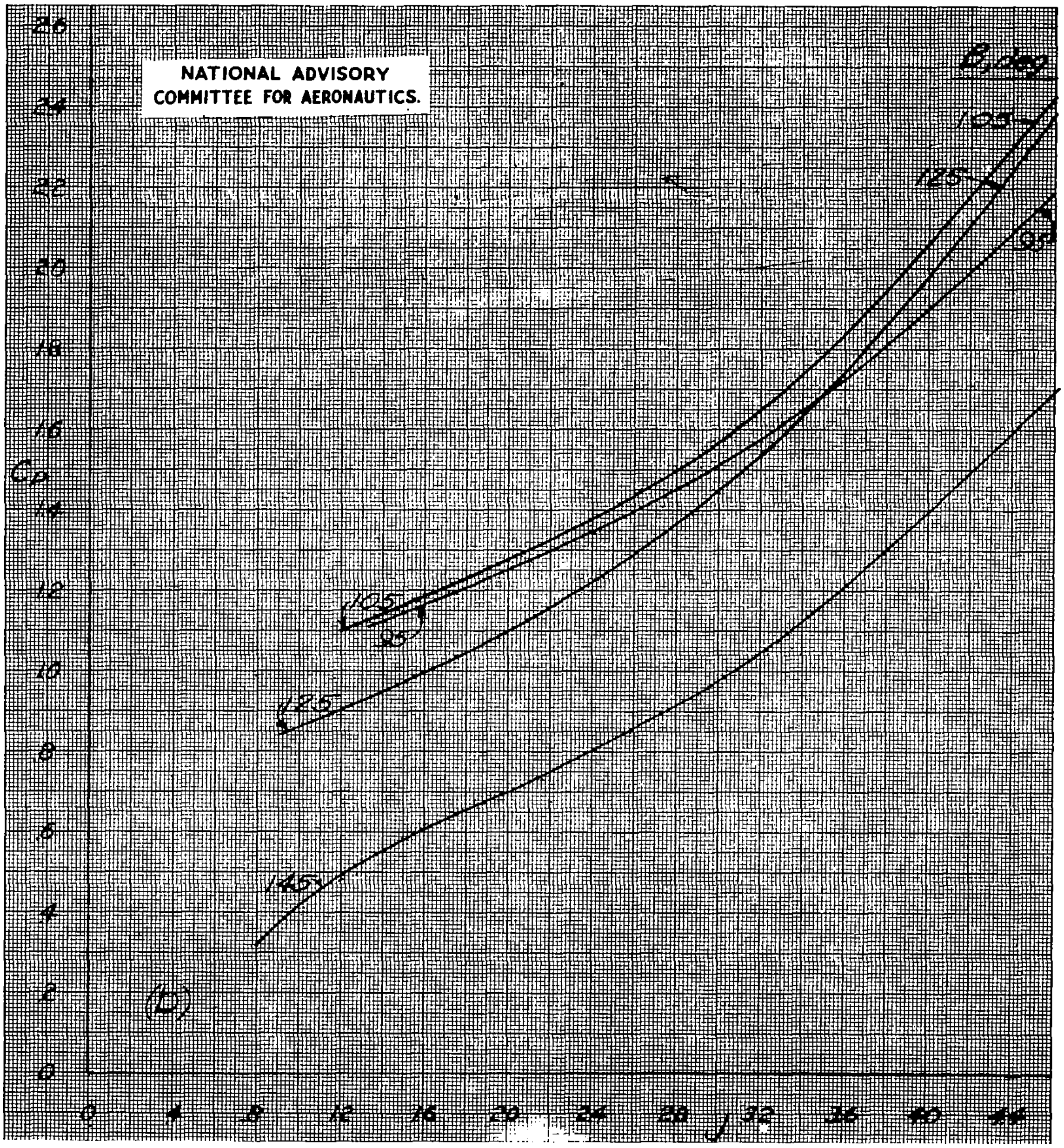

Figure 8.- Continued.

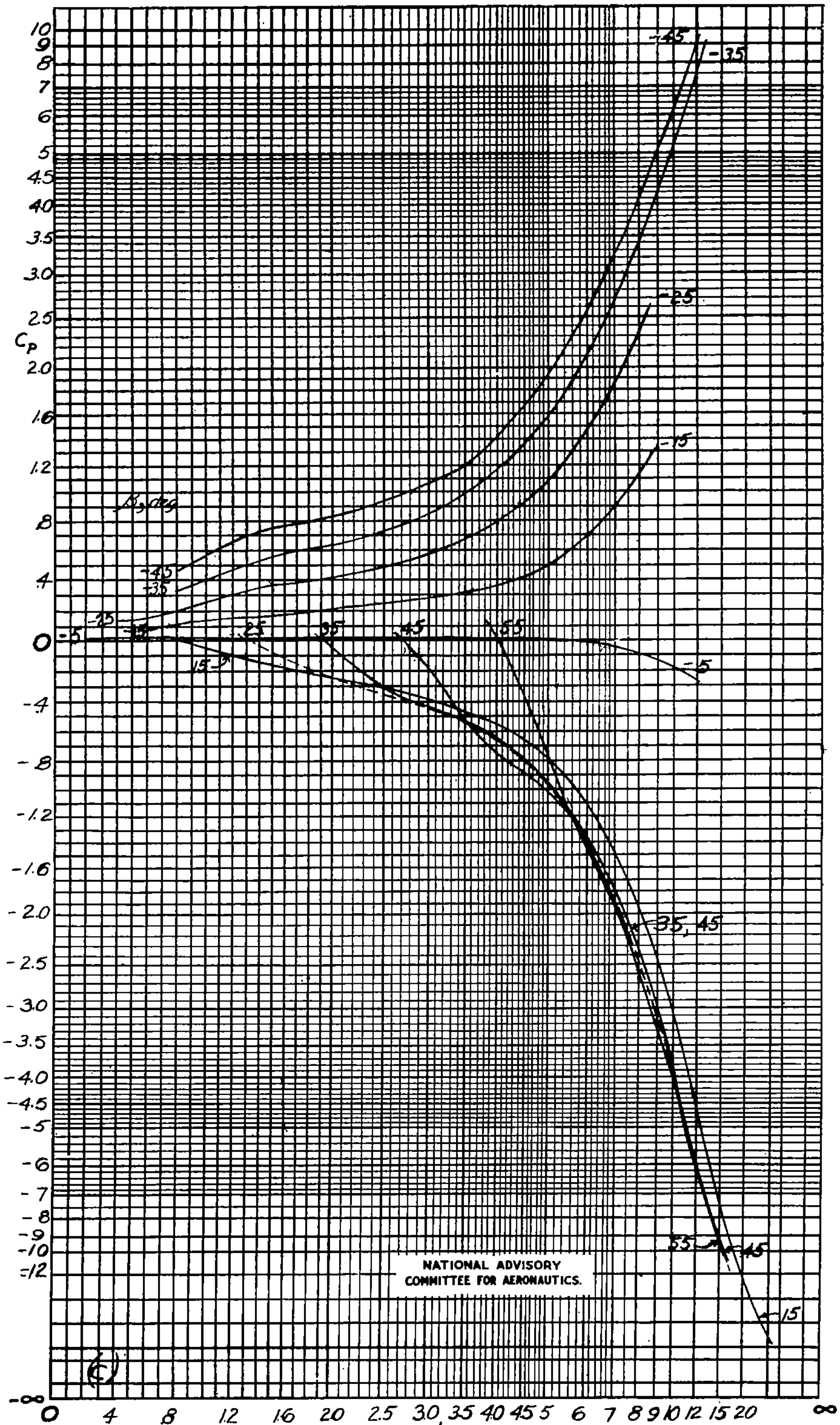

Figure 8.- Continued

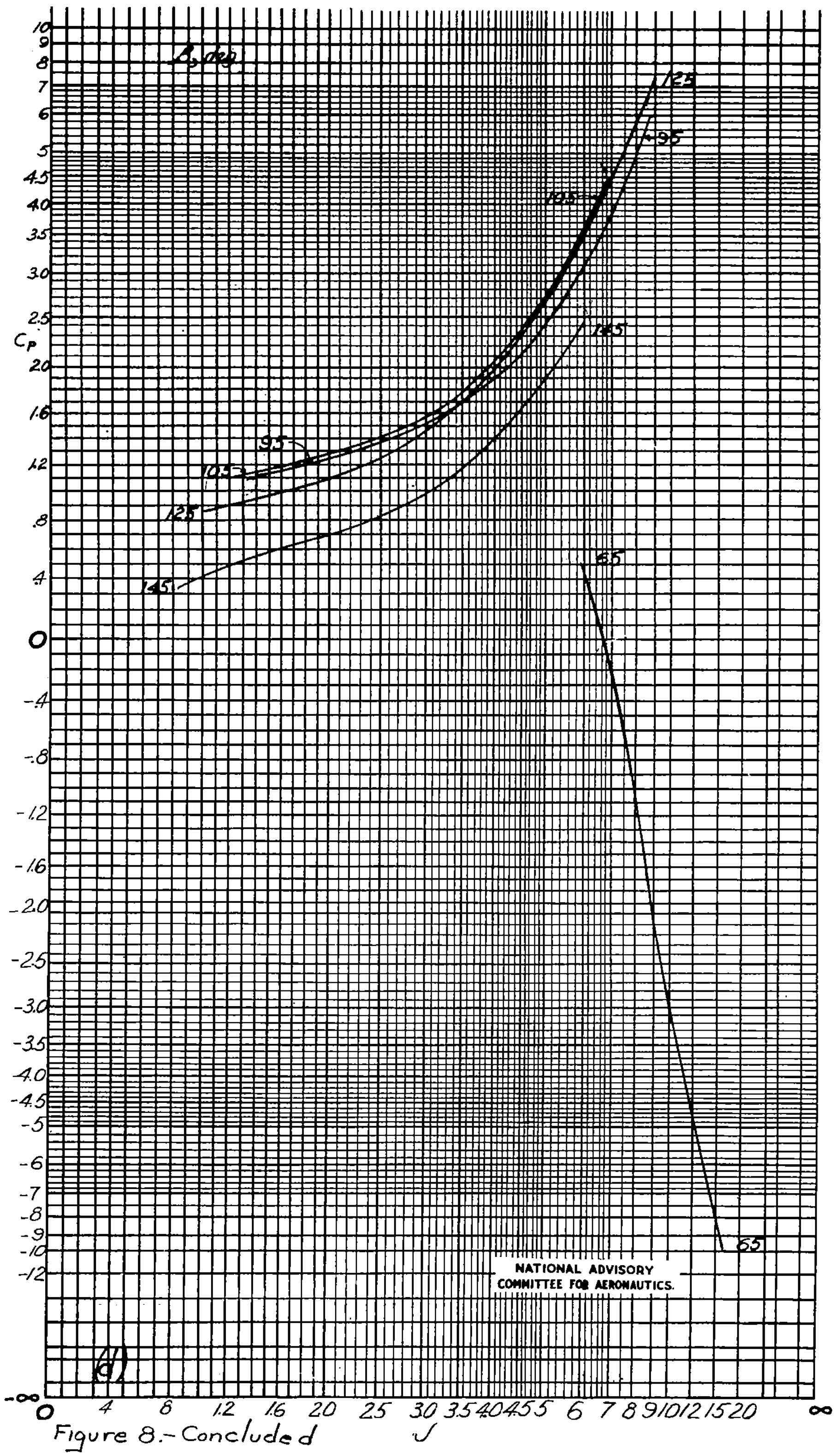

Figure 8.- Concluded

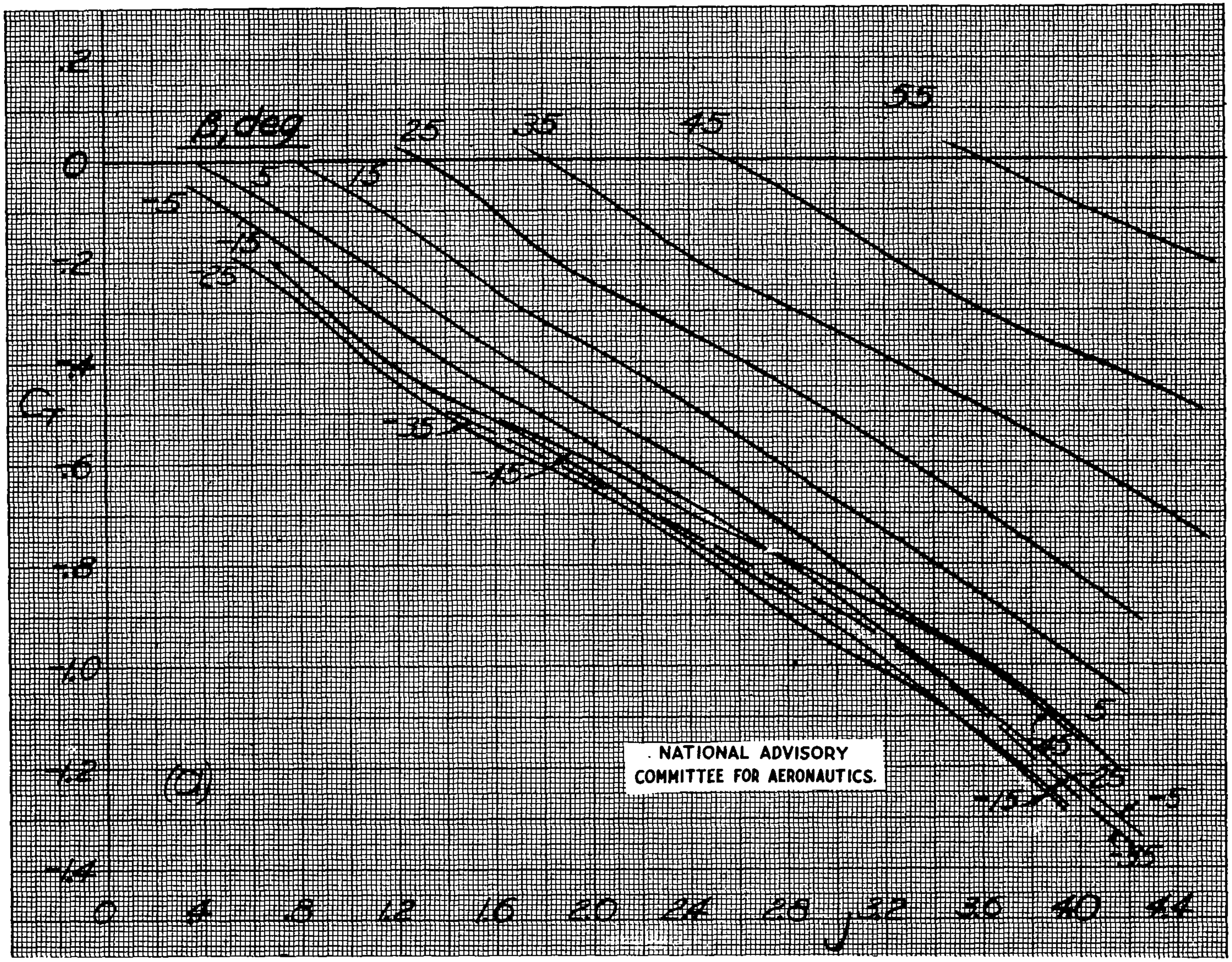

Figure 9.- Variation of thrust coefficient with advance ratio, four narrow blades, dual rotation.

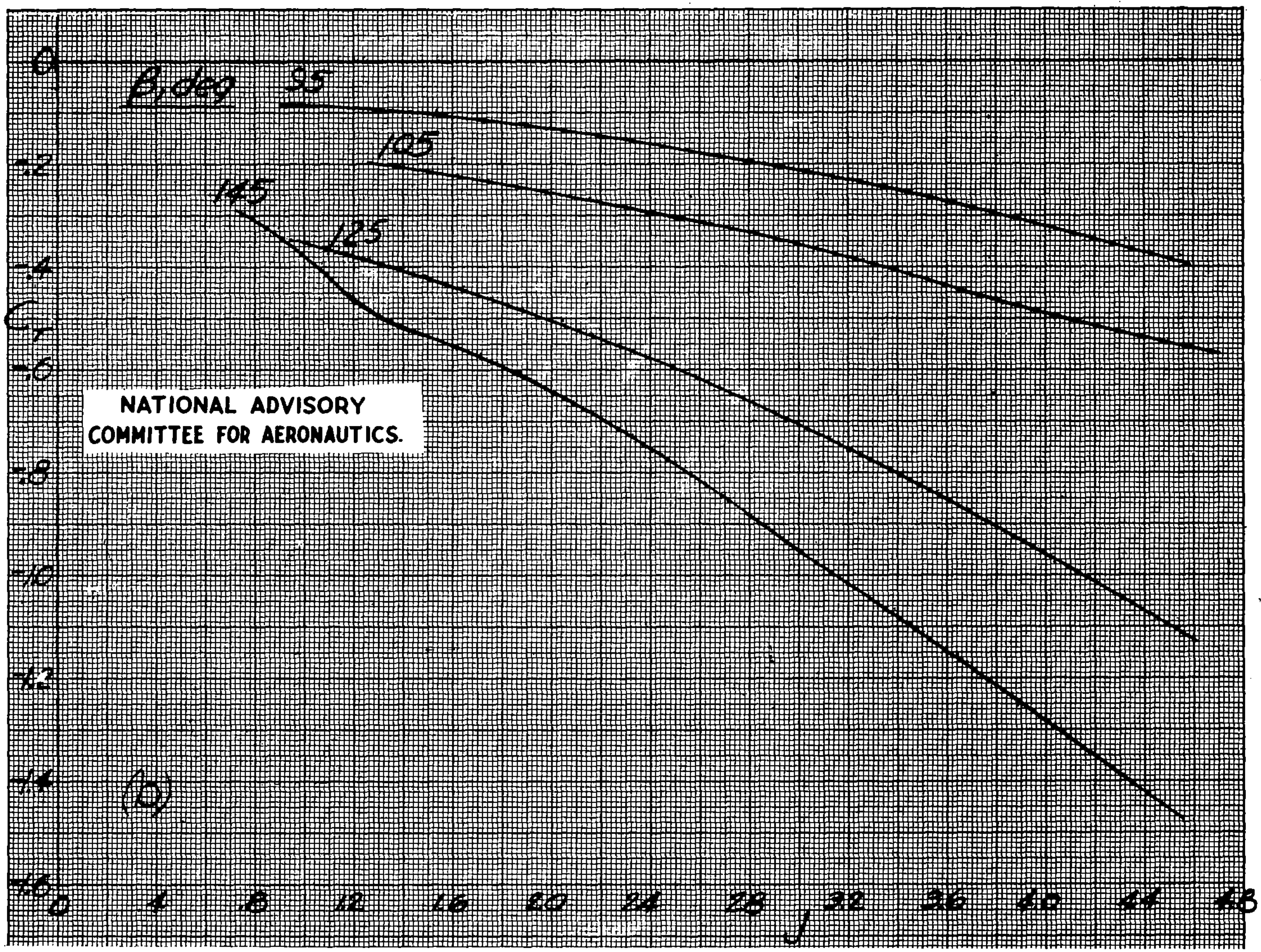

Figure 9.- Continued.

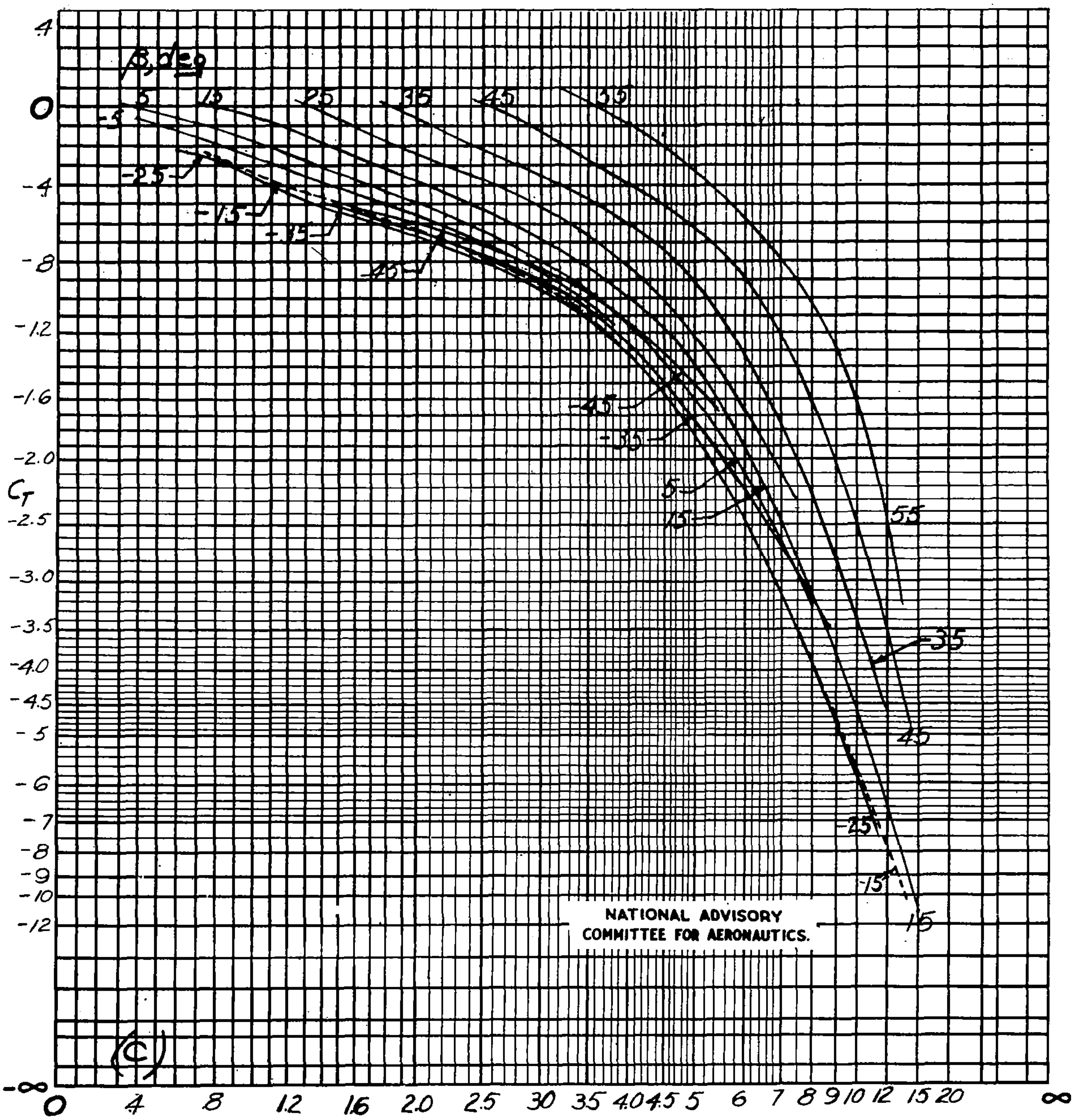

Figure 9.- Continued

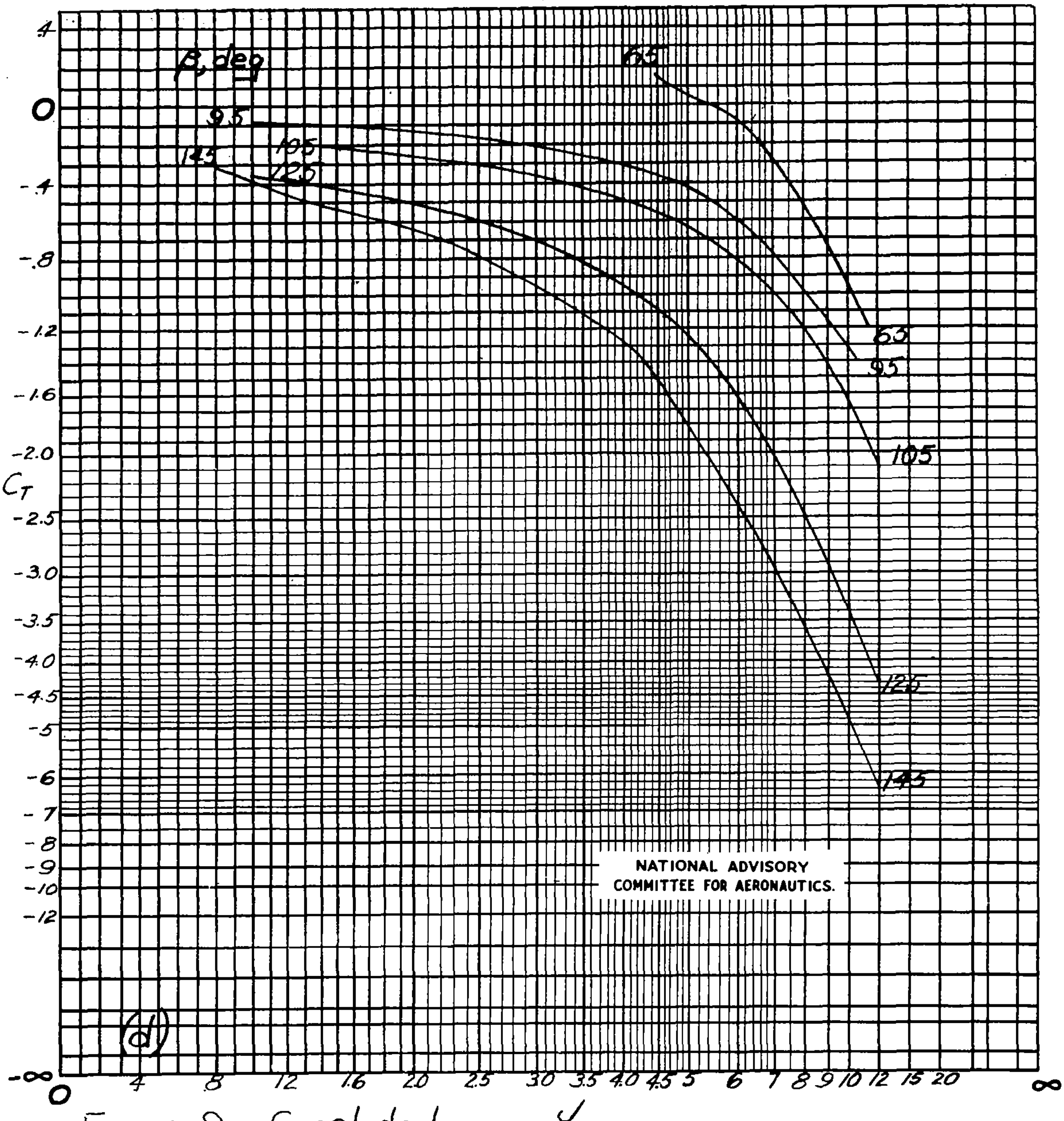

Figure 9.- Concluded

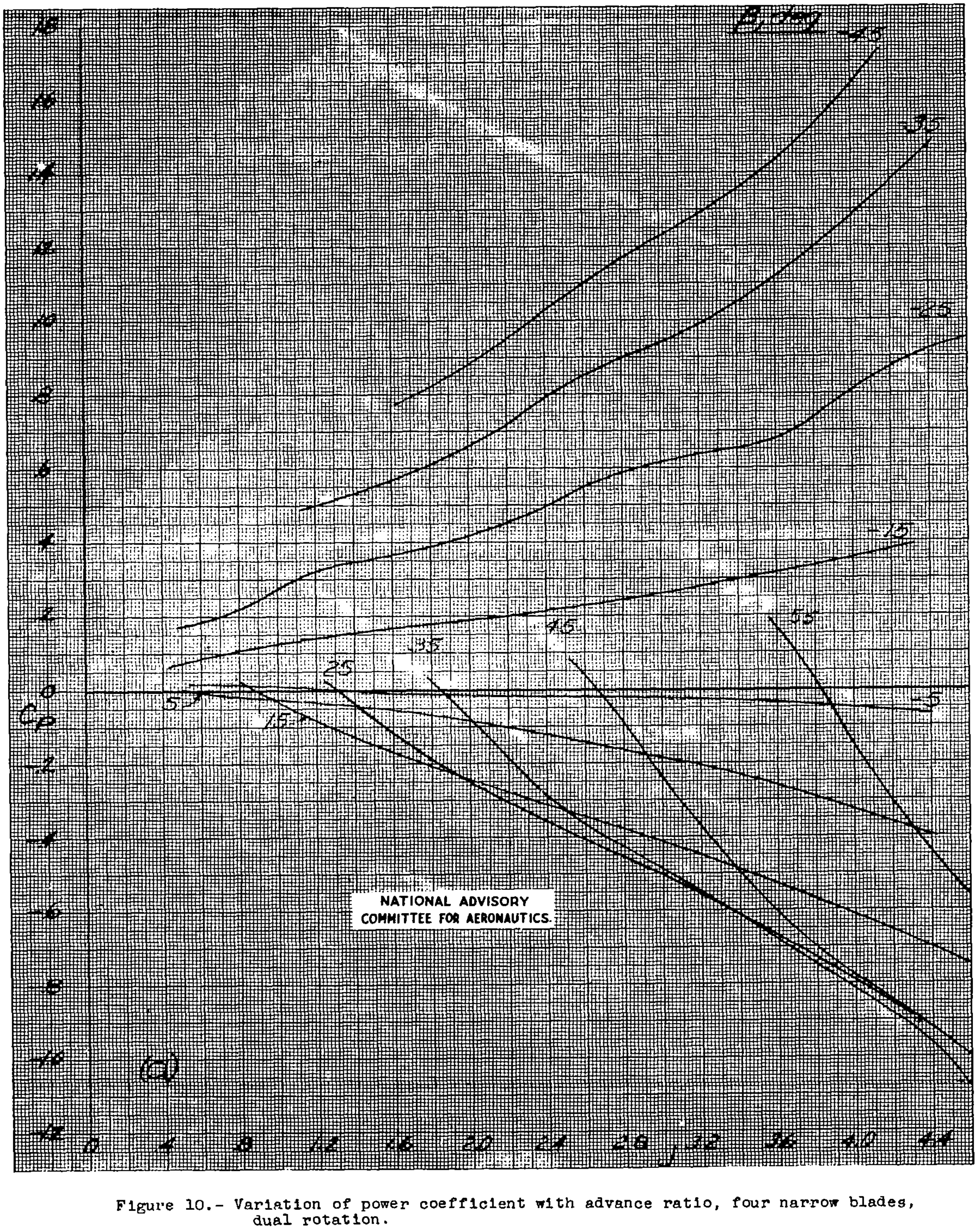

Figure 10.- Variation of power coefficient with advance ratio, four narrow blades, dual rotation.

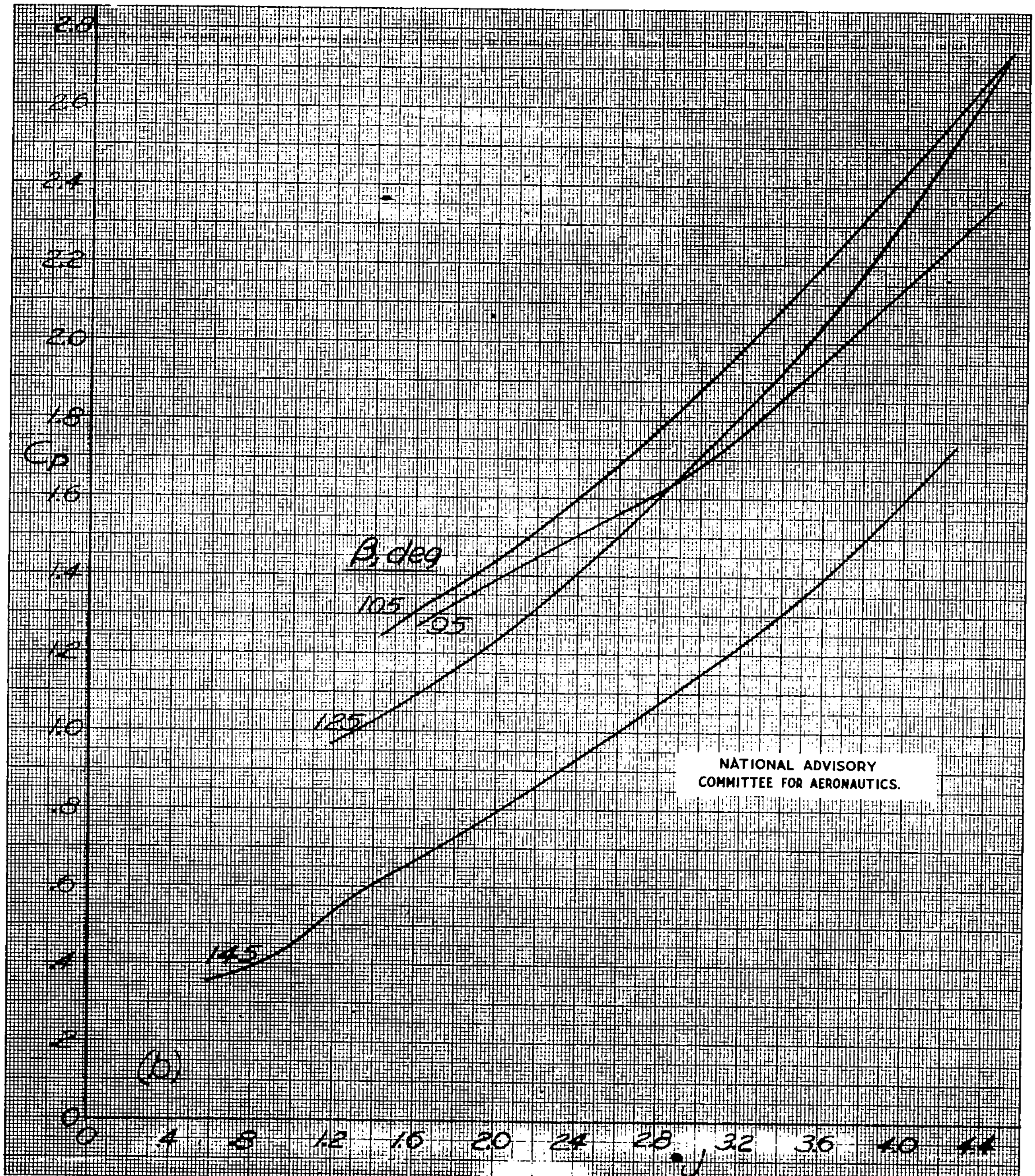

Figure 10.- Continued.

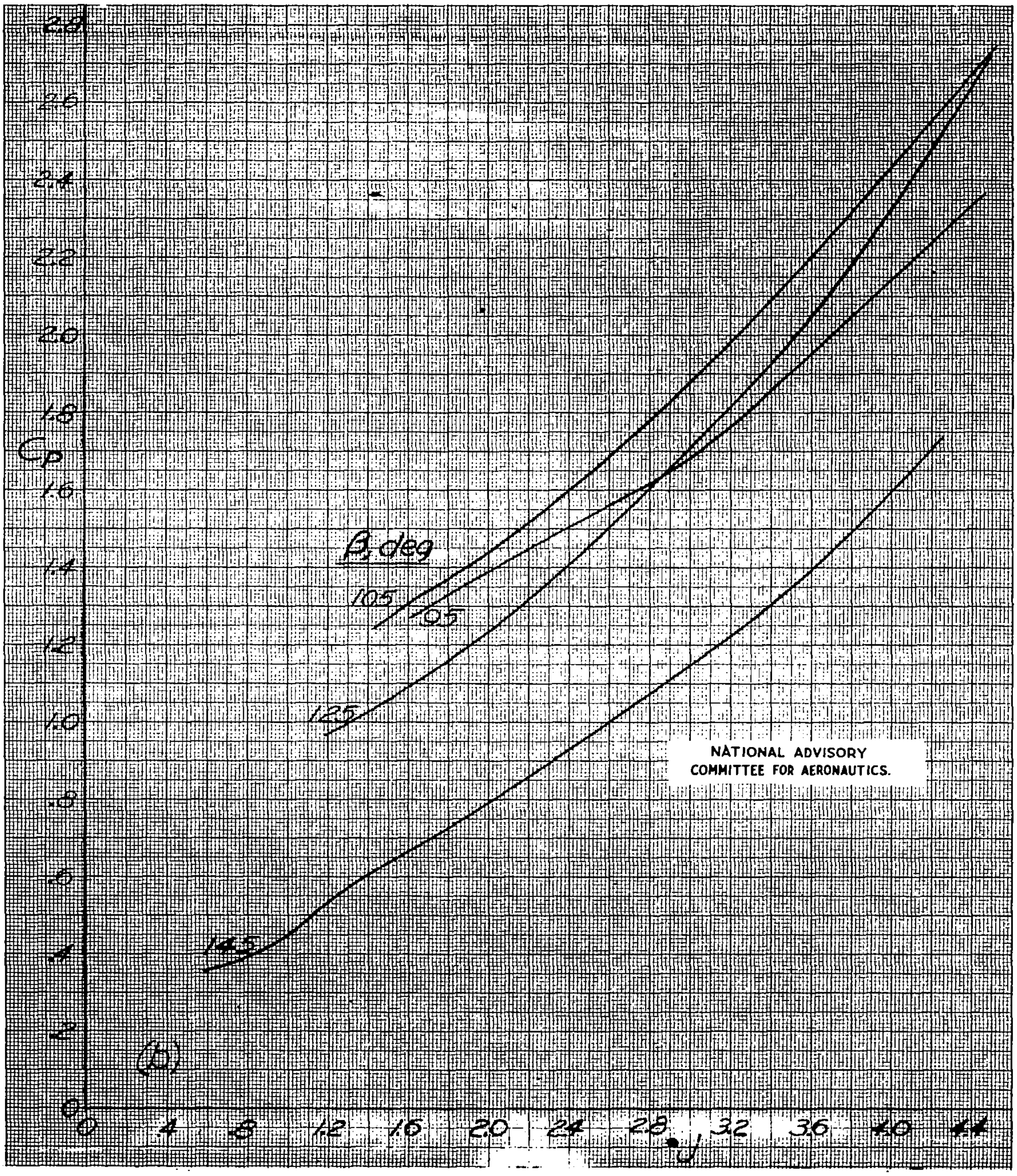

Figure 10.- Continued.

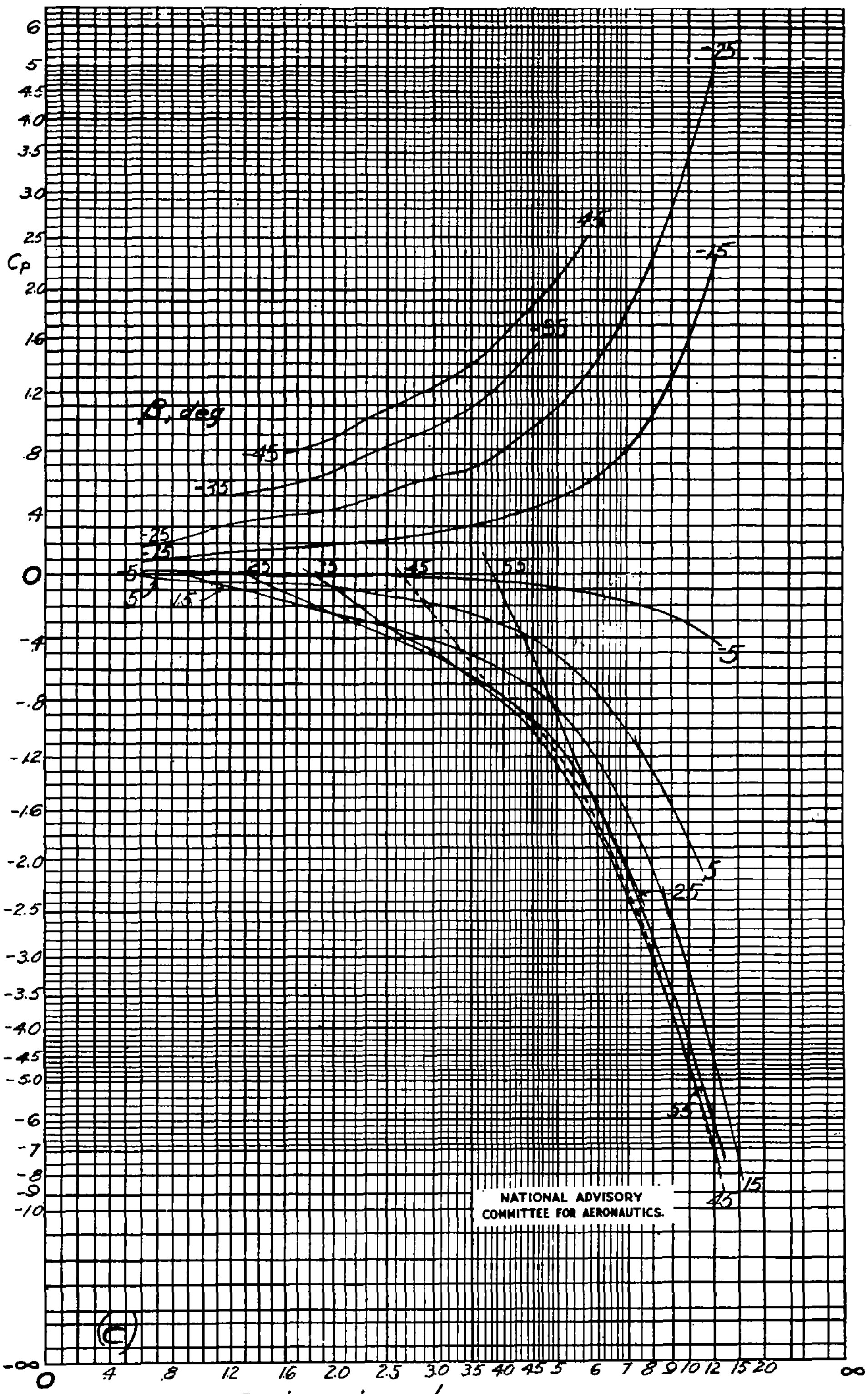

Figure 10.- Continued

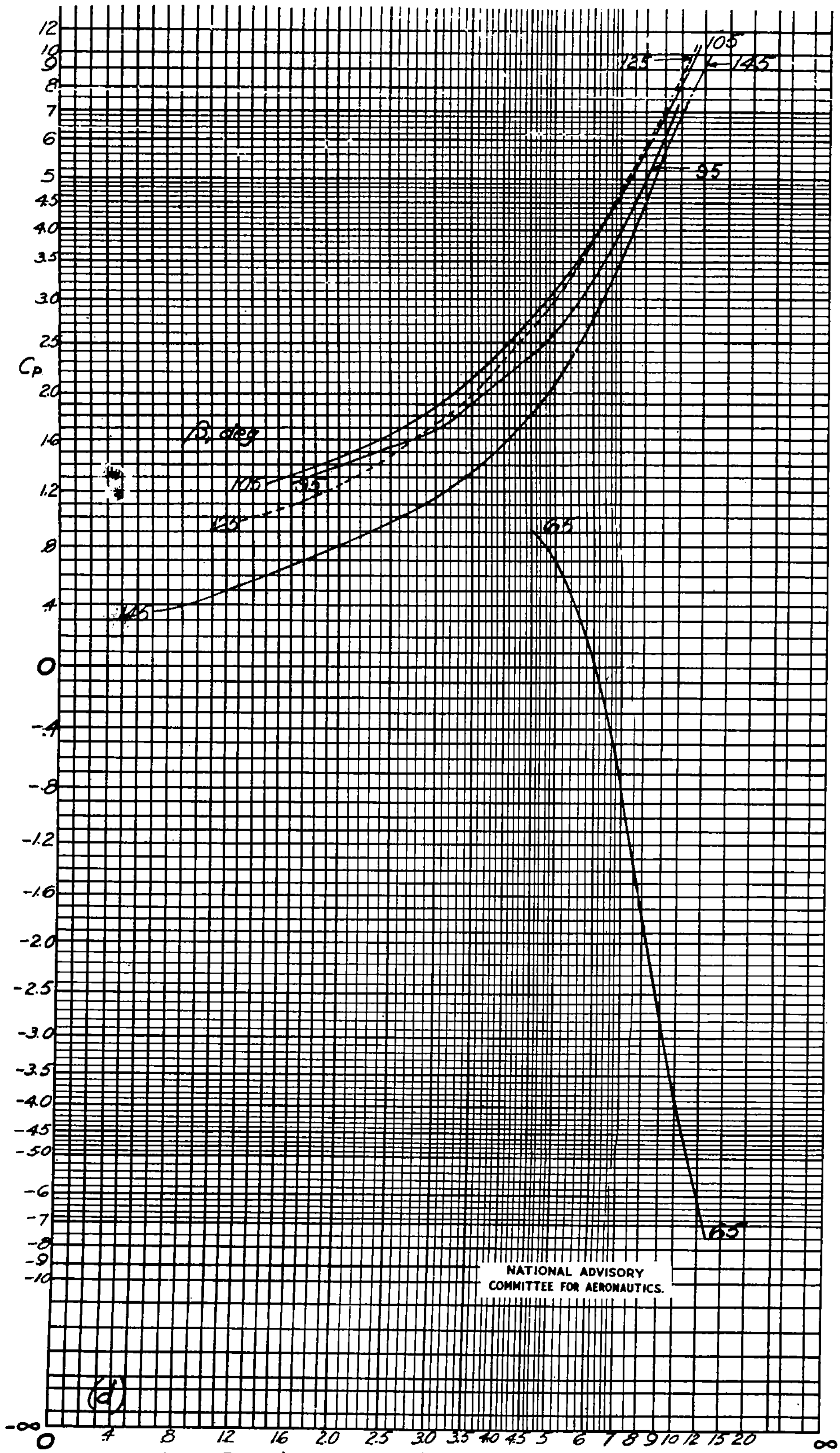

Figure 10.- Concluded

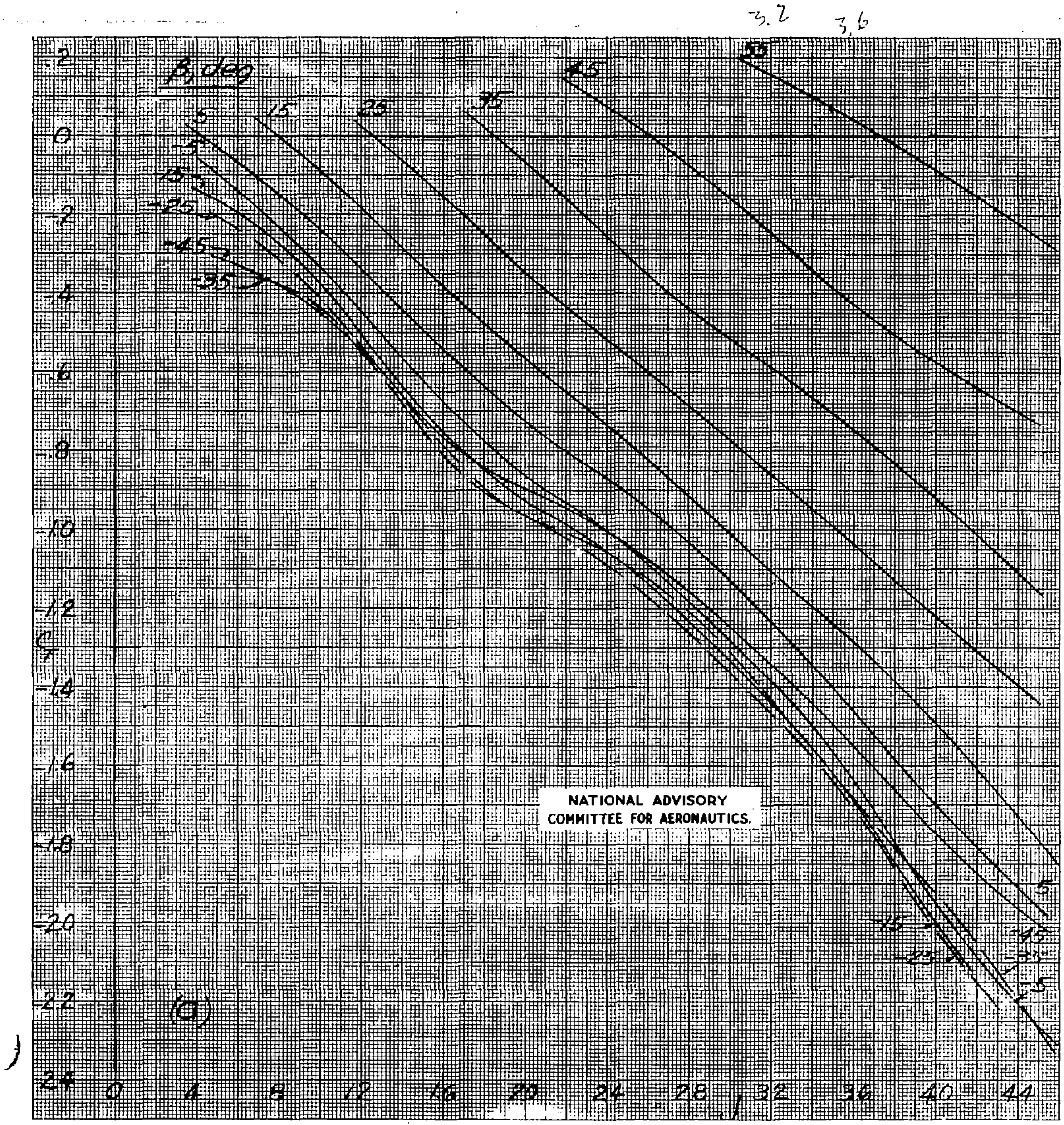

Figure 11.- Variation of thrust coefficient with advance ratio, six narrow blades, dual rotation.

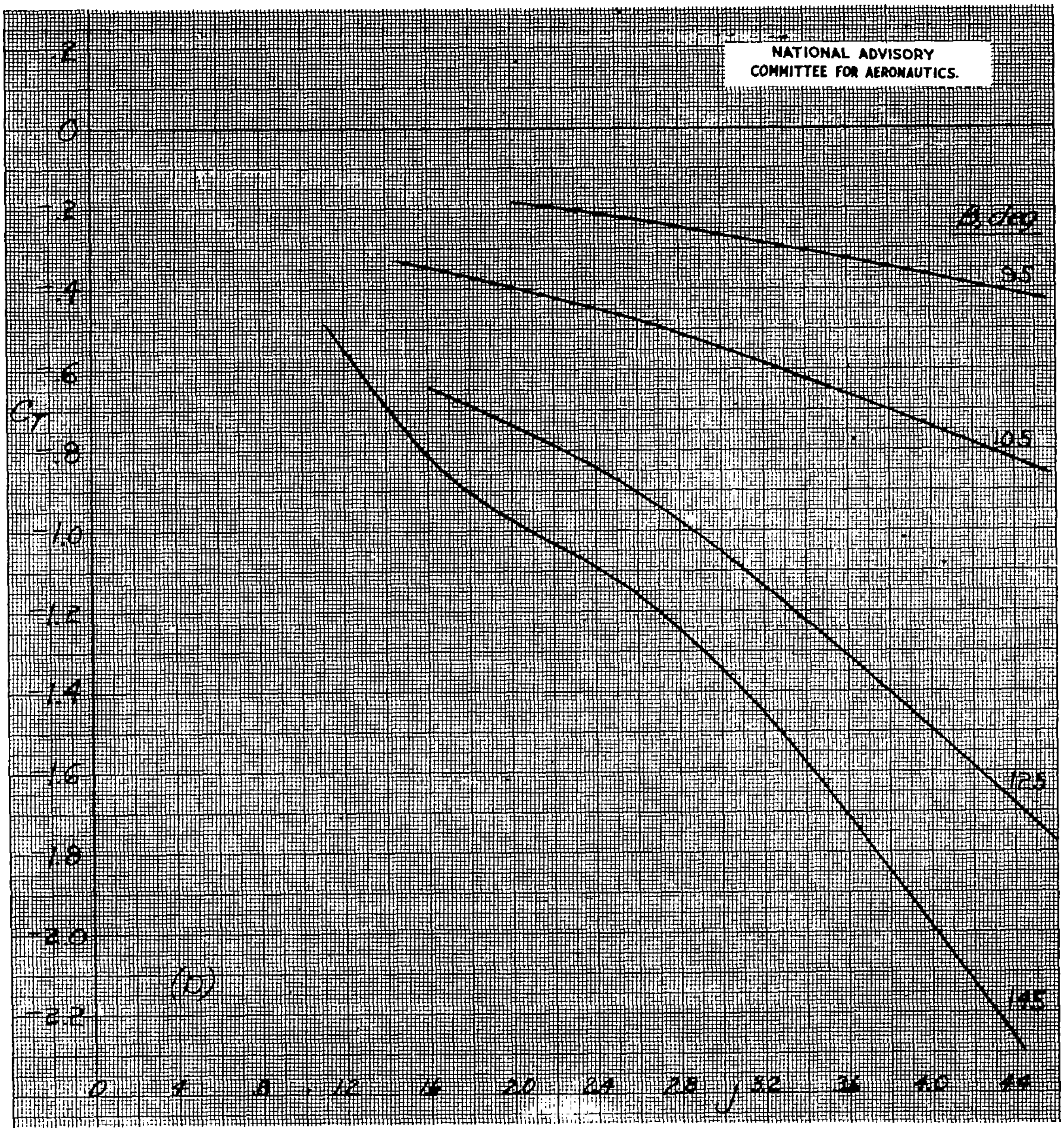

Figure 11.- Continued.

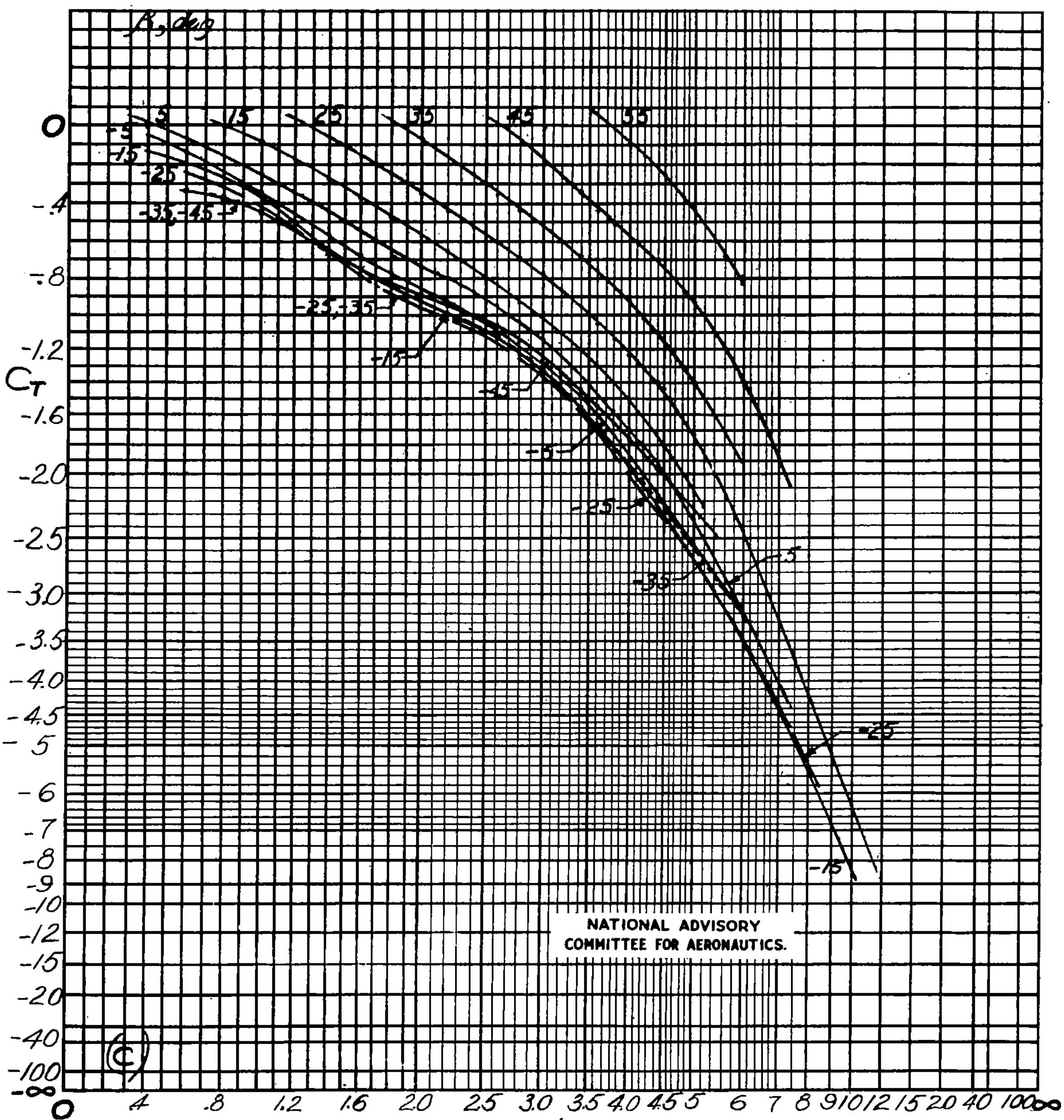

Figure 11.-Continued

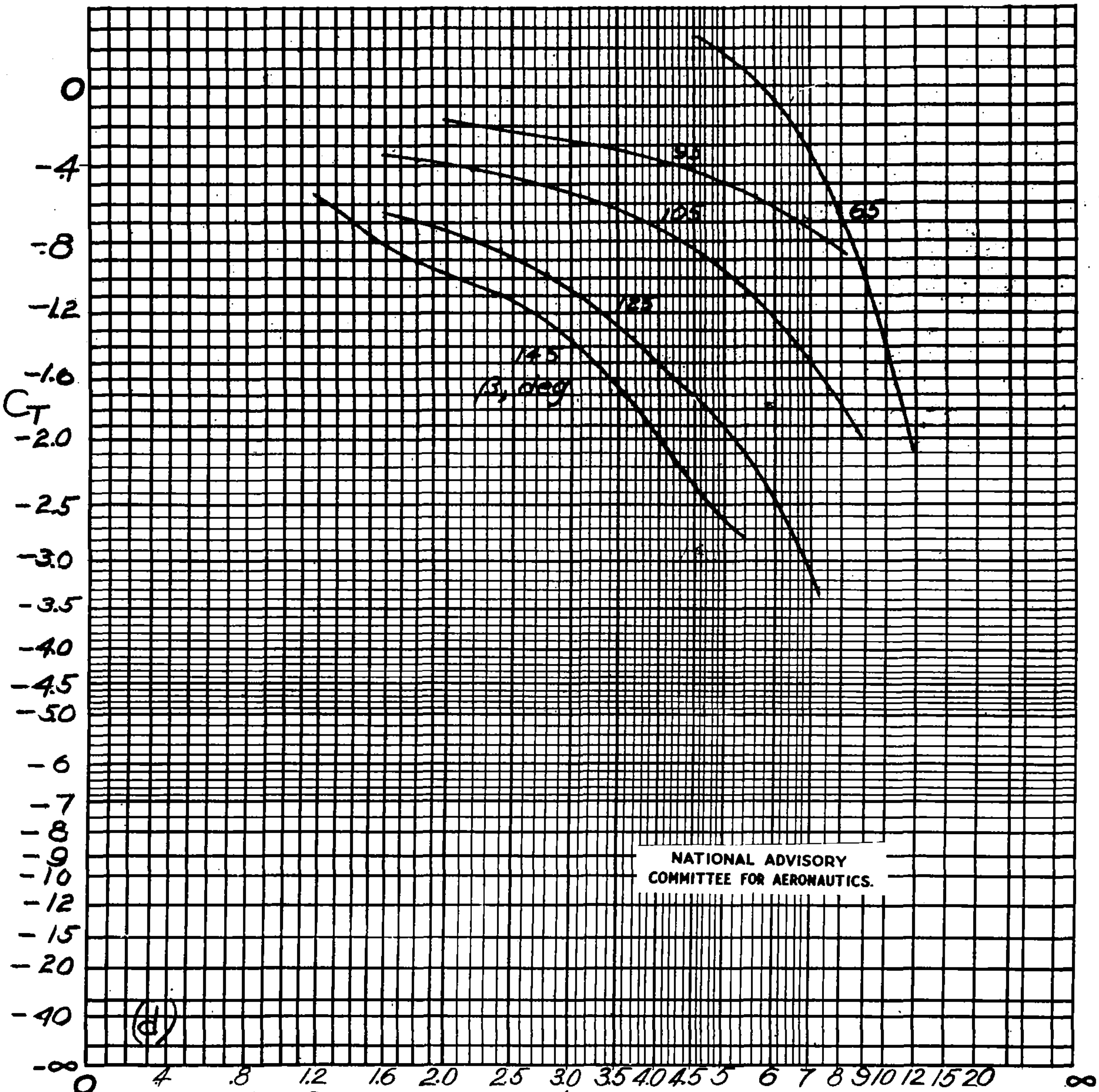

Figure 11.– Concluded

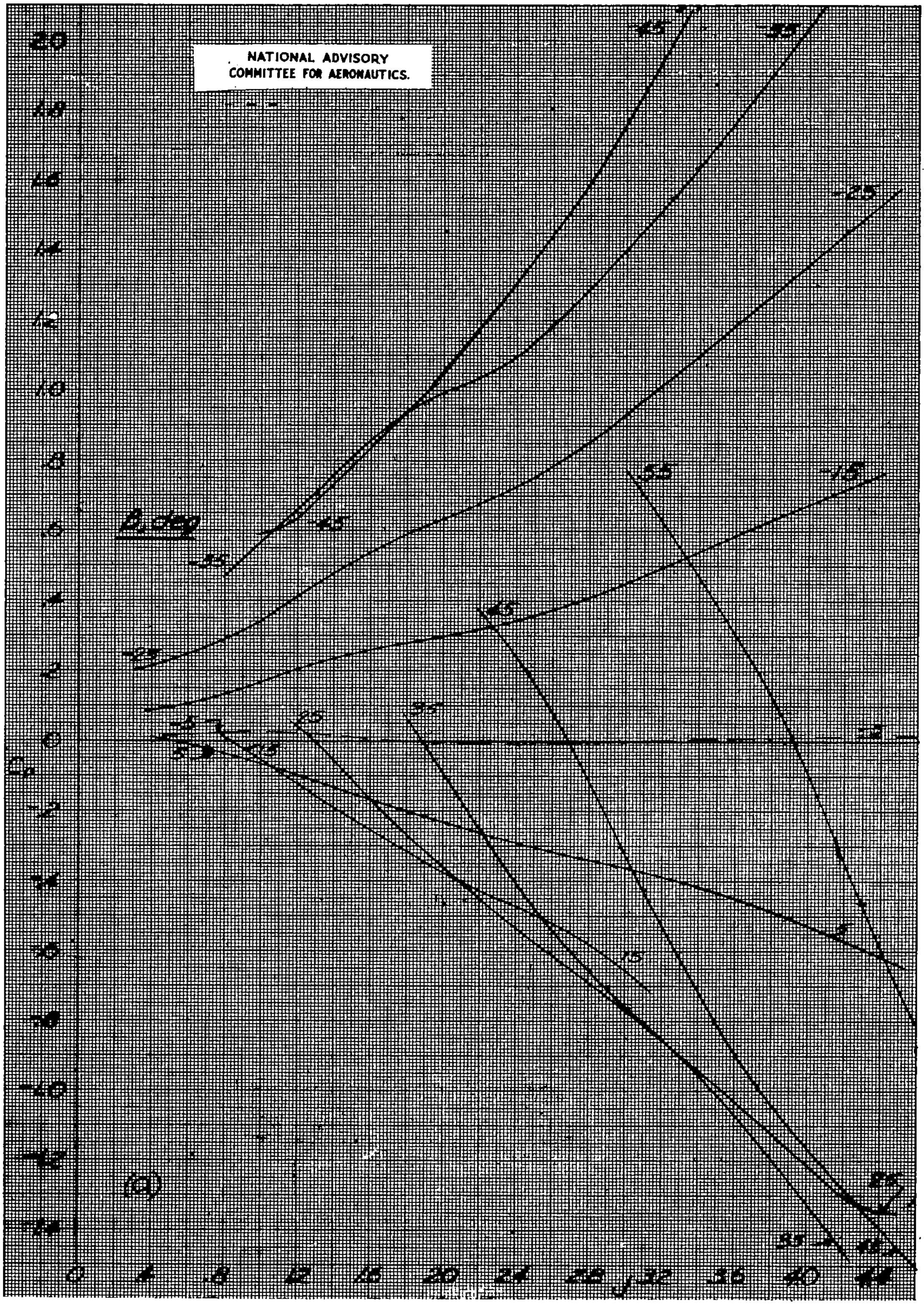

Figure 12.- Variation of power coefficient with advance ratio, six narrow blades, dual rotation.

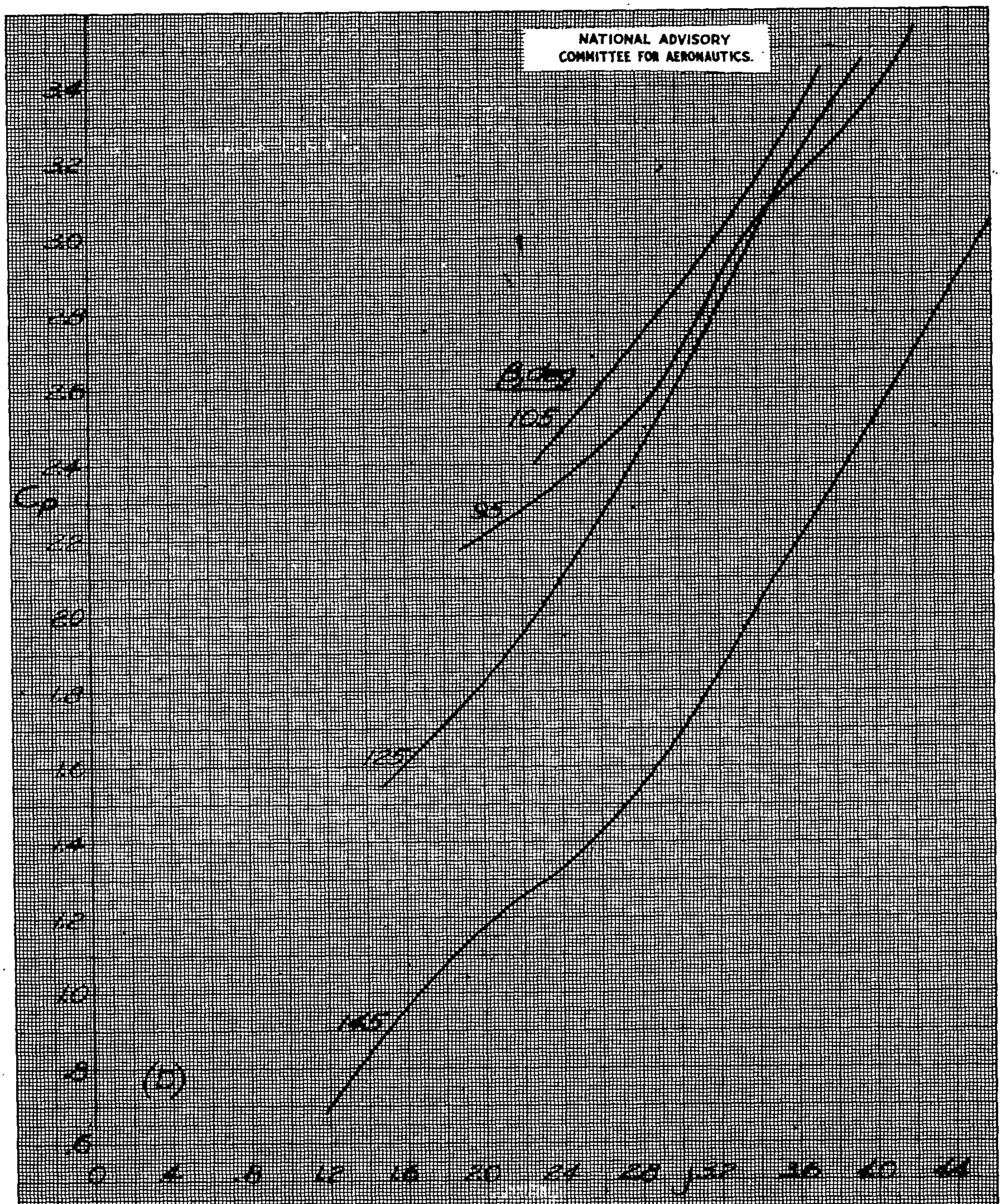

Figure 12.- Continued.

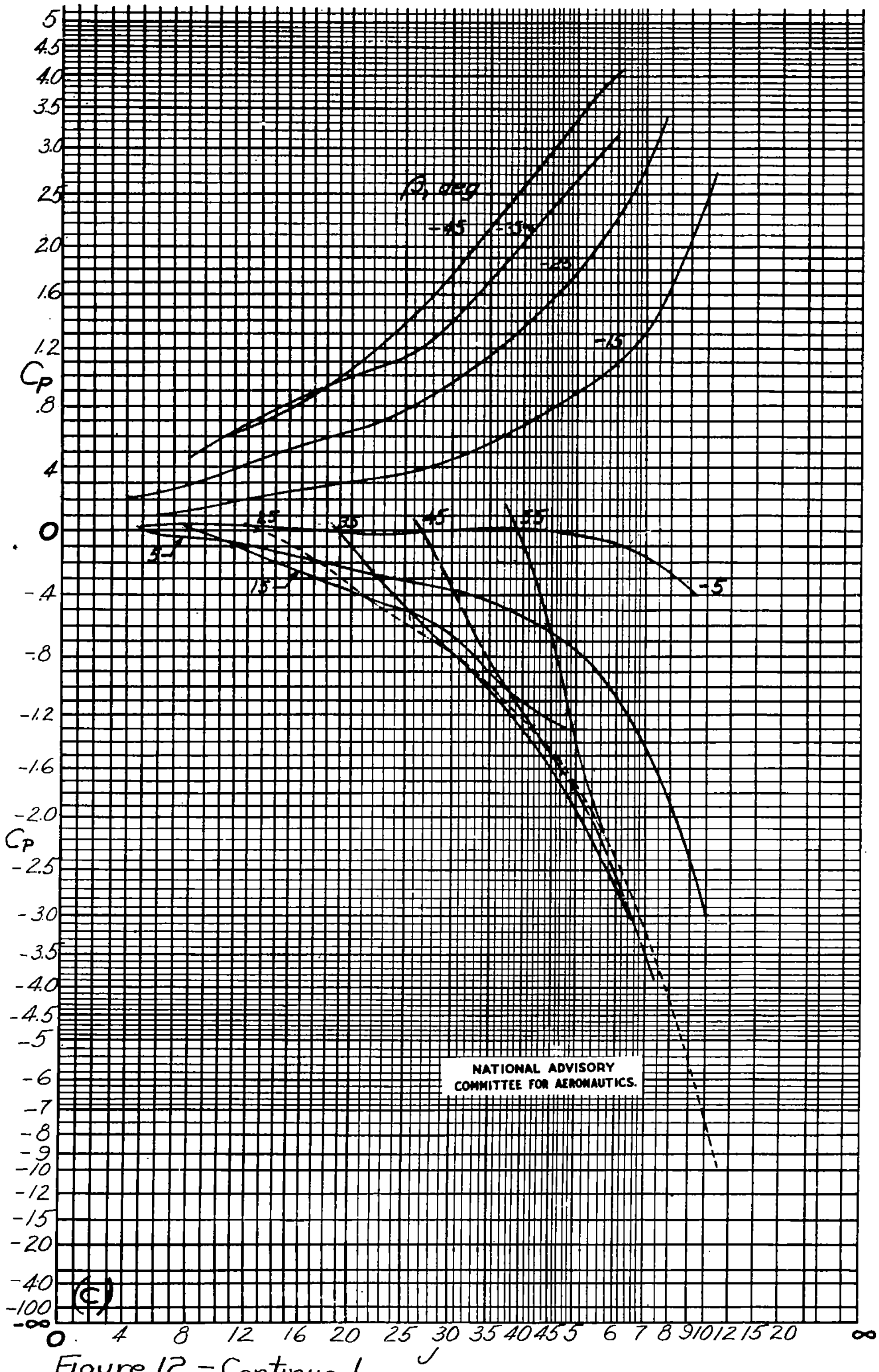

Figure 12.- Continued

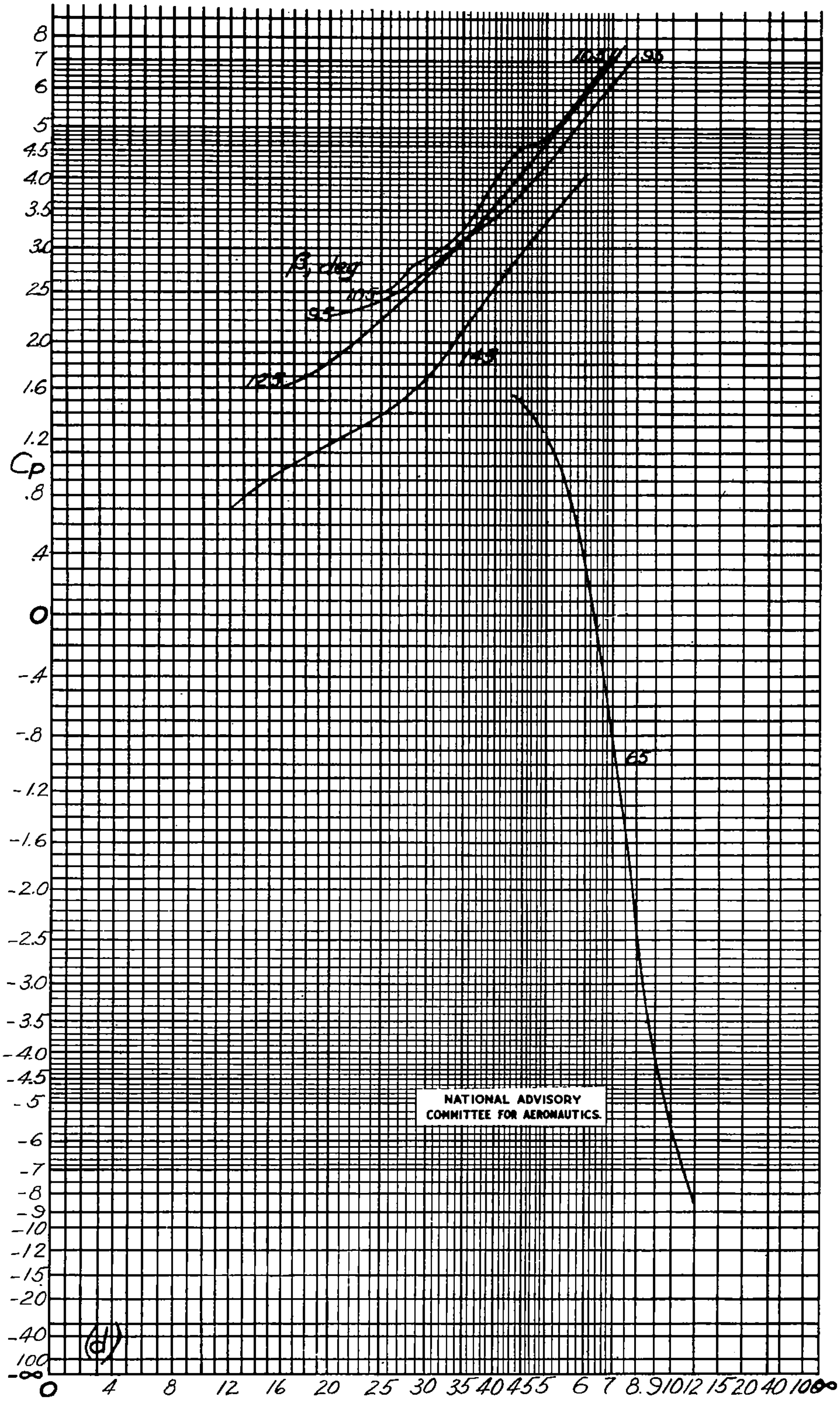

Figure 12.- Concluded

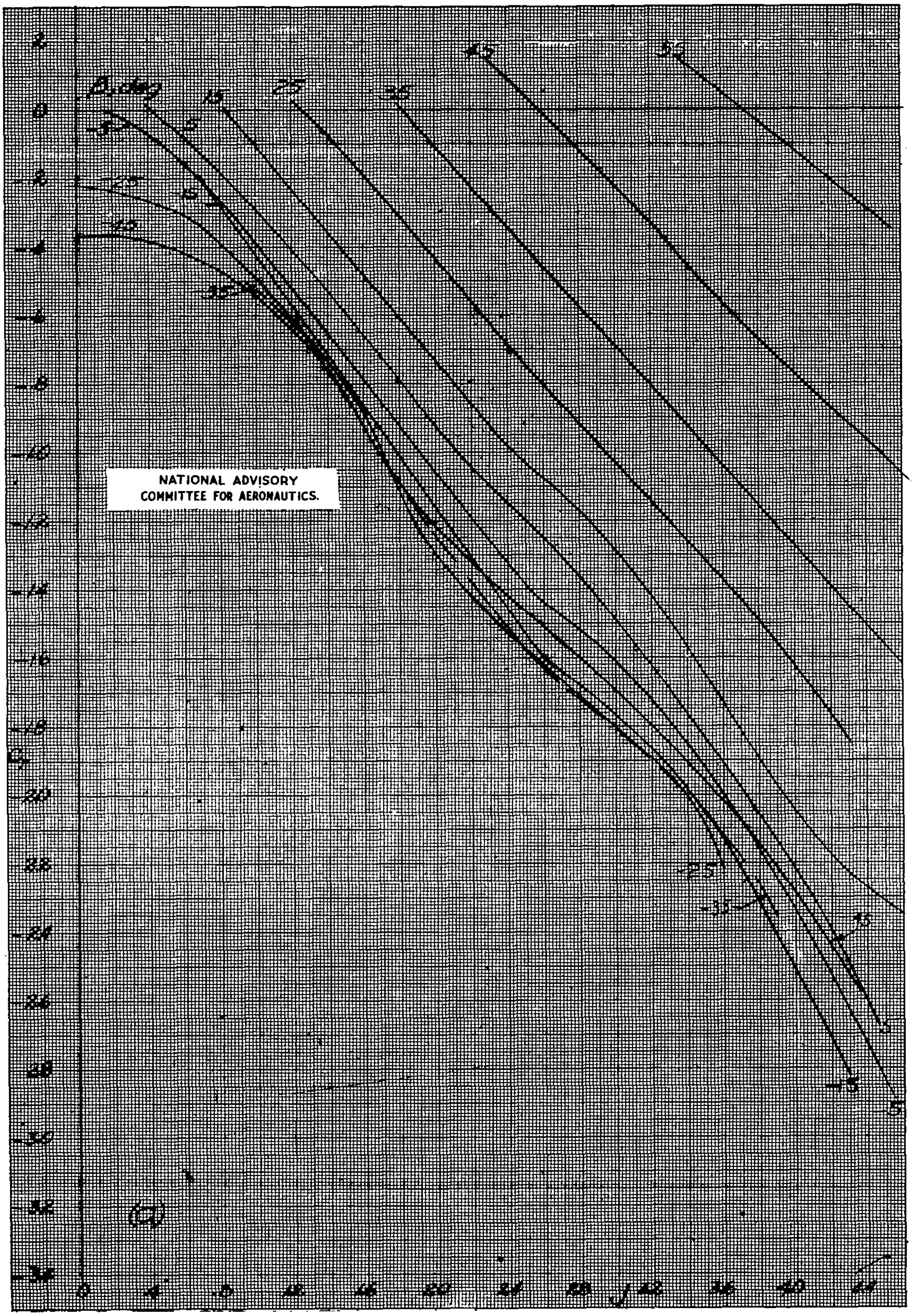

Figure 13.- Variation of thrust coefficient with advance ratio, eight narrow blades, dual rotation.

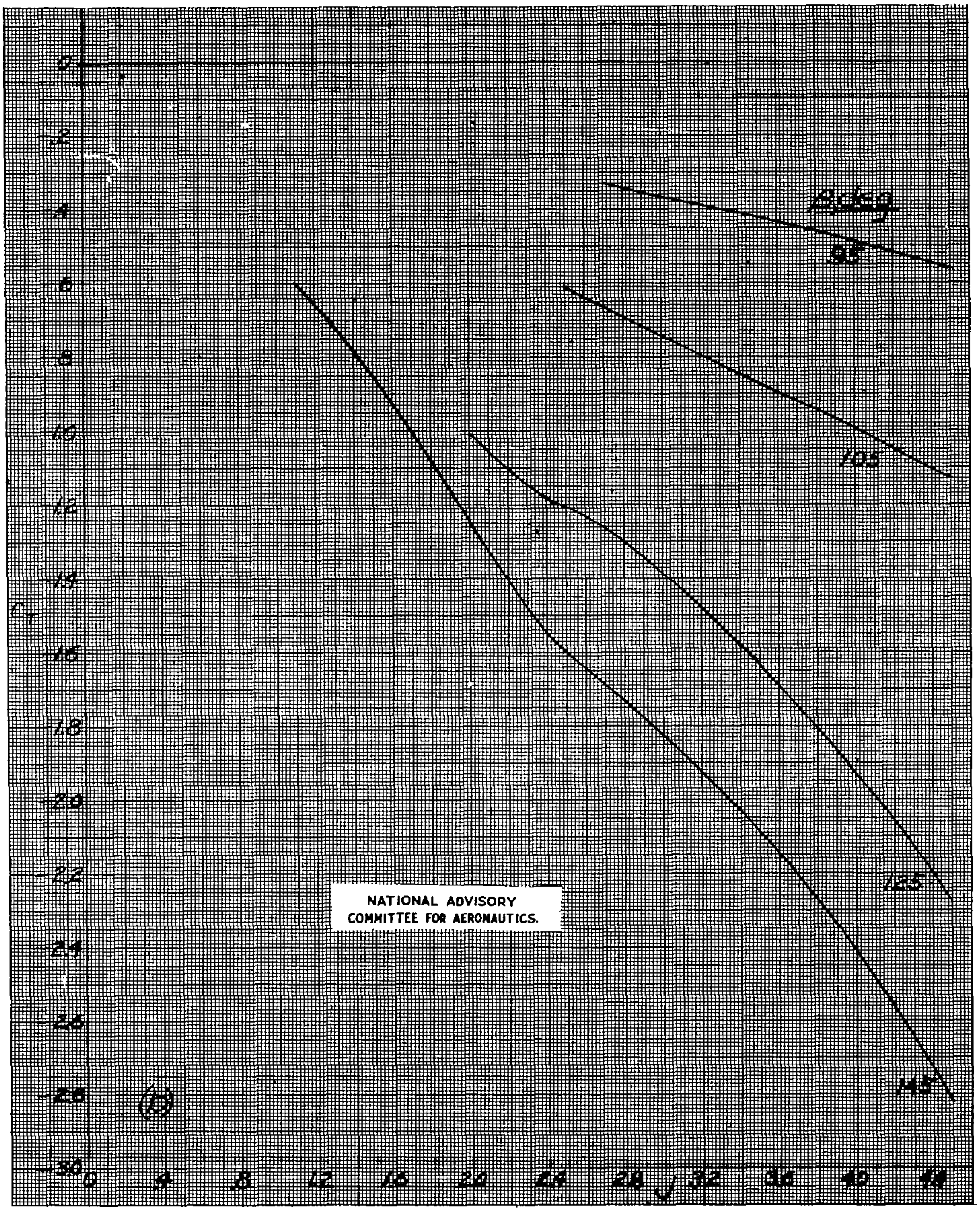

Figure 13.- Continued.

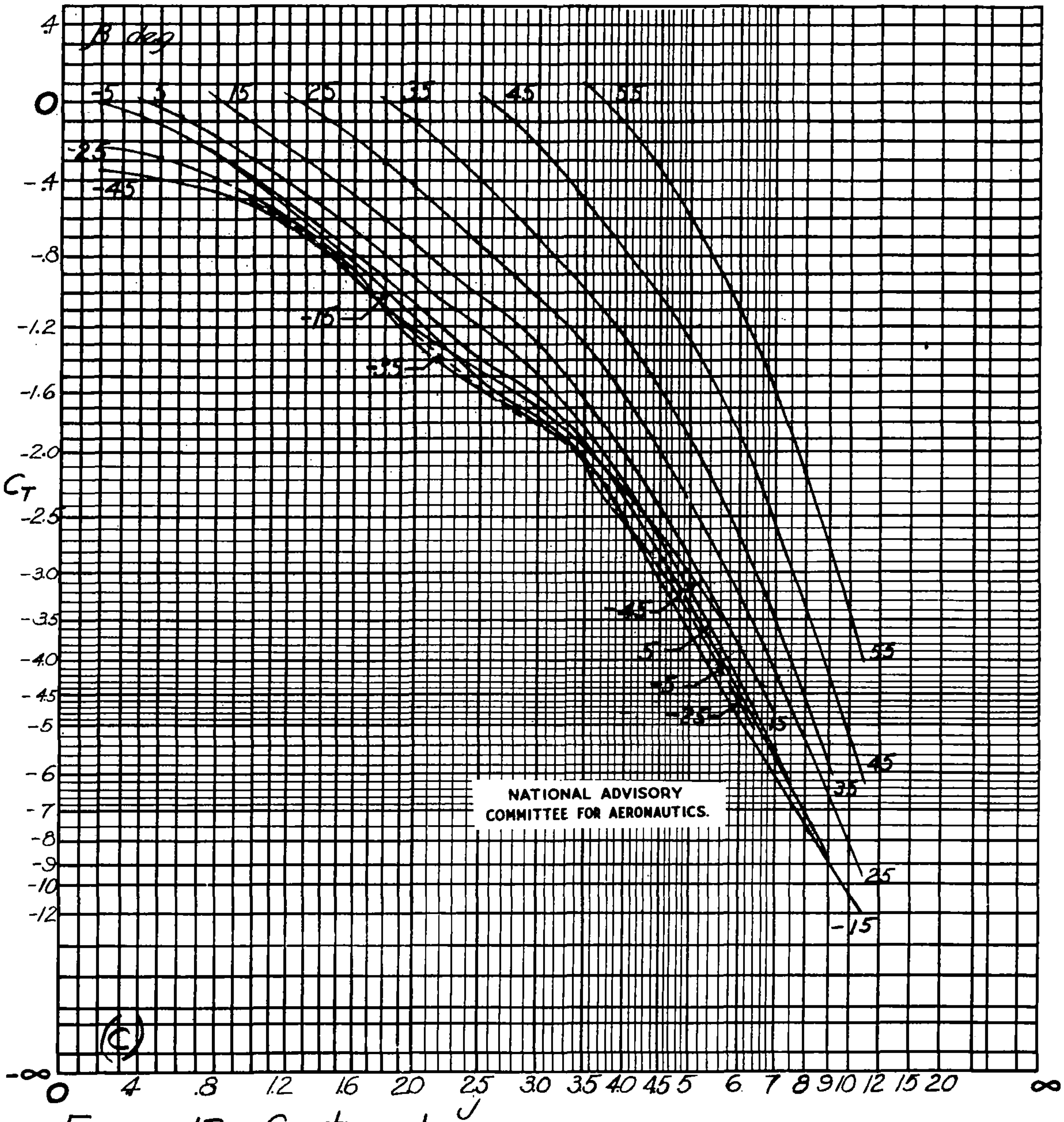

Figure 13.- Continued

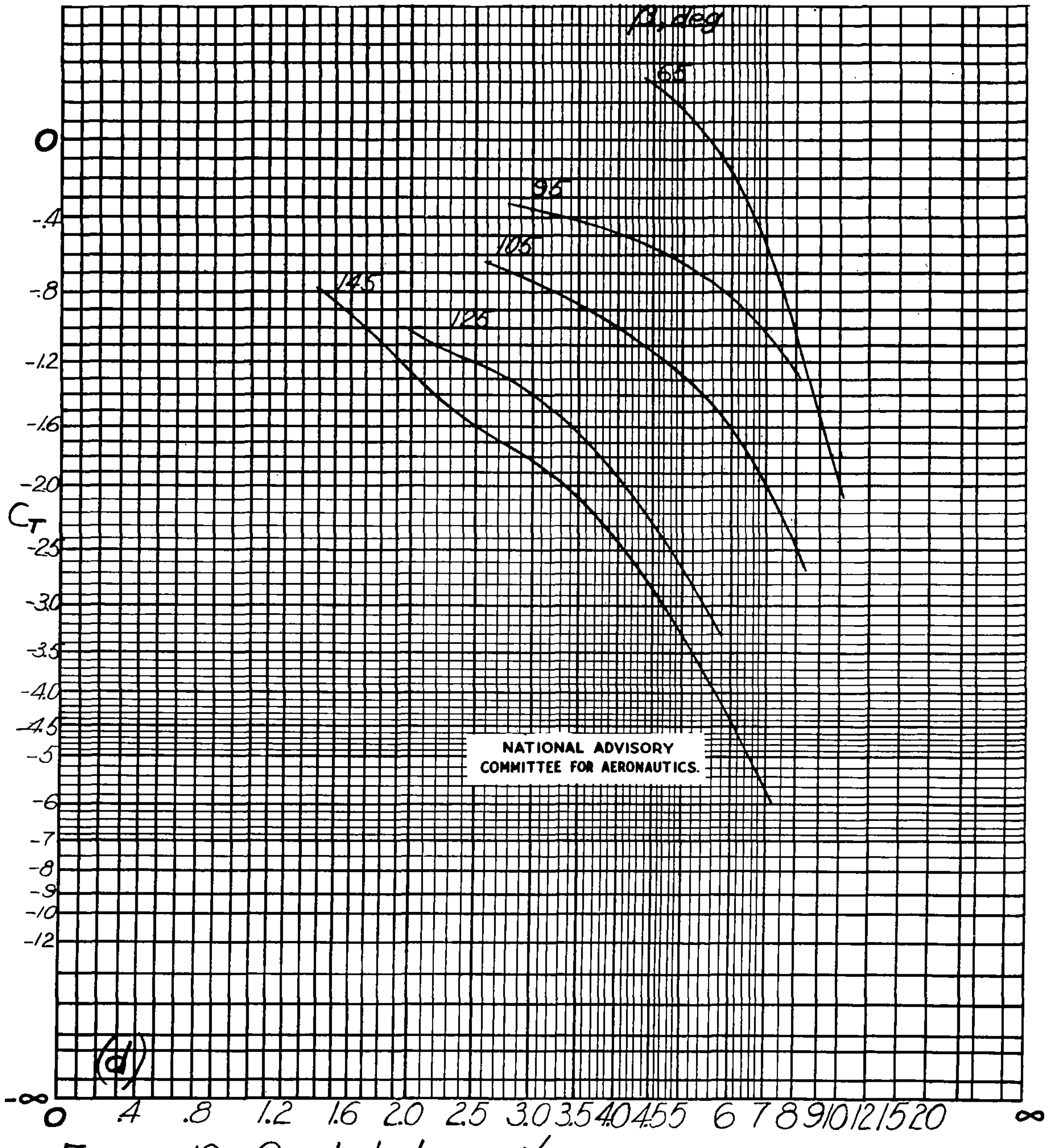

Figure 13.- Concluded

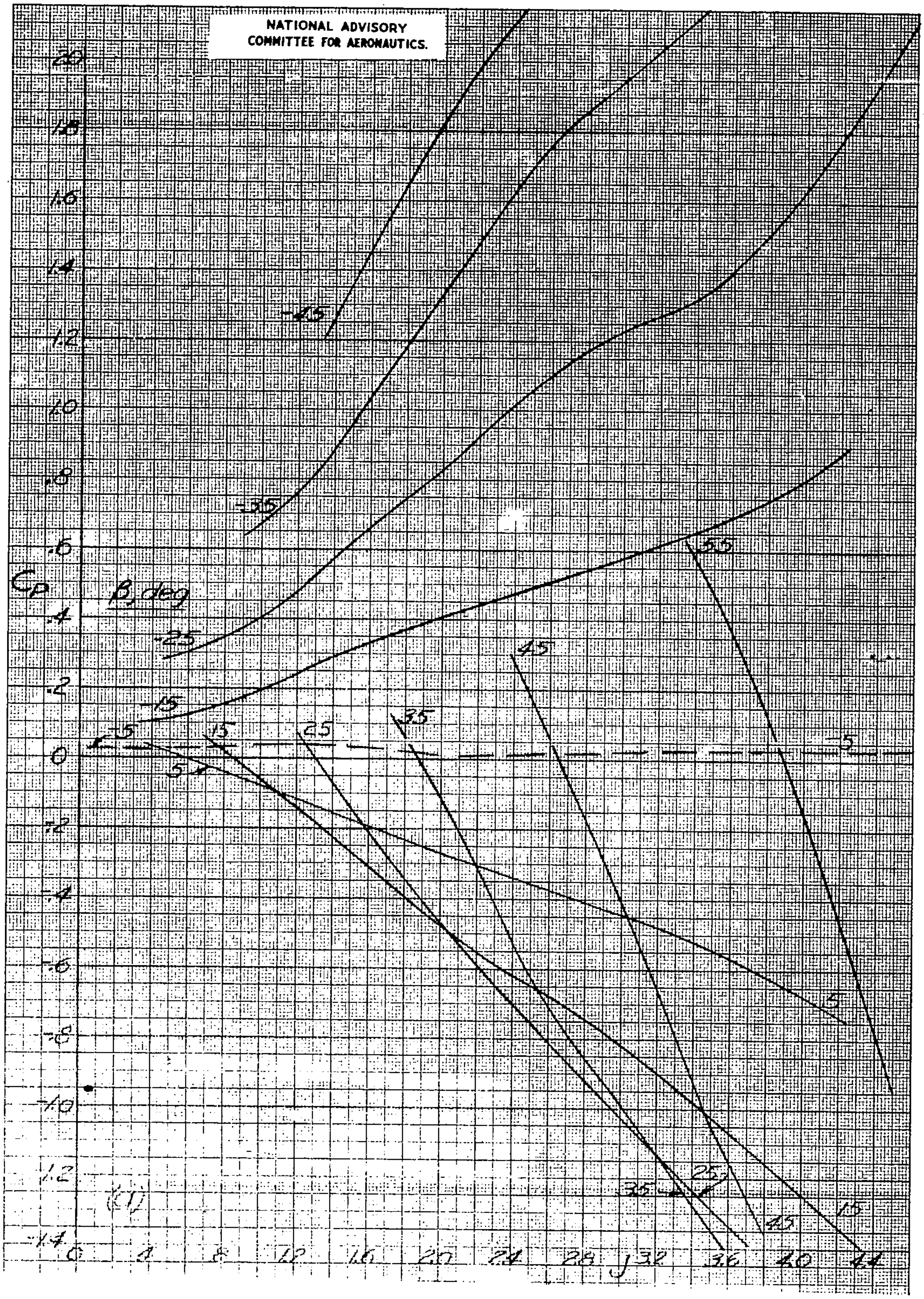

Figure 18.- Variation of power coefficient with advance ratio, eight narrow blades, dual rotation.

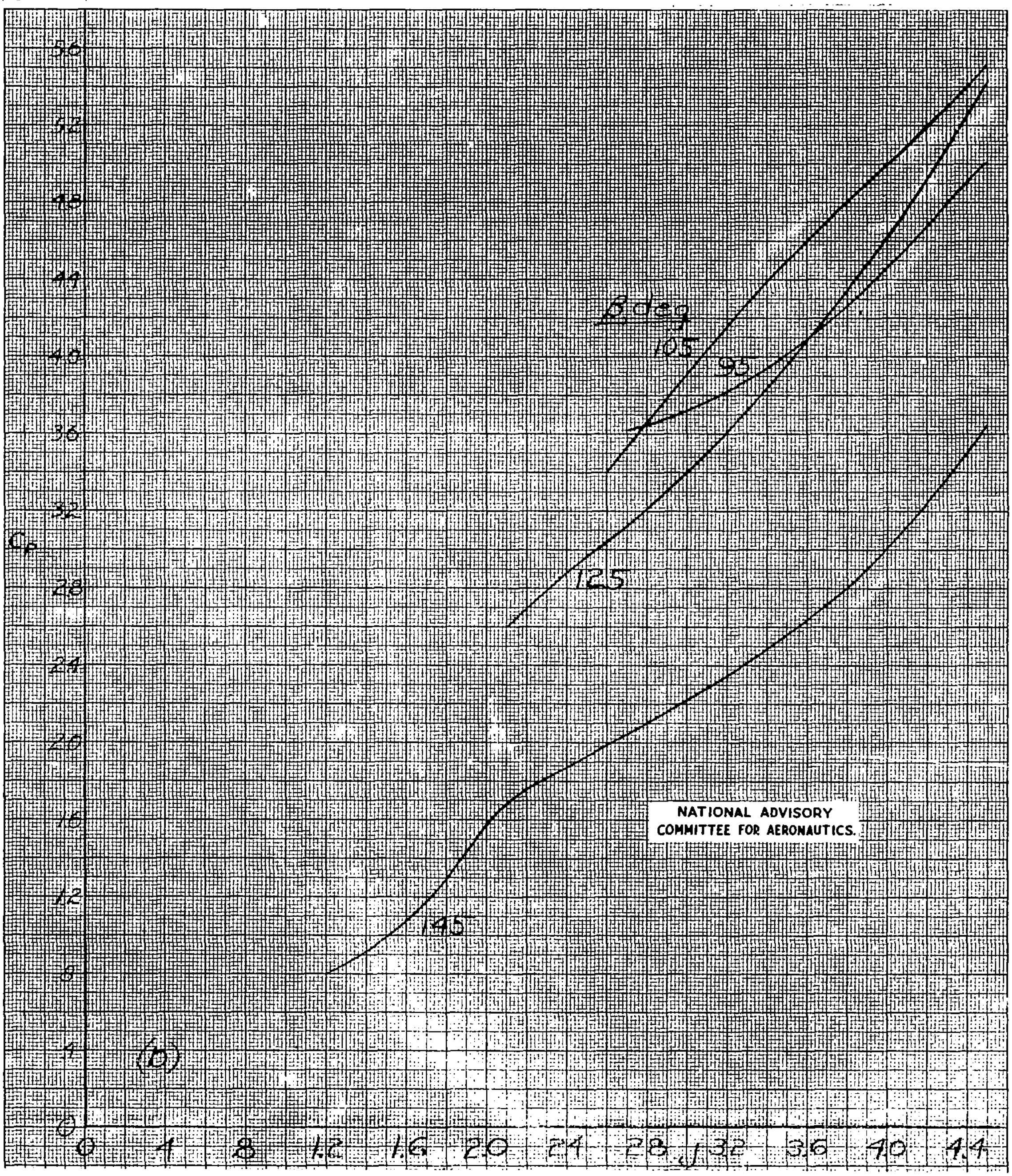

Figure 14.- Continued.

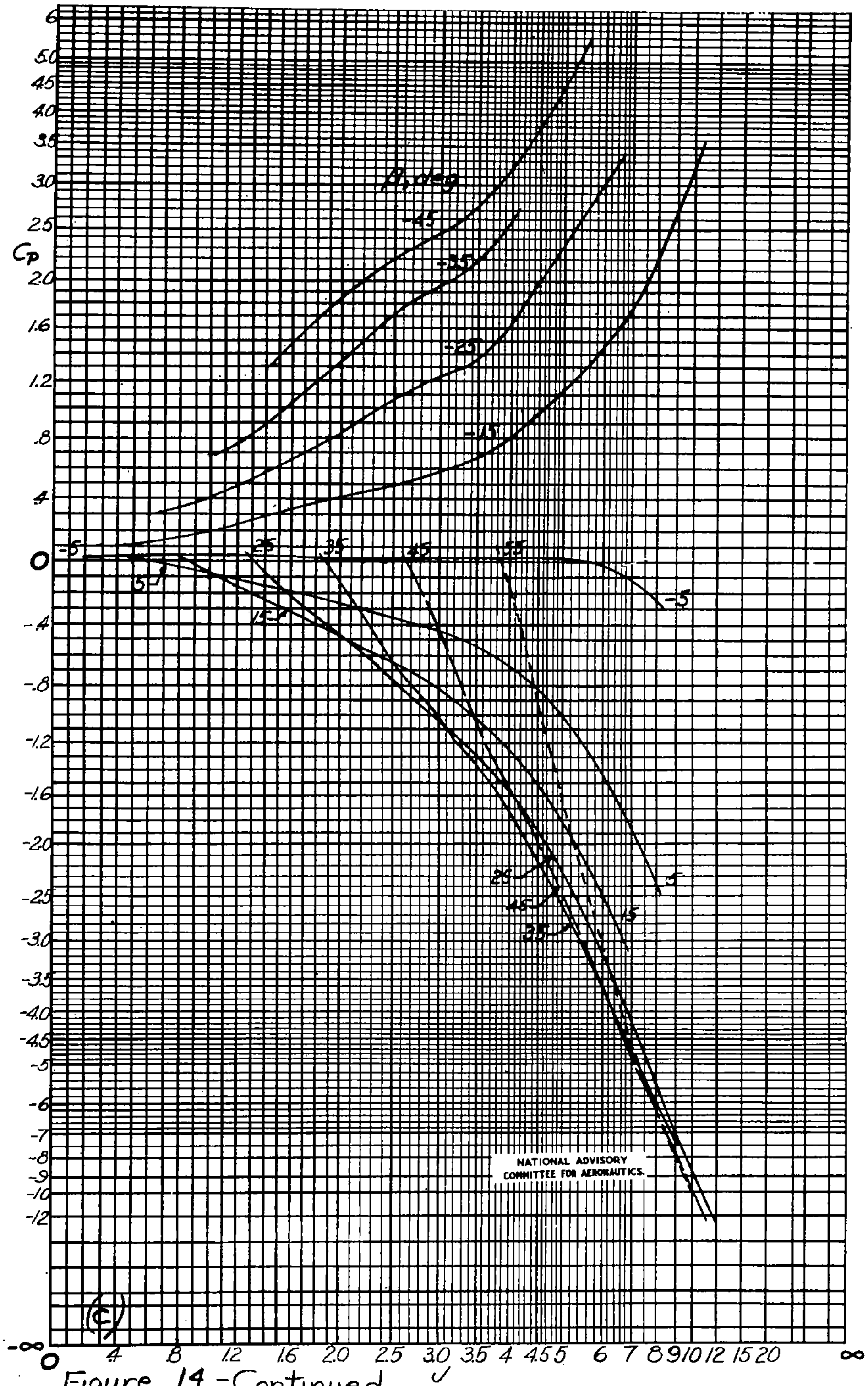

Figure 14.-Continued

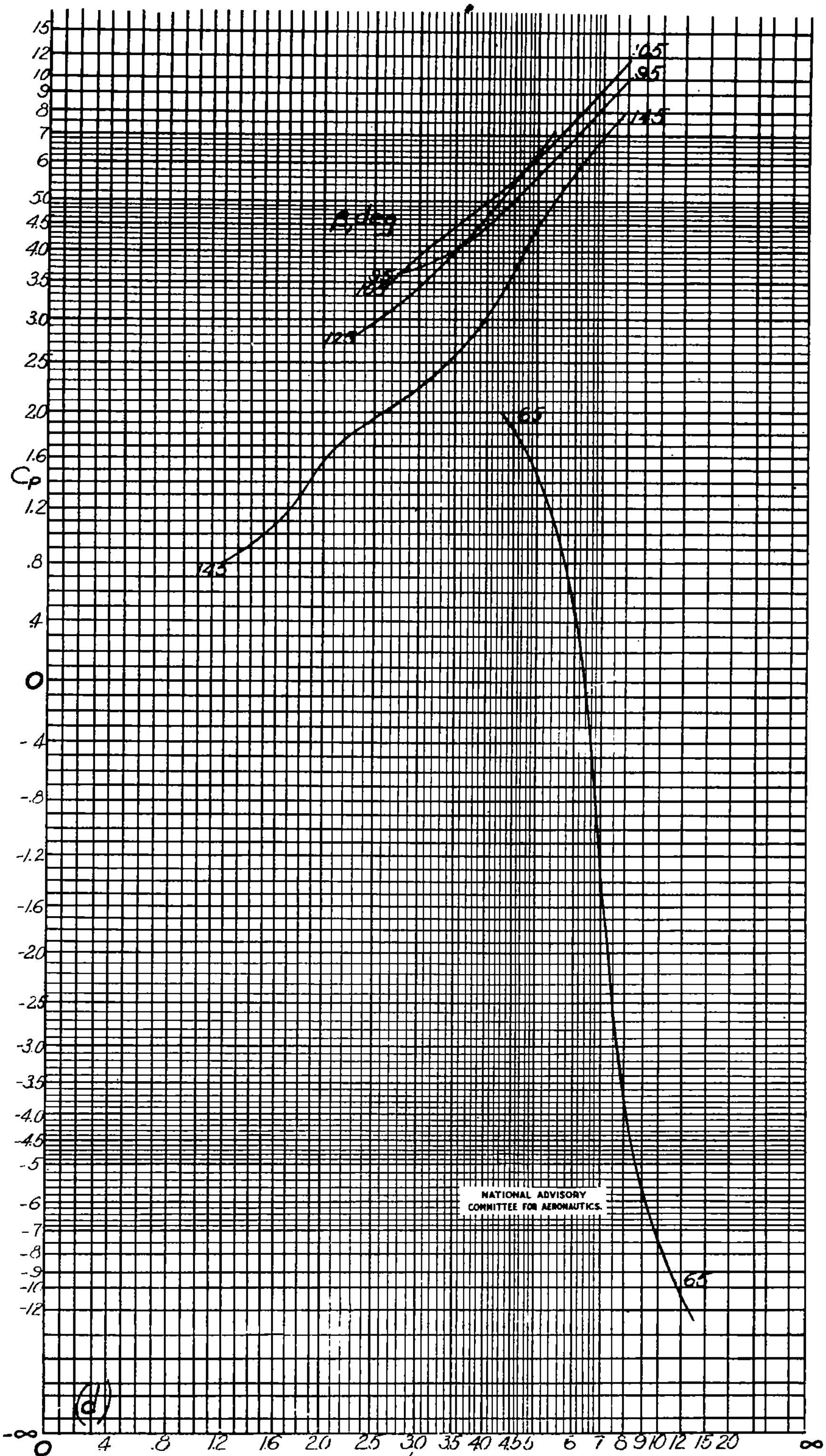

Figure 14.- Concluded

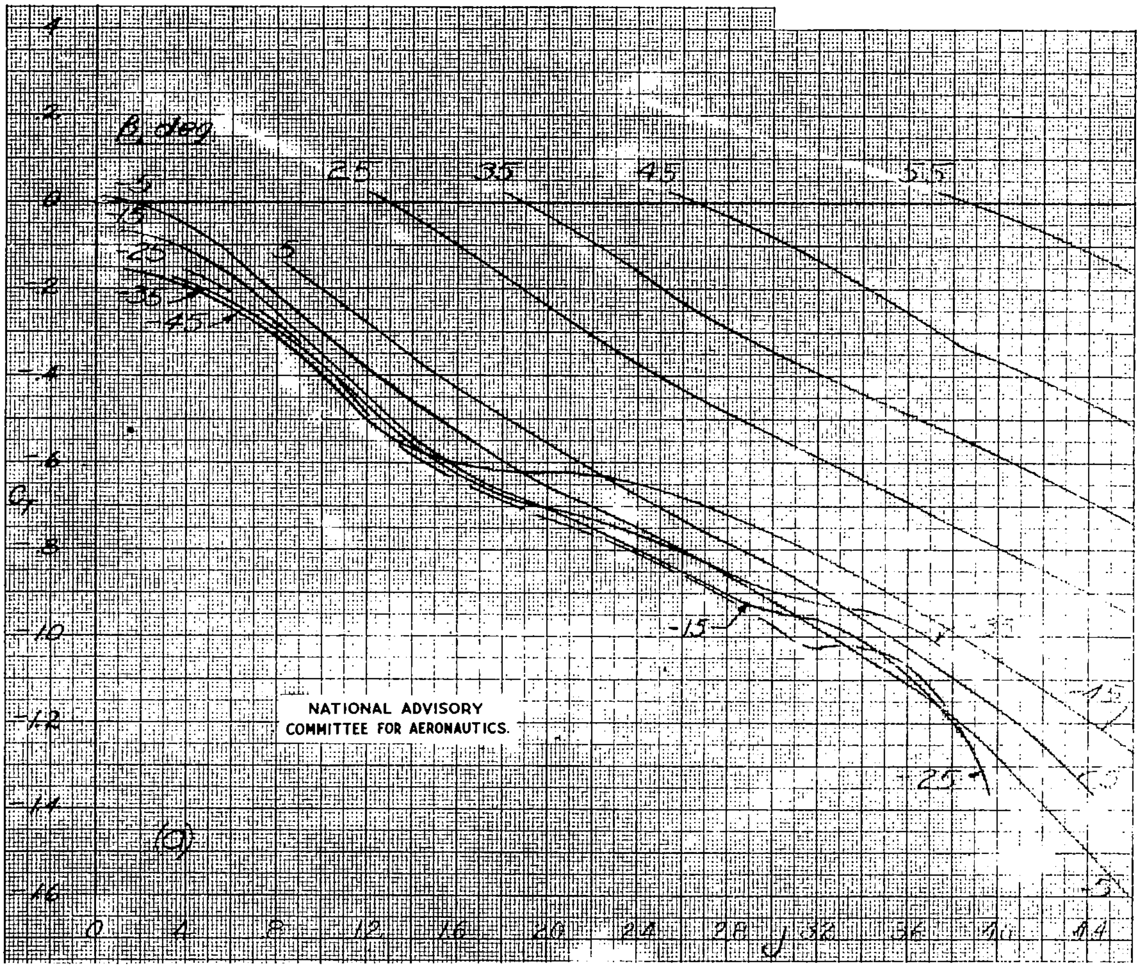

Figure 15.- Variation of thrust coefficient with advance ratio, three wide blades.

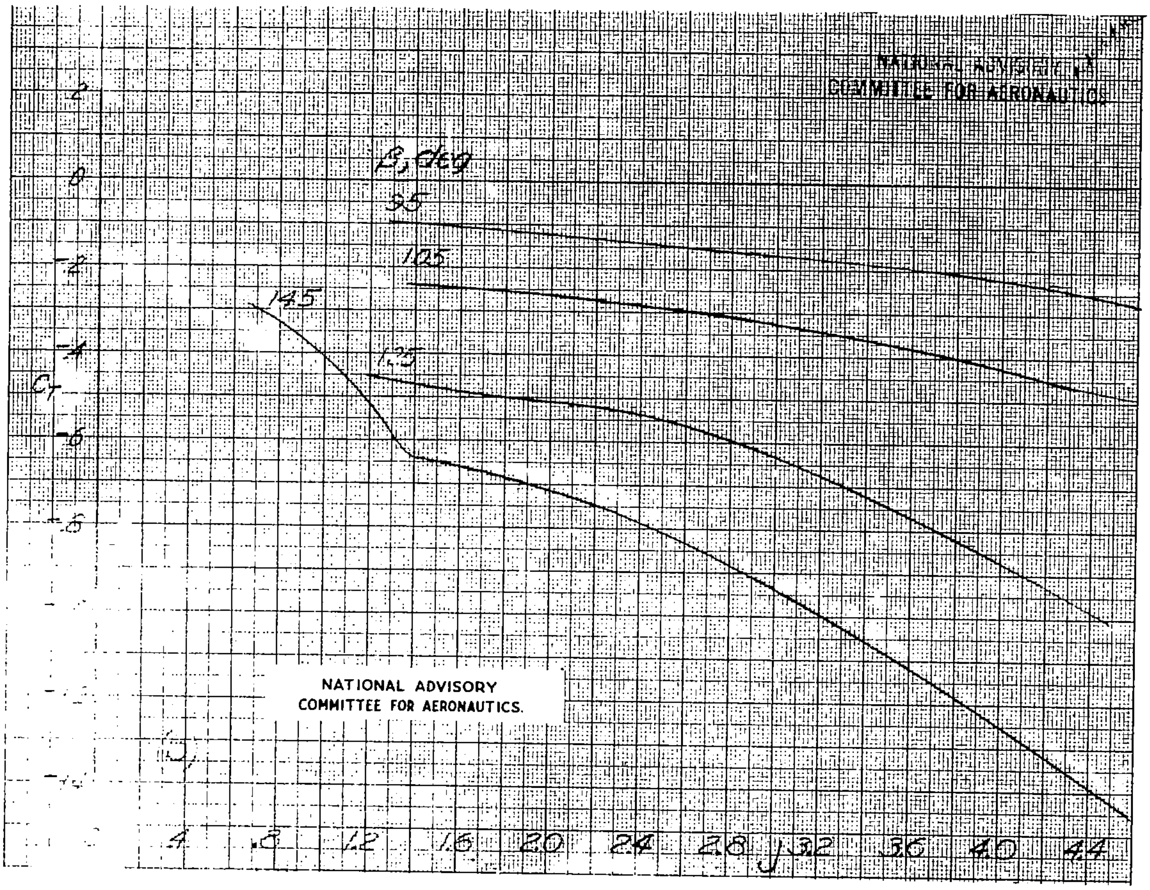

Figure 1F.- Continued.

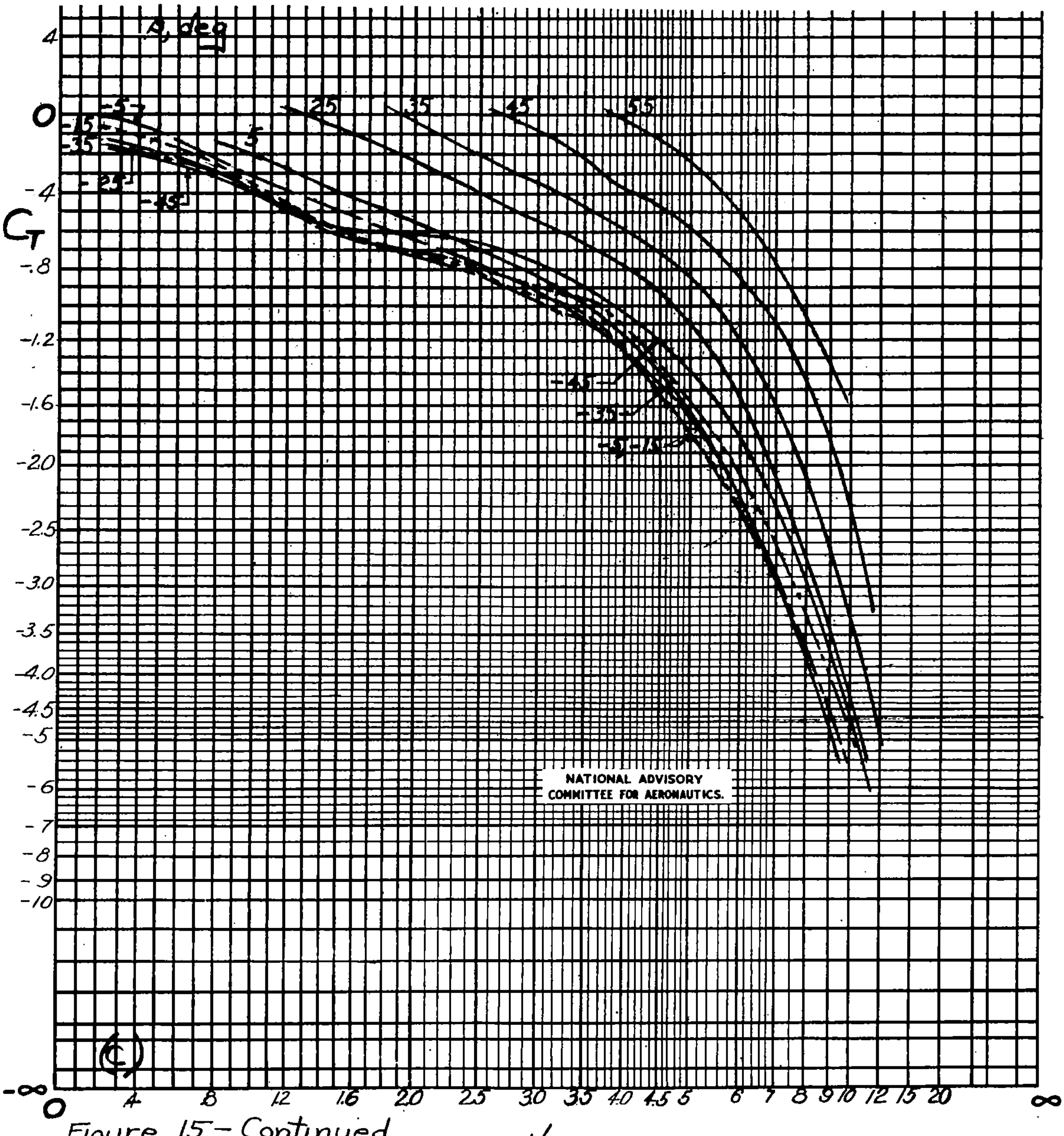

Figure 15.- Continued

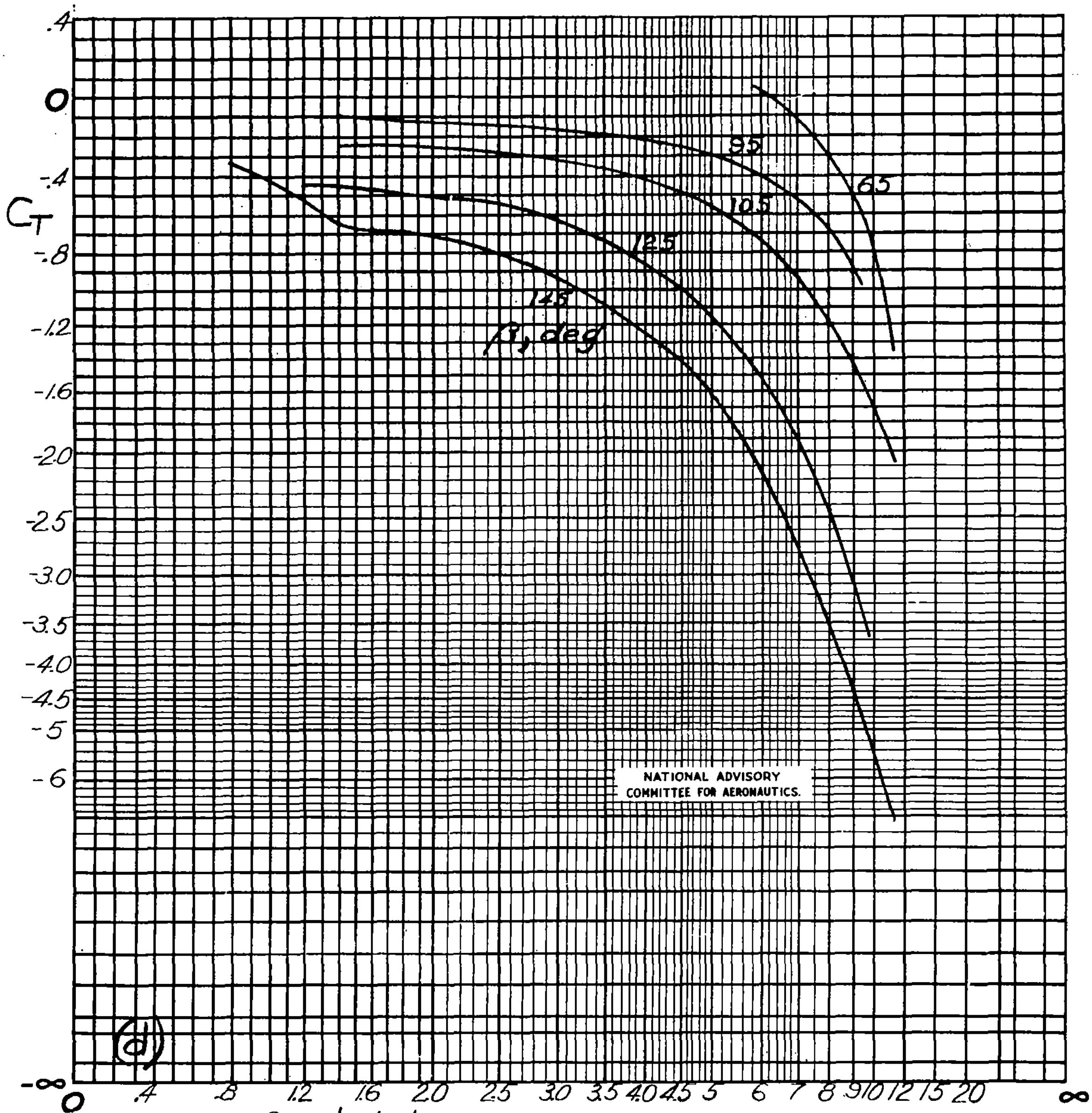

Figure 15.– Concluded

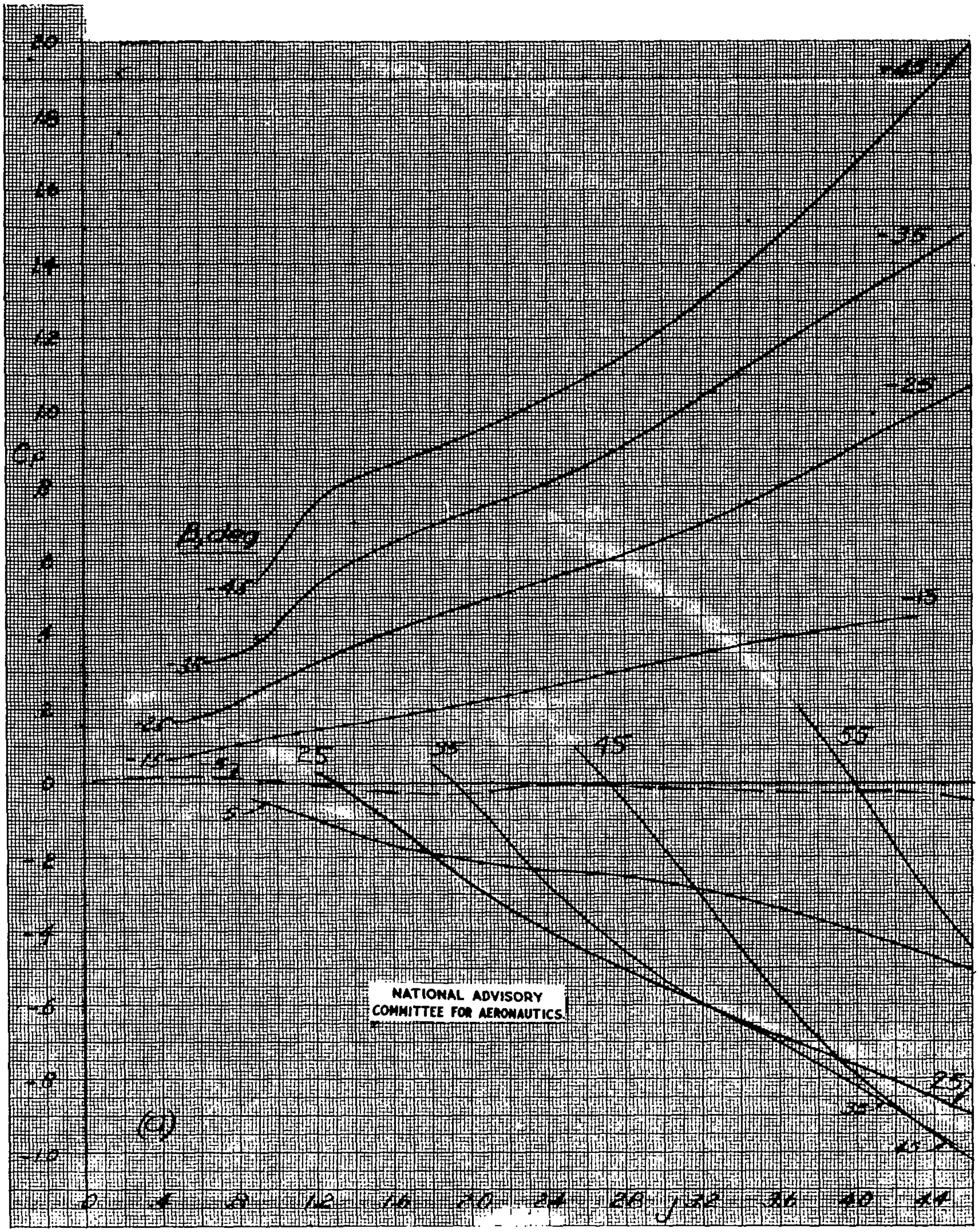

Figure 16.- Variation of power coefficient with advance ratio, three wide blades.

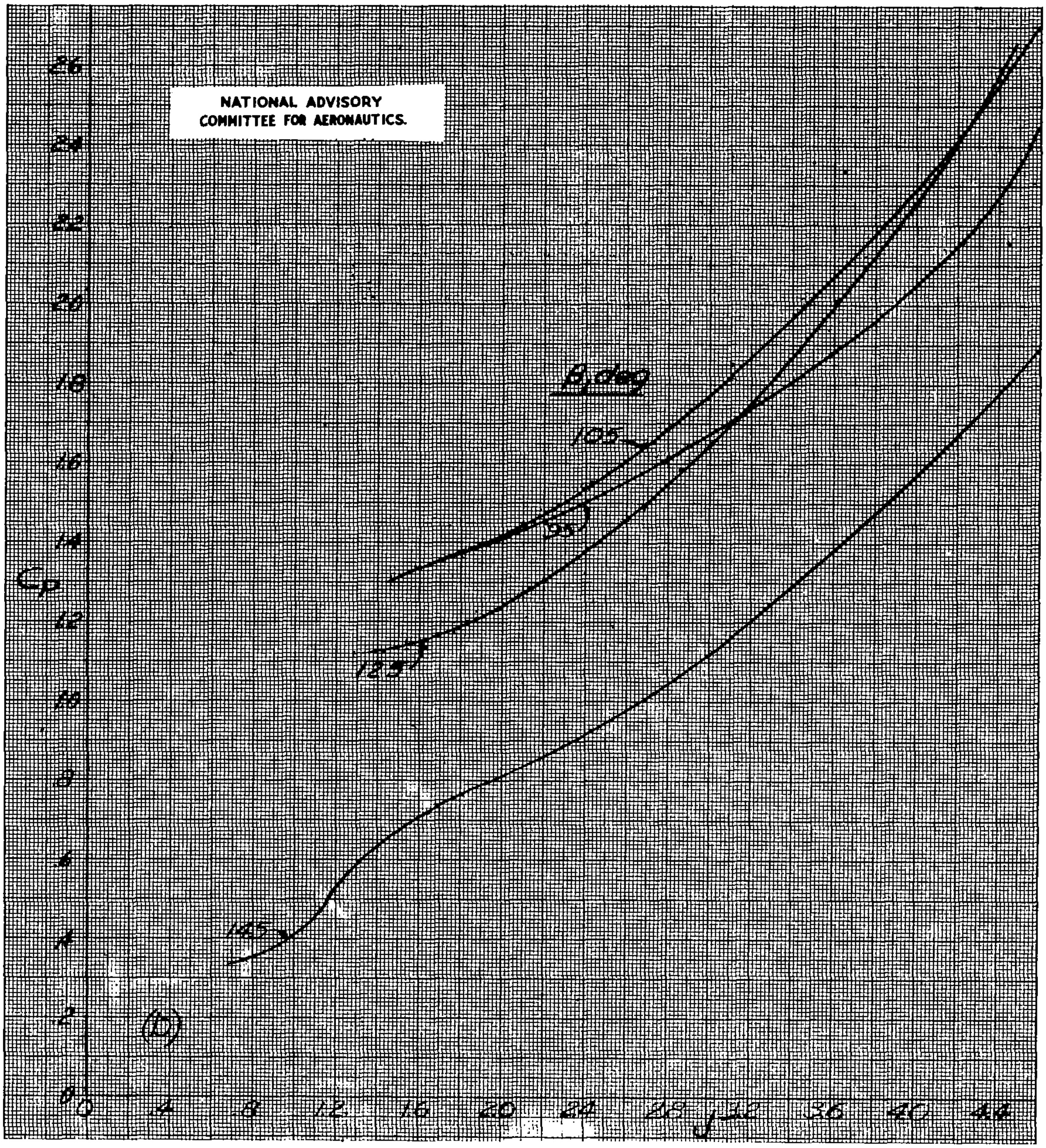

Figure 16.- Continued.

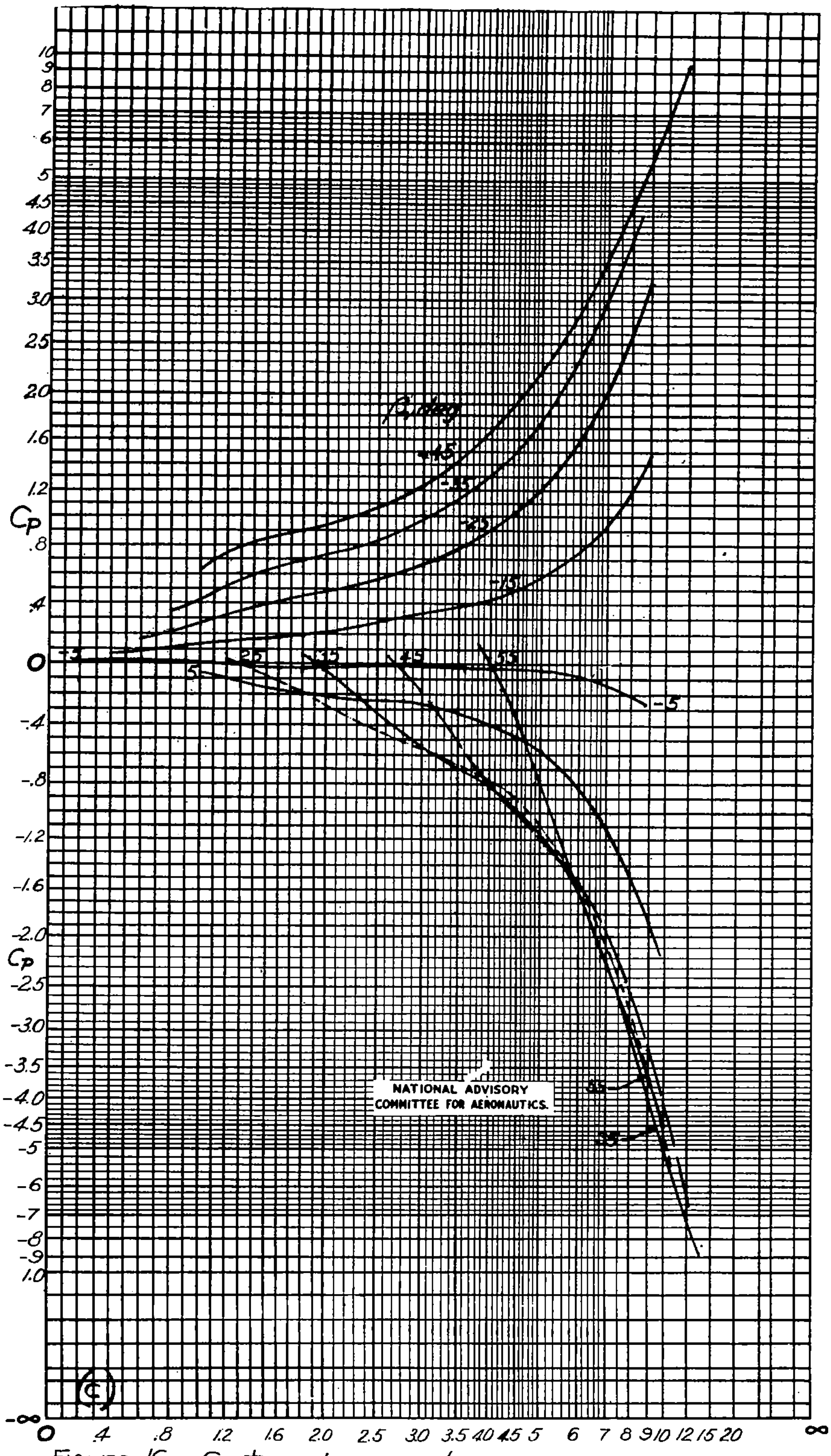

Figure 16.– Continued

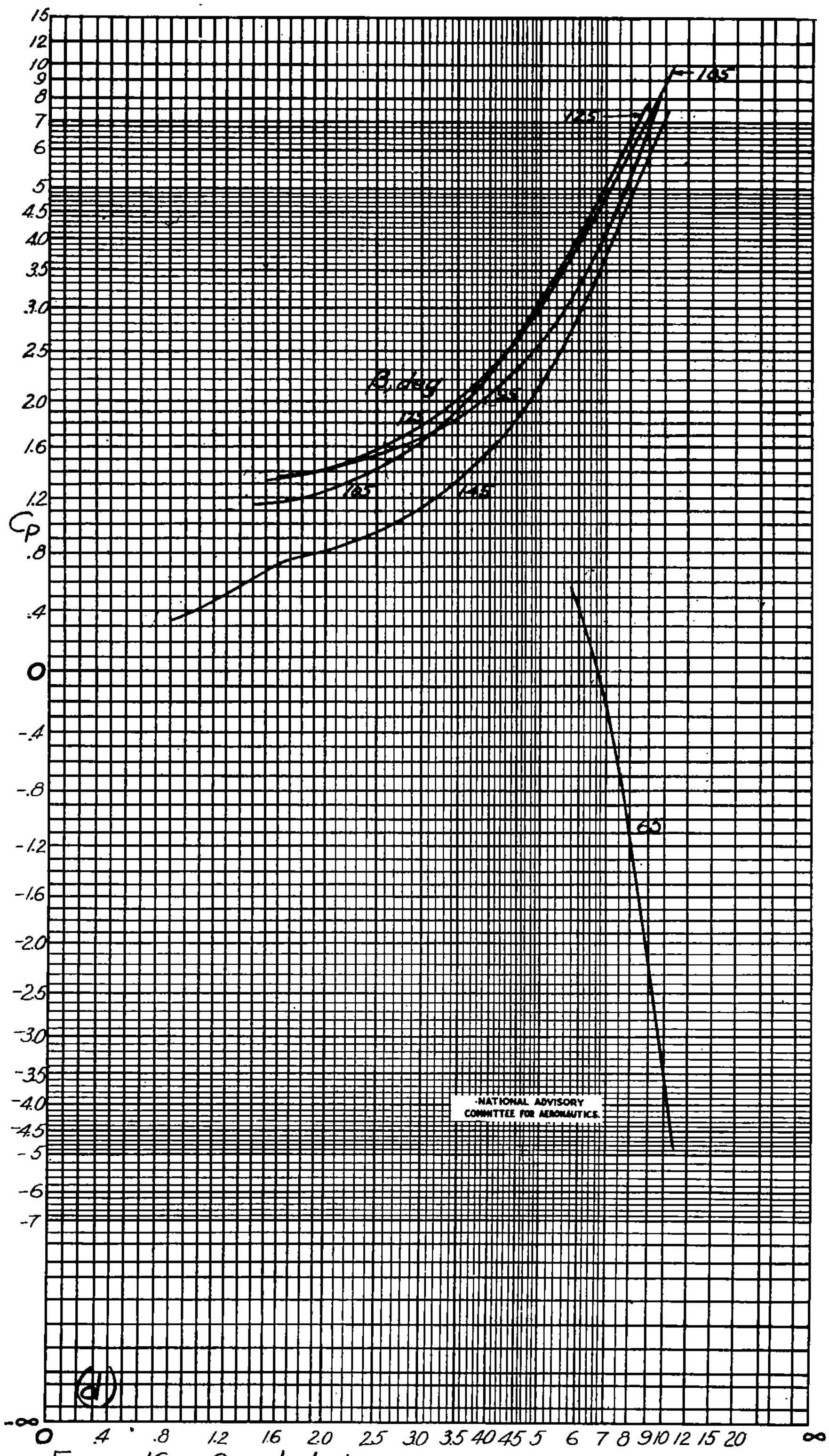

Figure 16.- Concluded

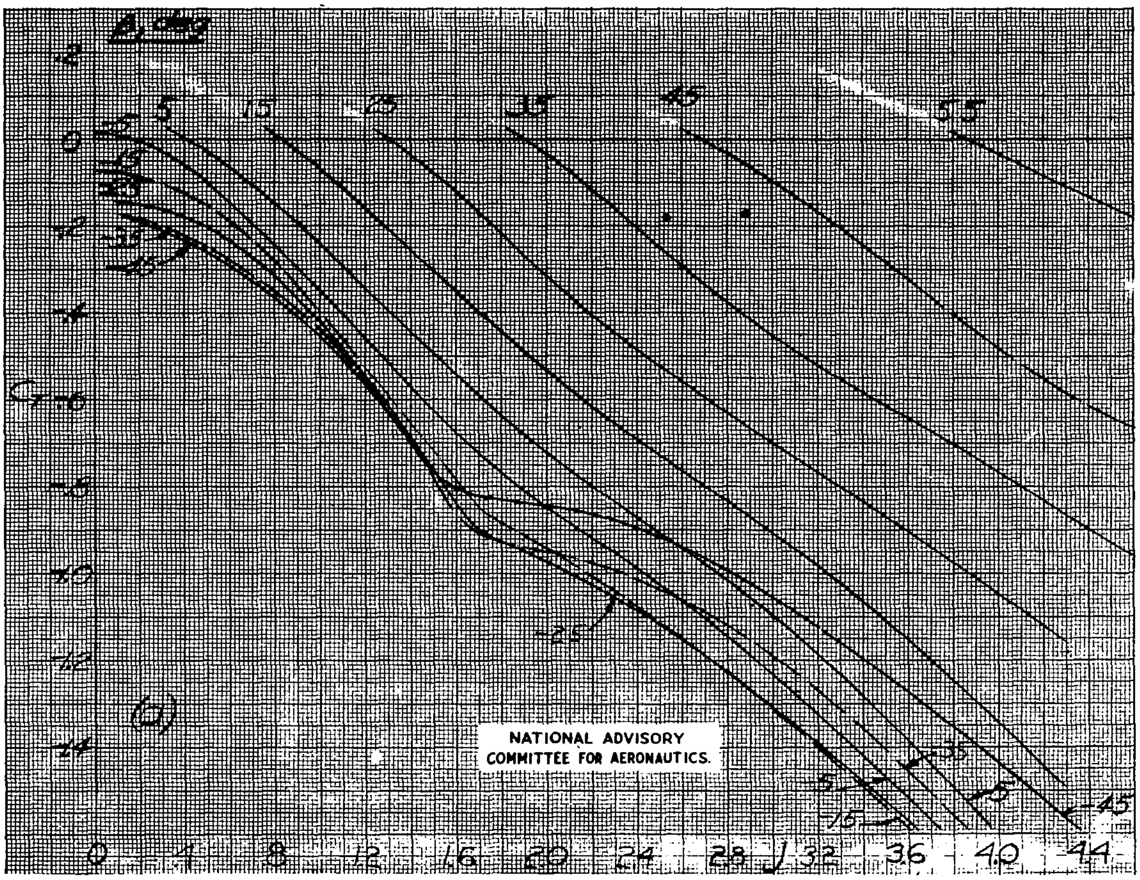

Figure 17.- Variation of thrust coefficient with advance ratio, four wide blades, single rotation.

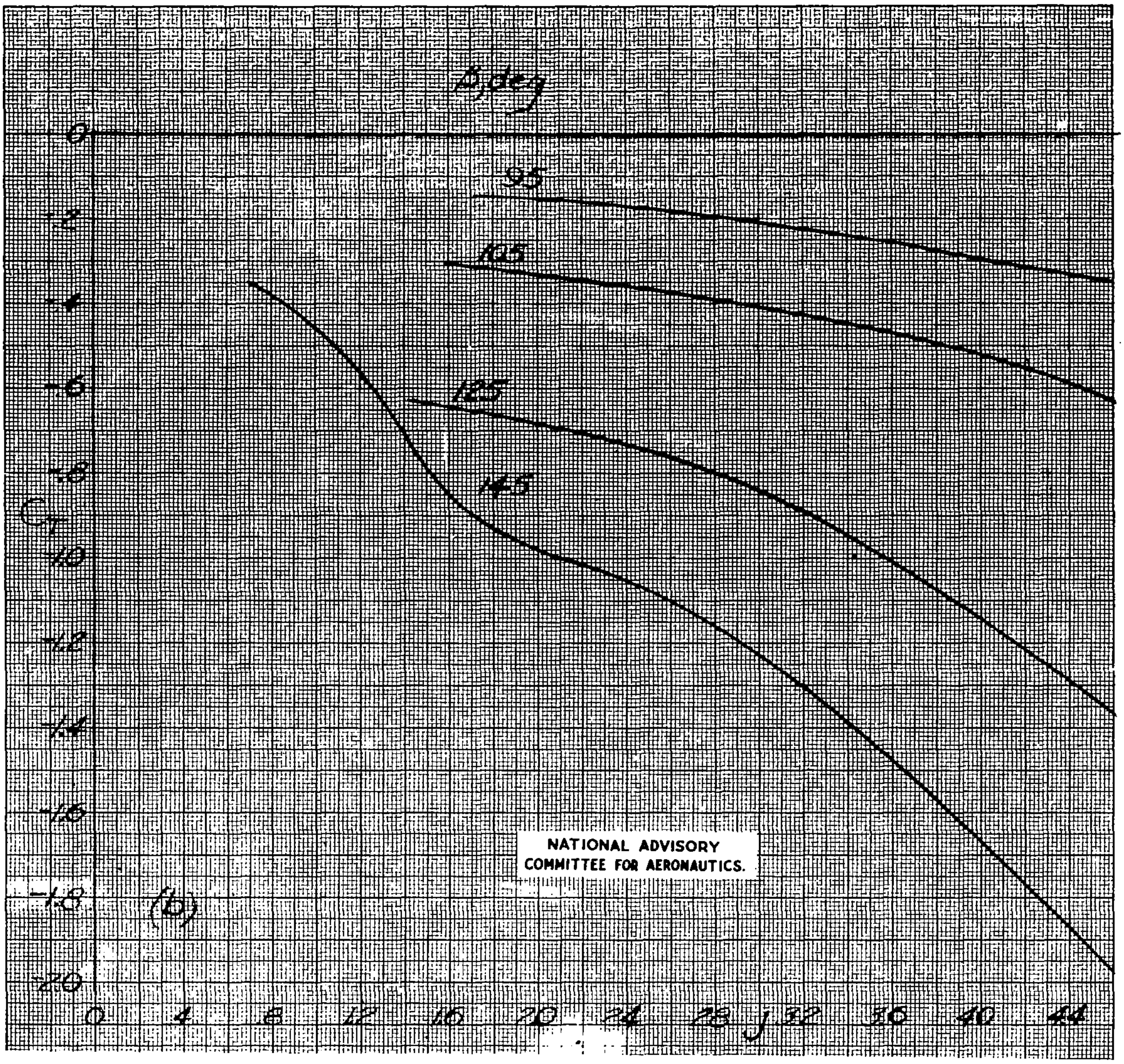

Figure 17.- Continued.

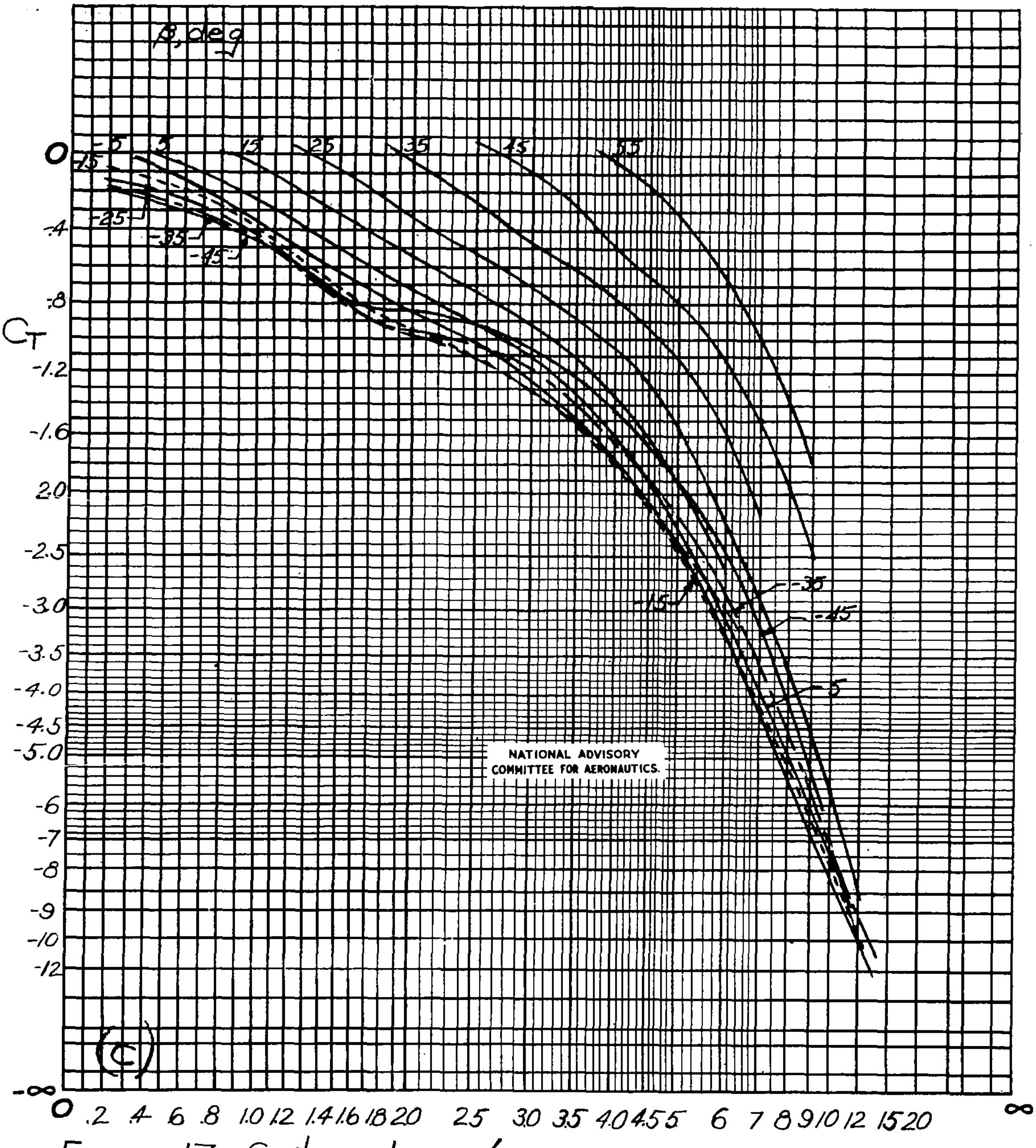

Figure 17.- Continued

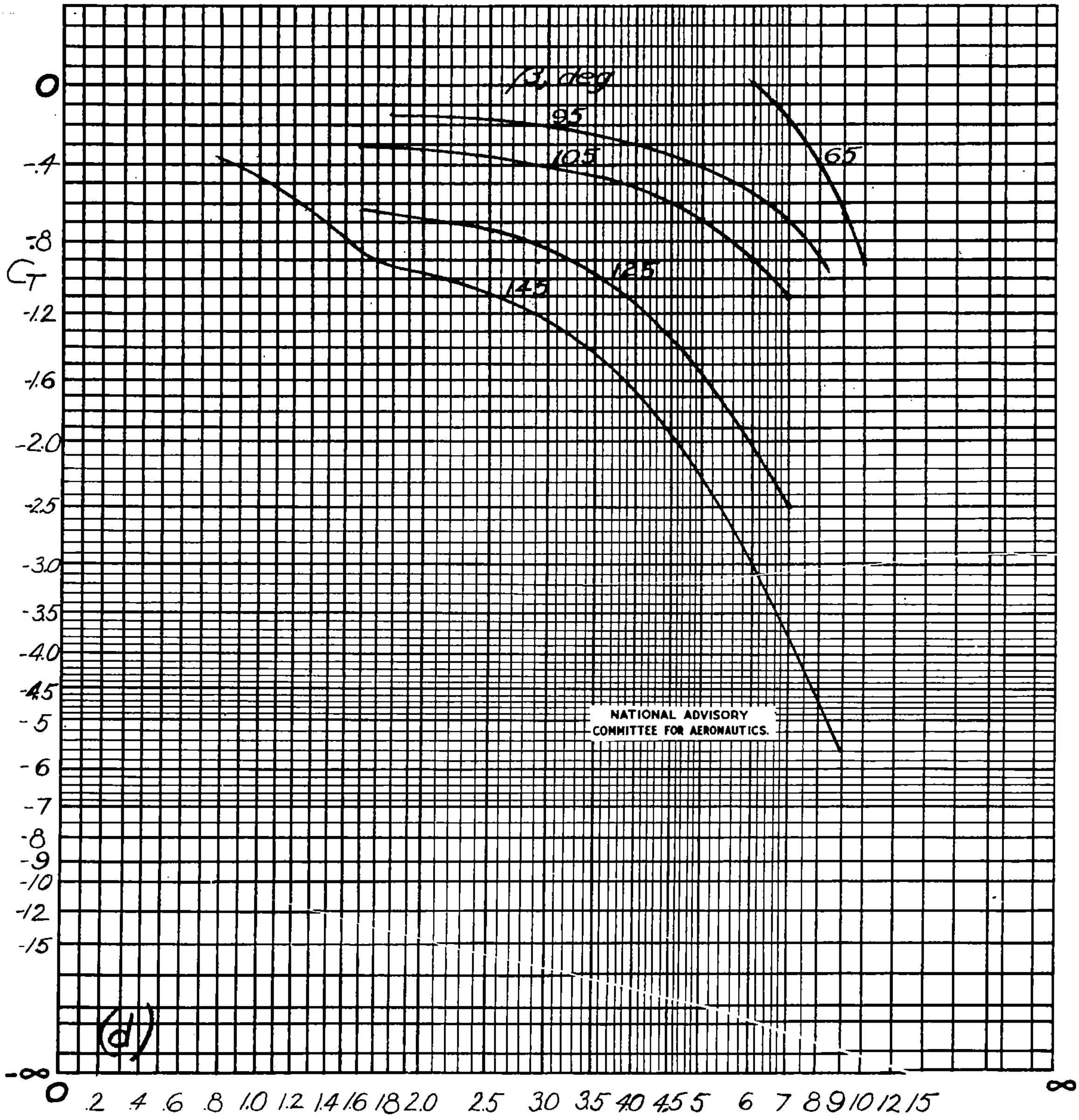

Figure 17.- Concluded

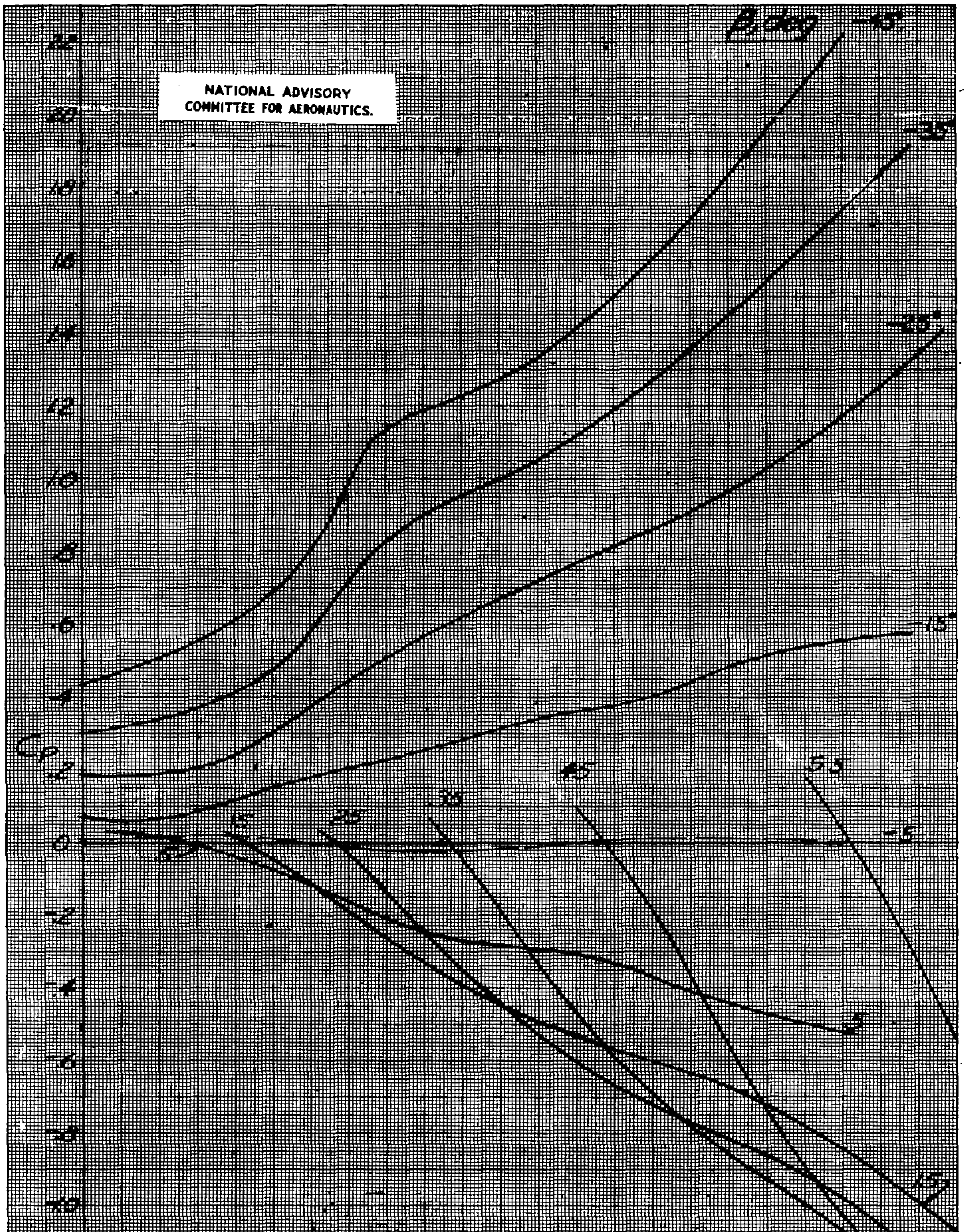

Figure 15.- Variation of power coefficient with advance ratio, four wide blades, single rotation.

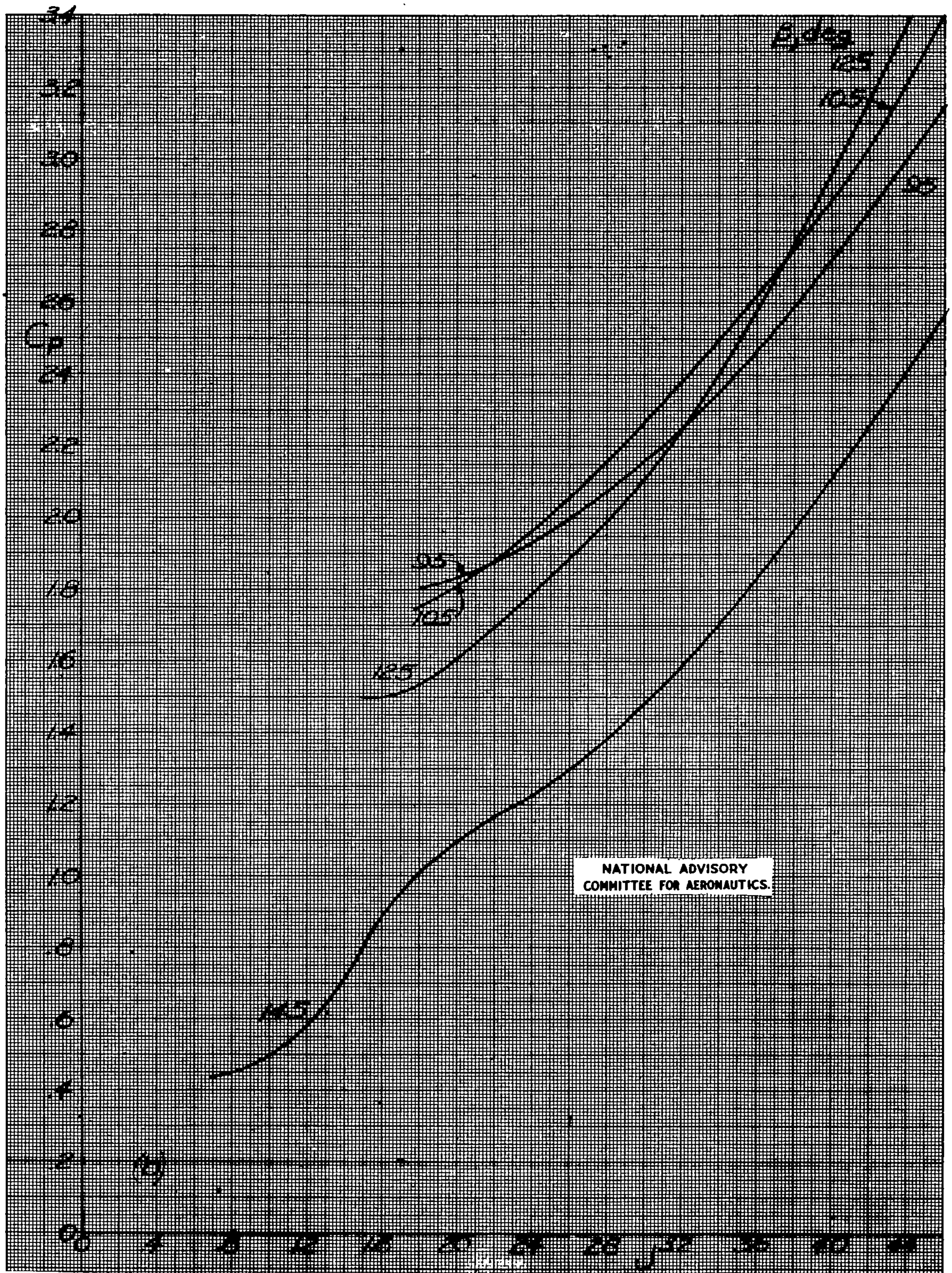

Figure 18.- Continued.

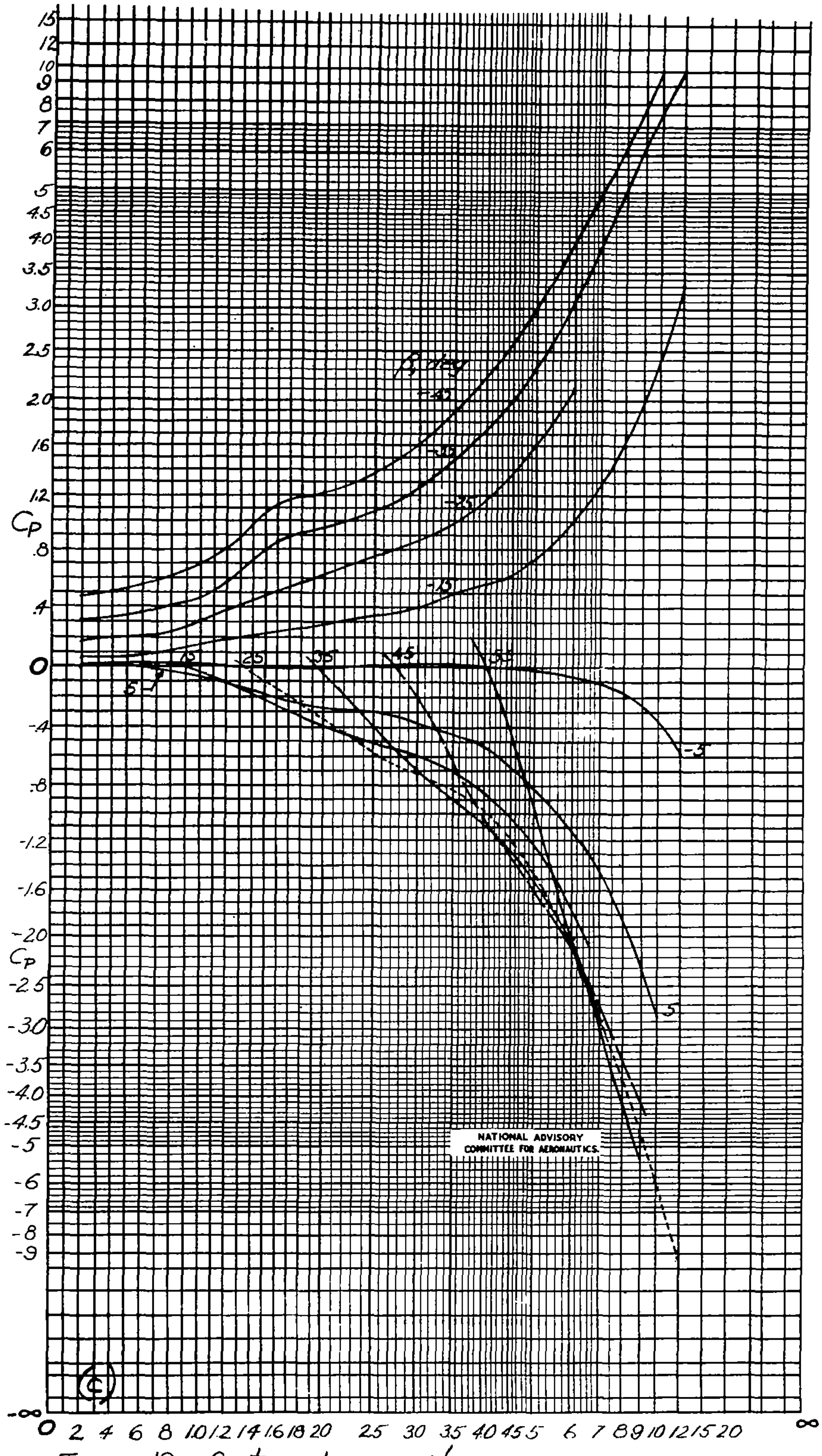

Figure 18.- Continued

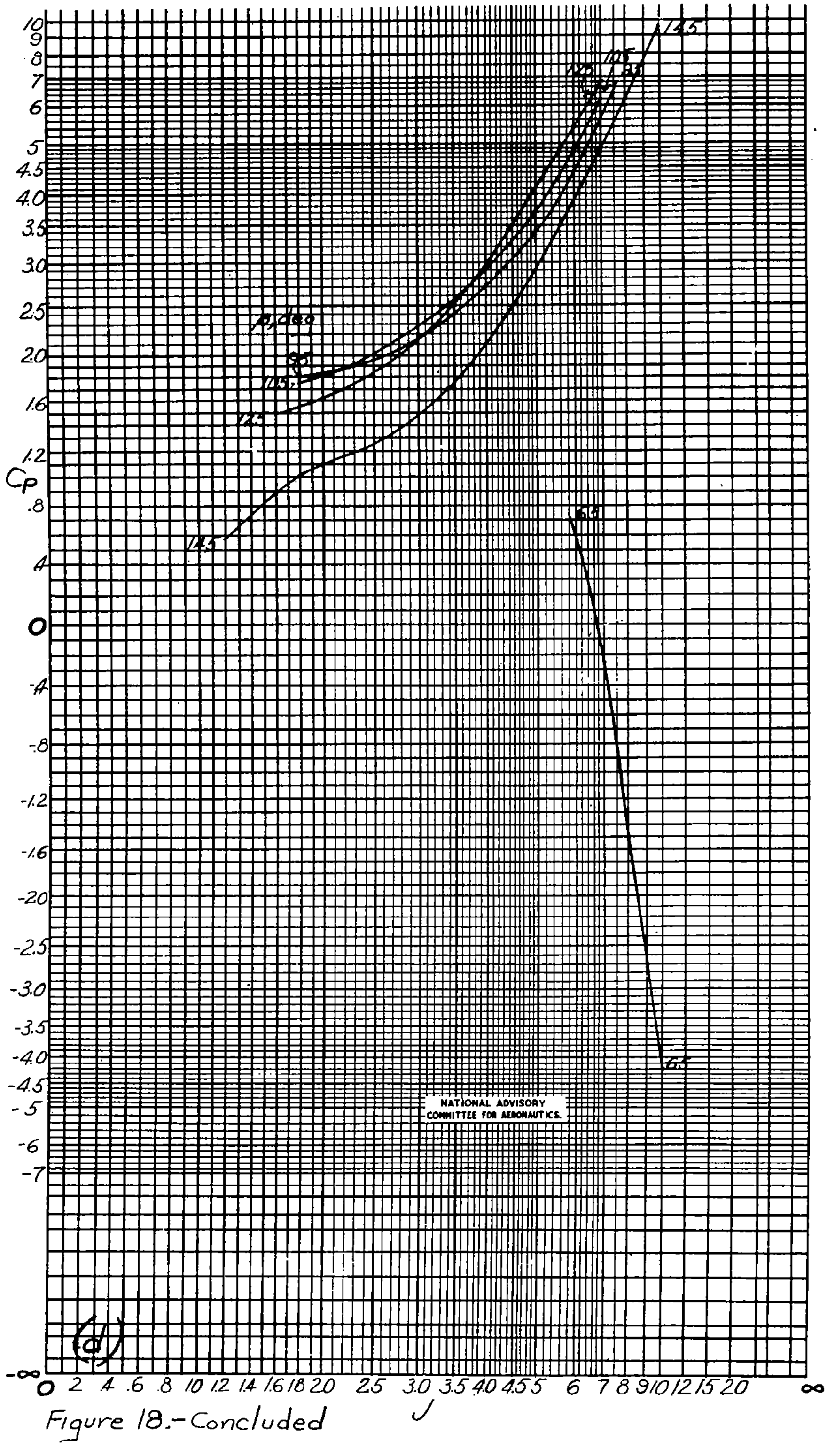

Figure 18.- Concluded

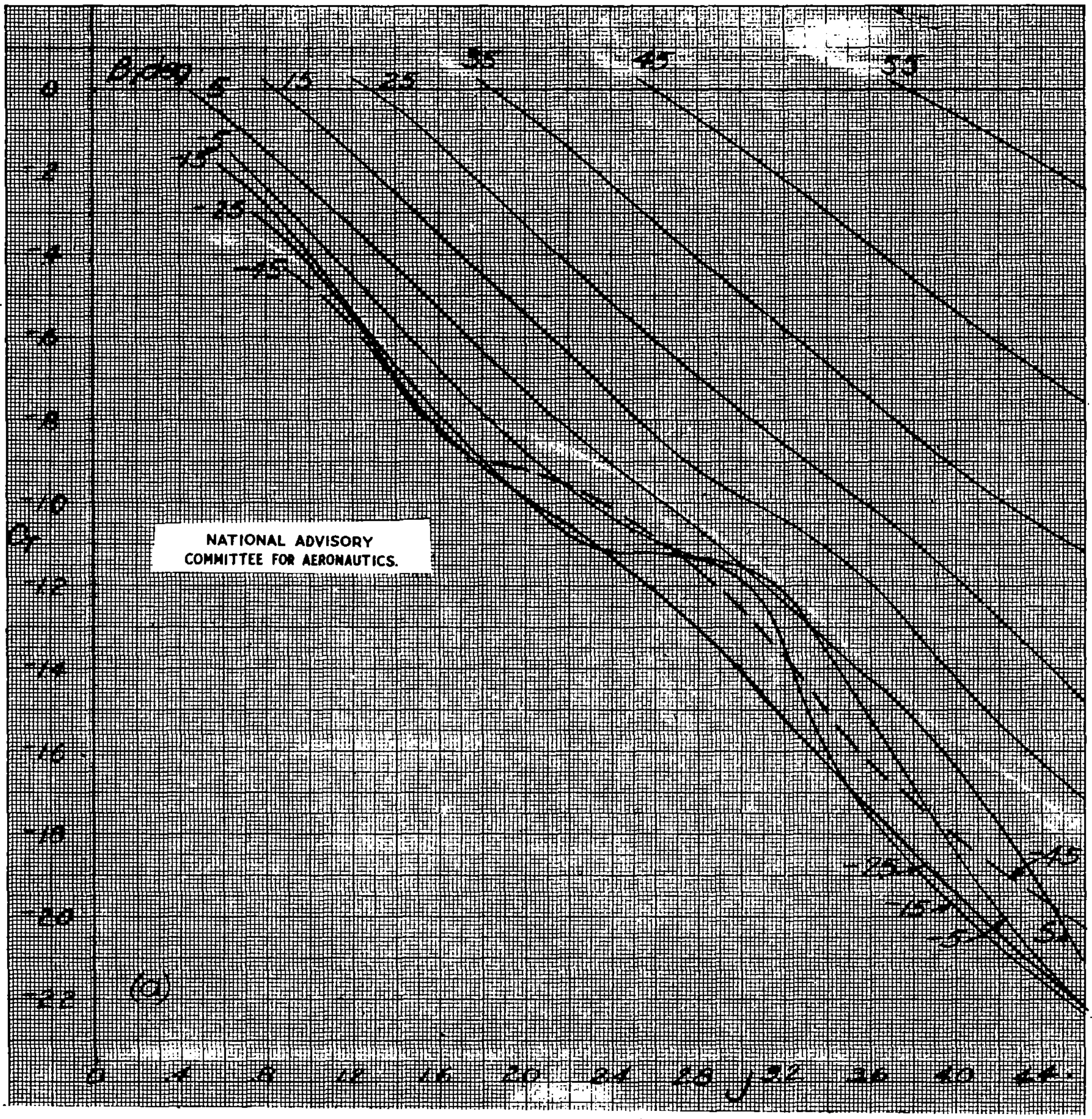

Figure 19.- Variation of thrust coefficient with advance ratio, four wide blades, dual rotation.

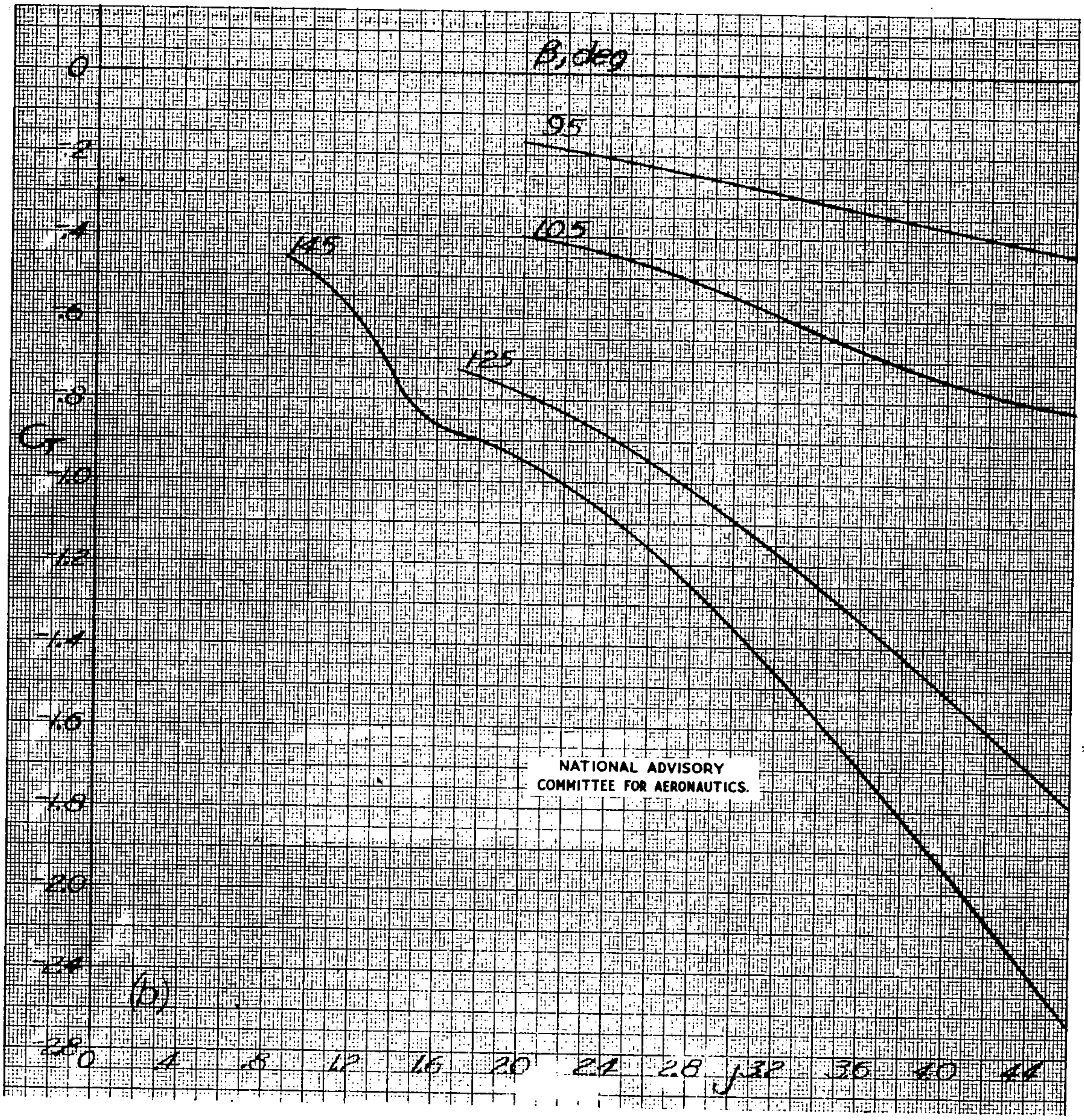

Figure 19.- Continued.

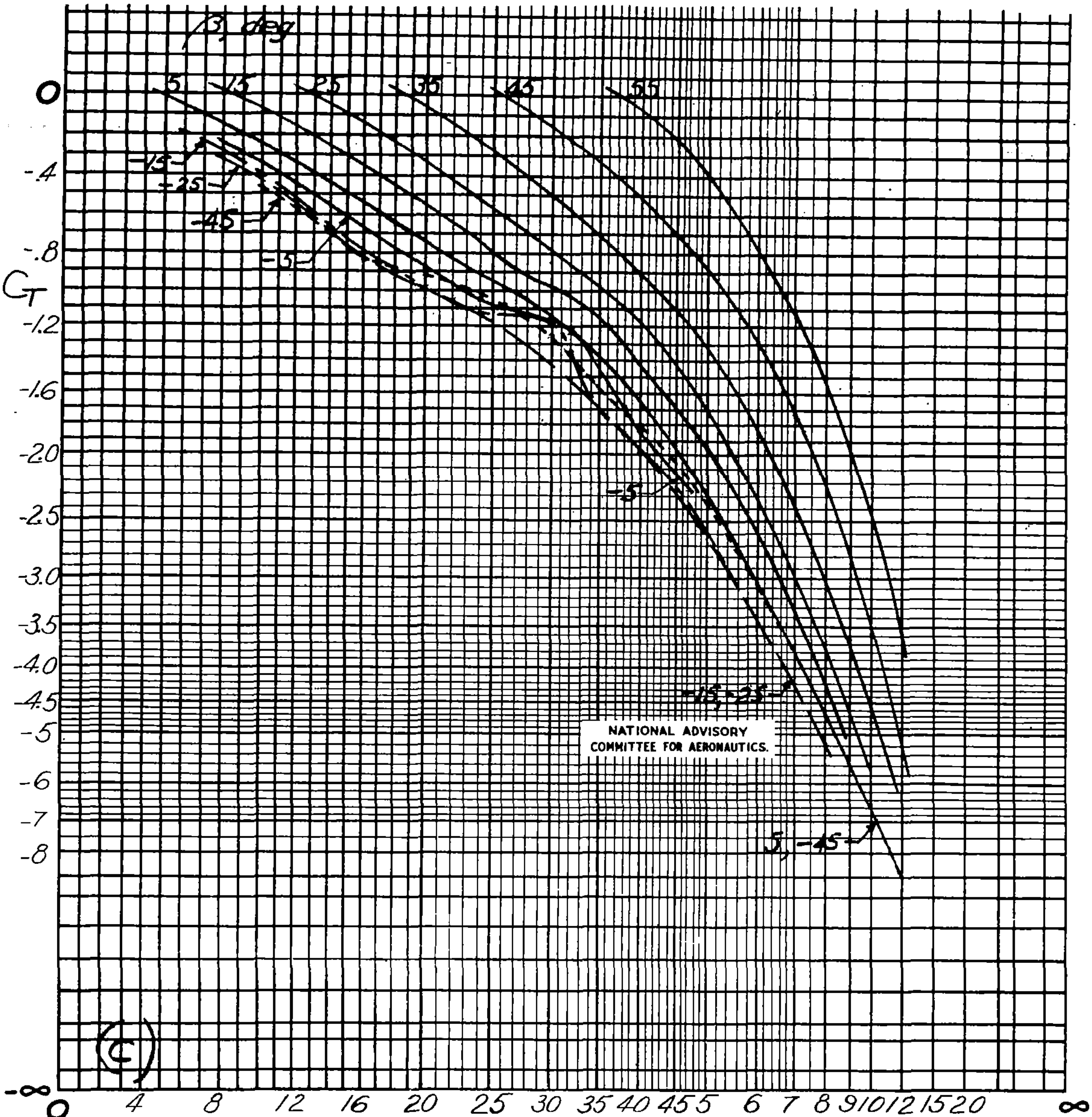

Figure 19.- Continued

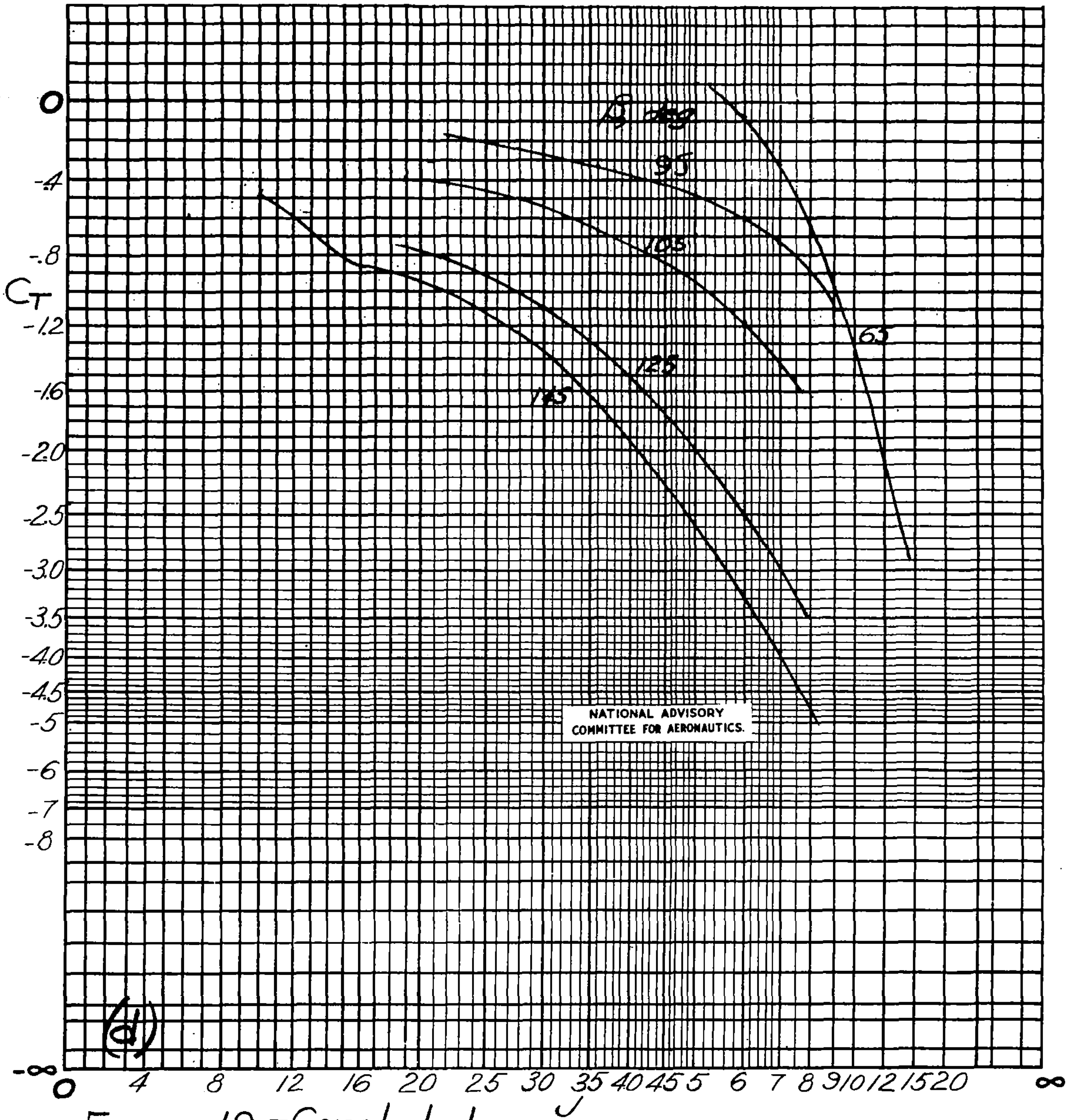

Figure 19.–Concluded

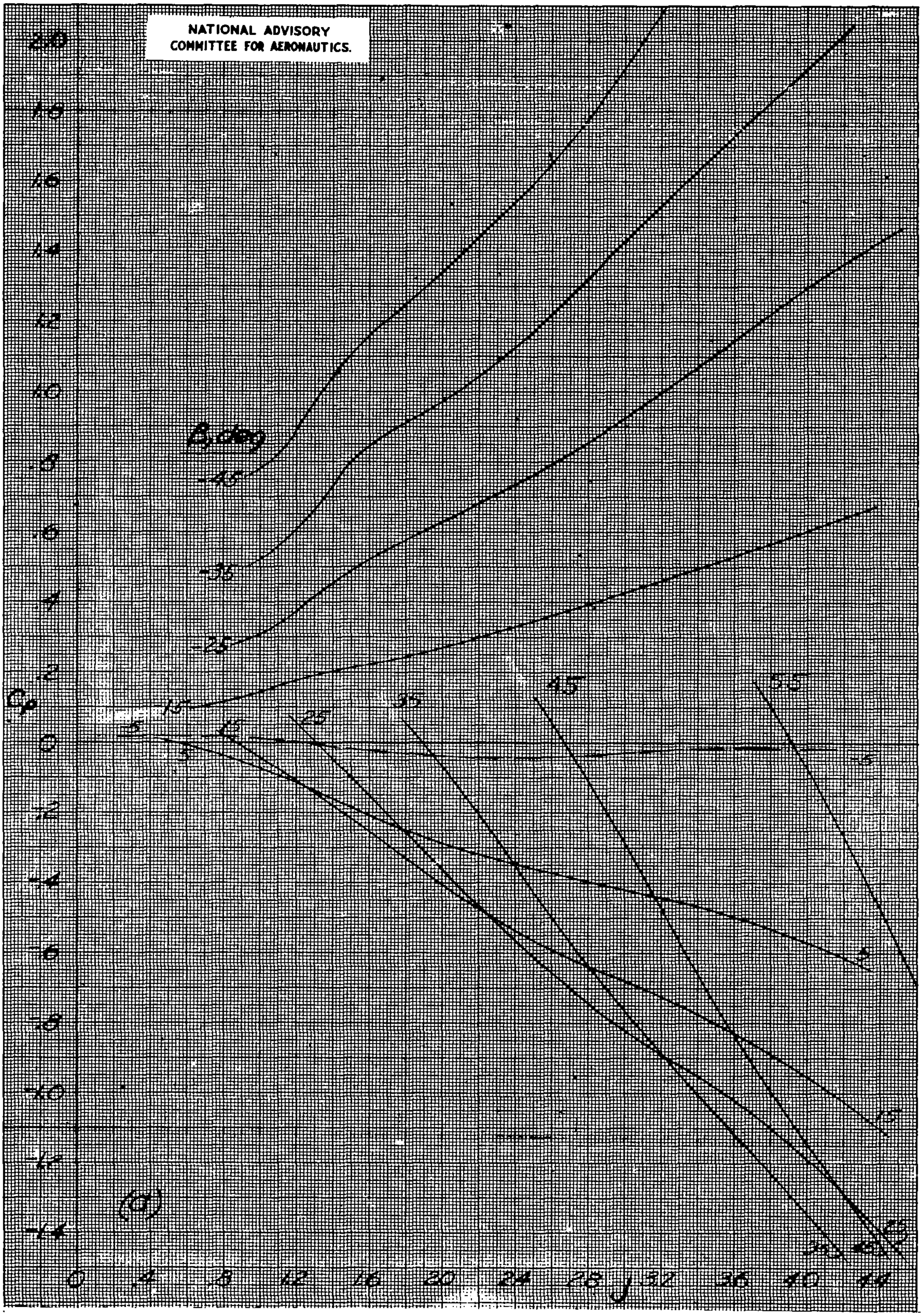

Figure 20.- Variation of power coefficient with advance ratio, four wide blades, dual rotation.

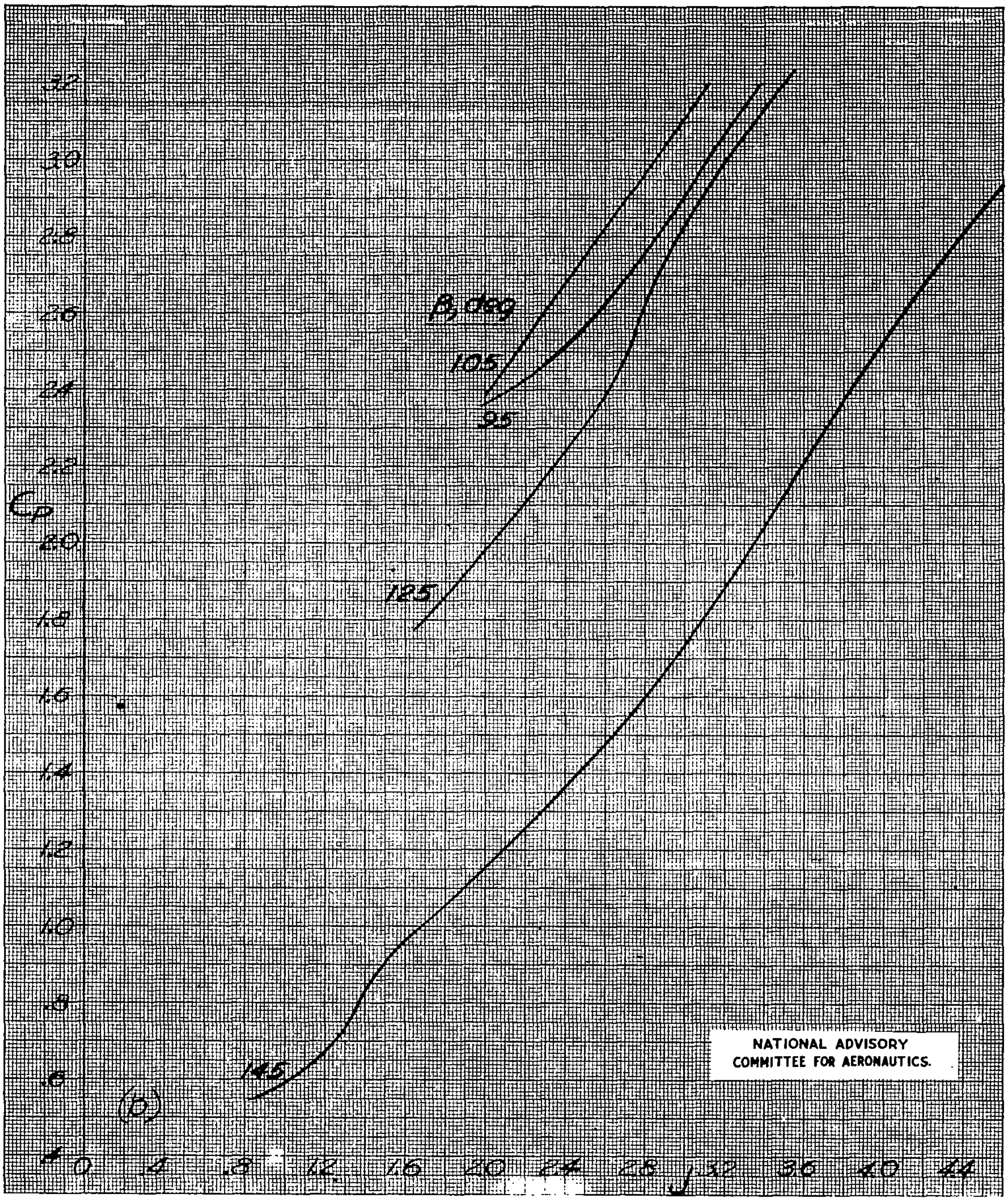

Figure 20.- Continued.

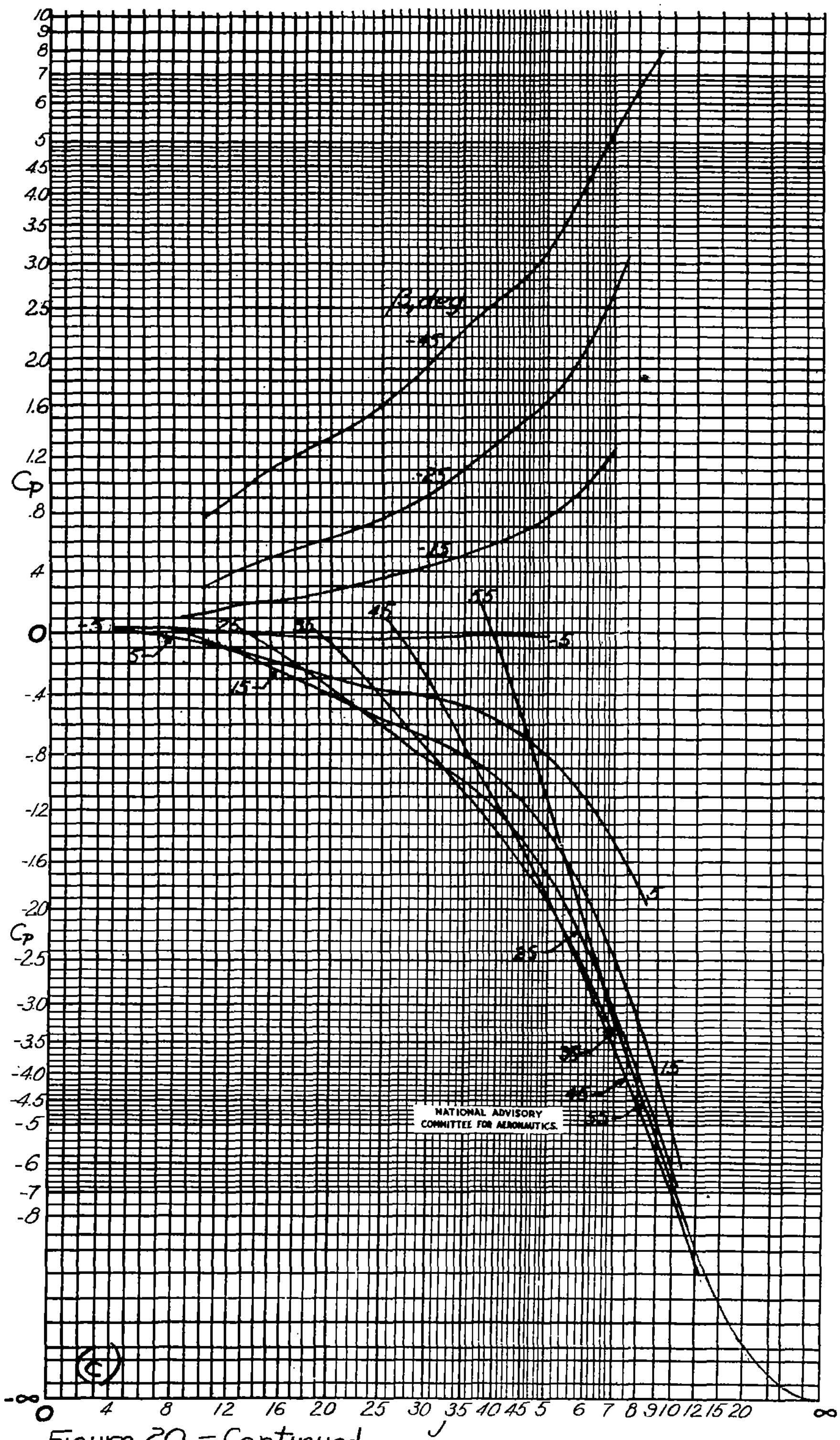

Figure 20.- Continued

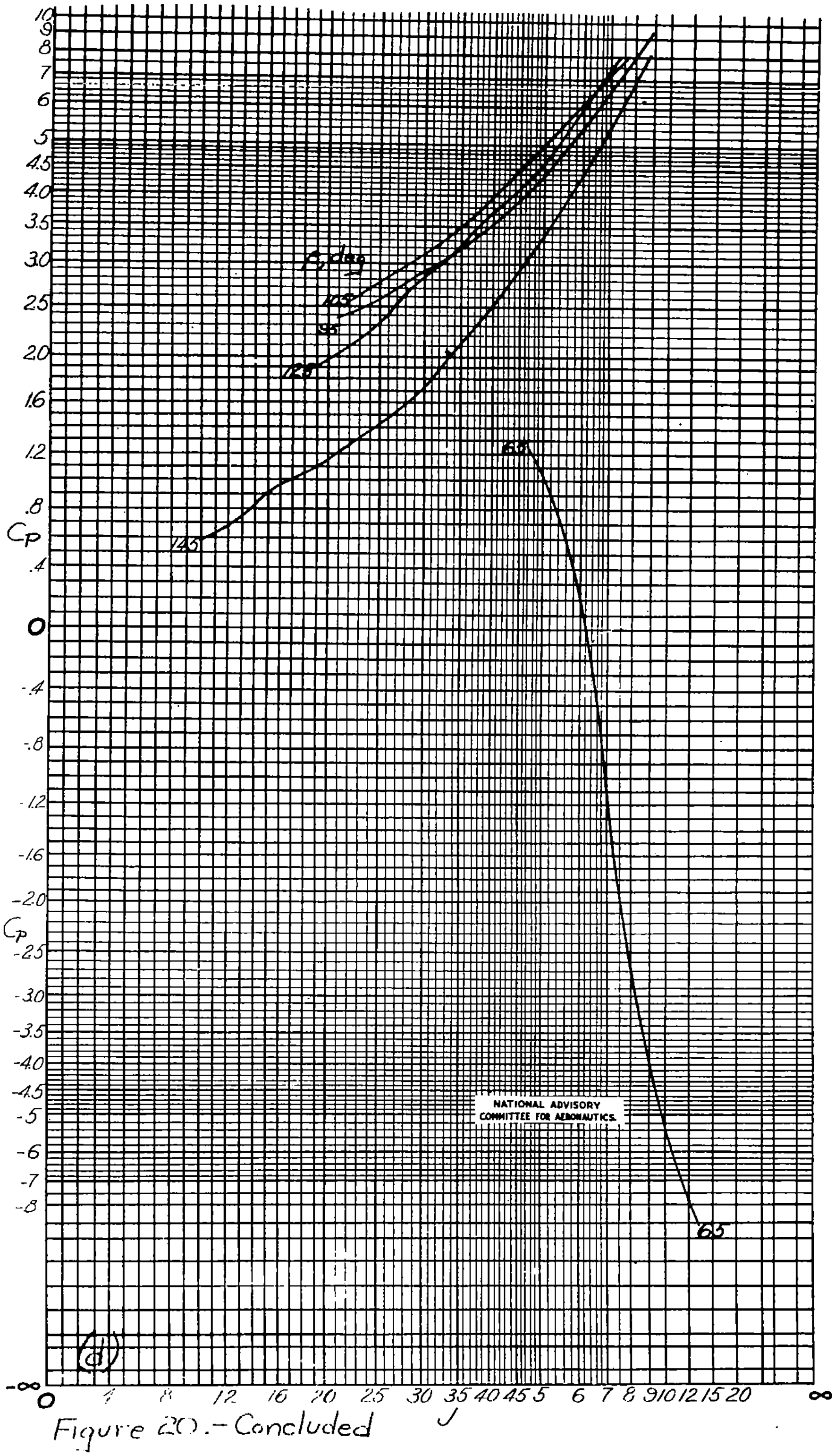

Figure 20.- Concluded

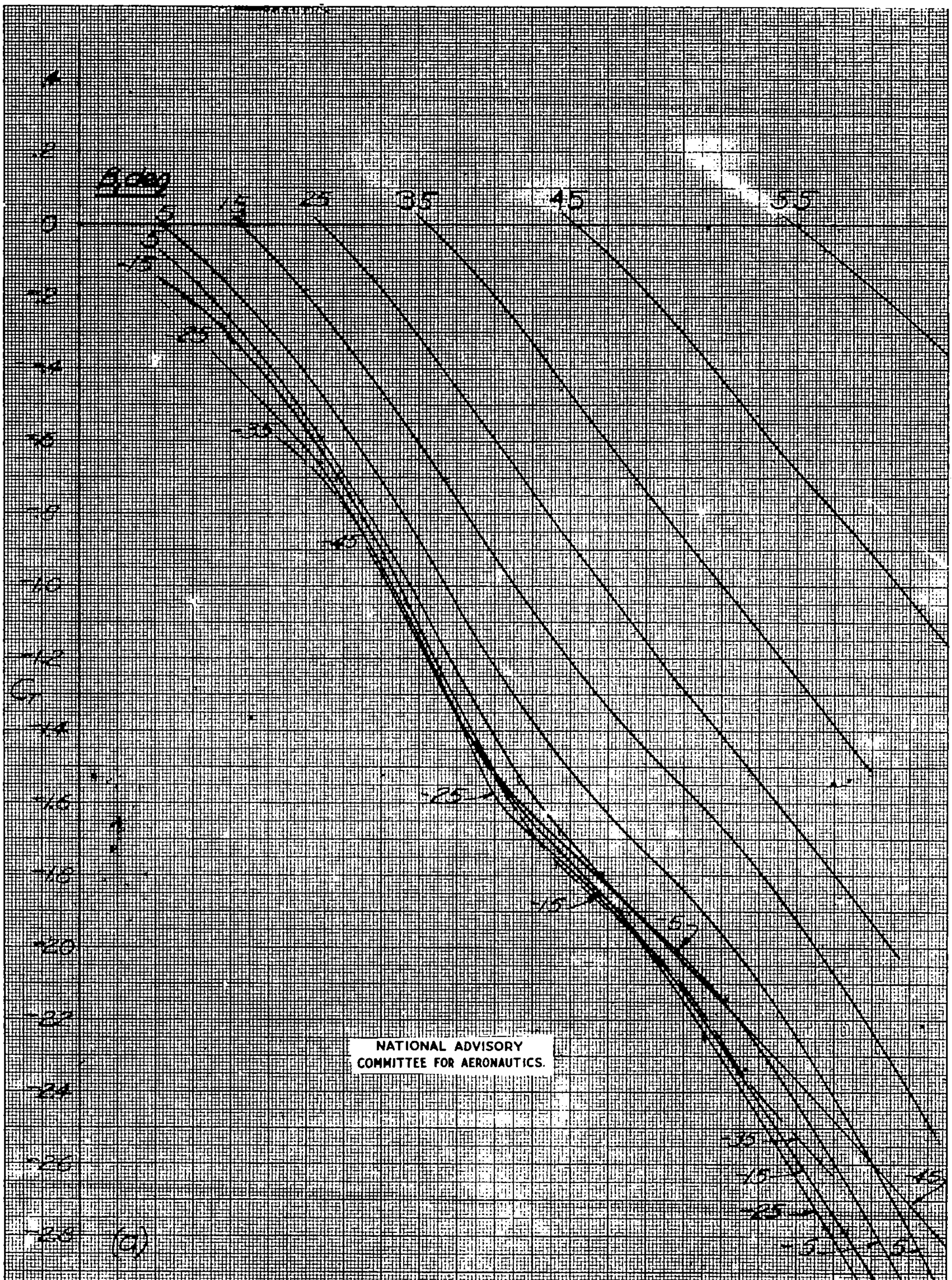

Figure 21.- Variation of thrust coefficient with advance ratio, six wide blades, dual rotation.

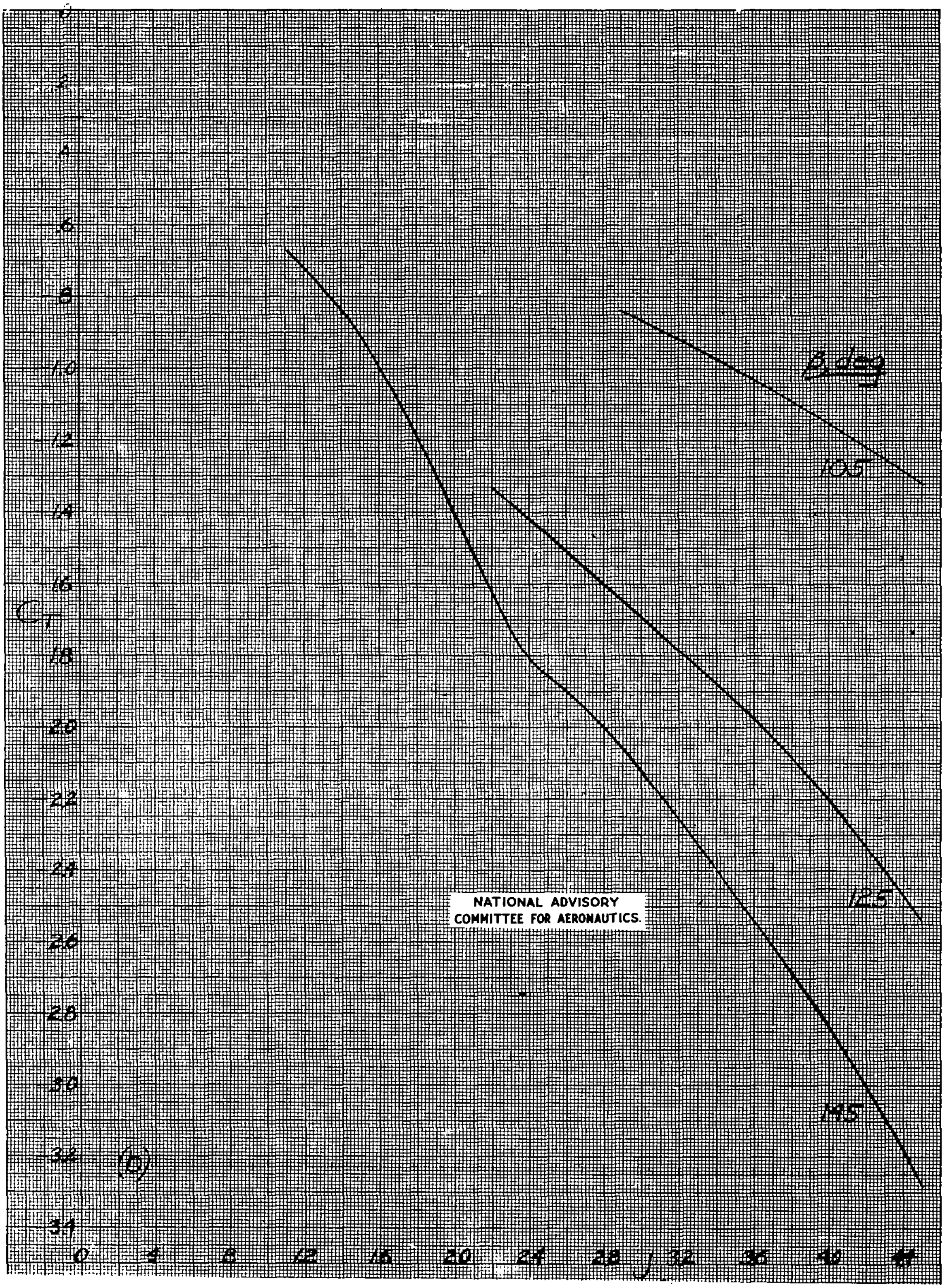

Figure 21.- Continued.

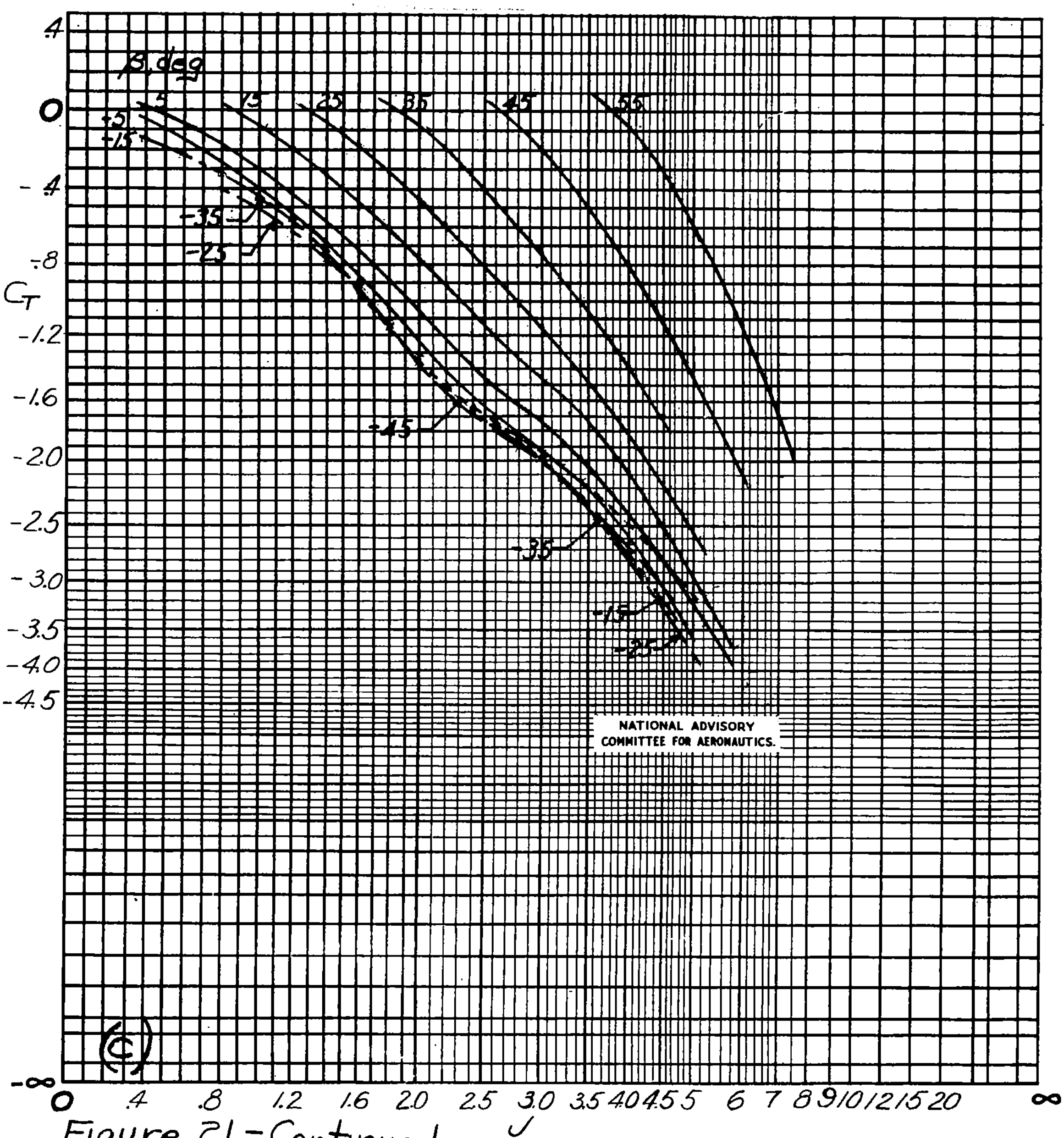

Figure 21.- Continued

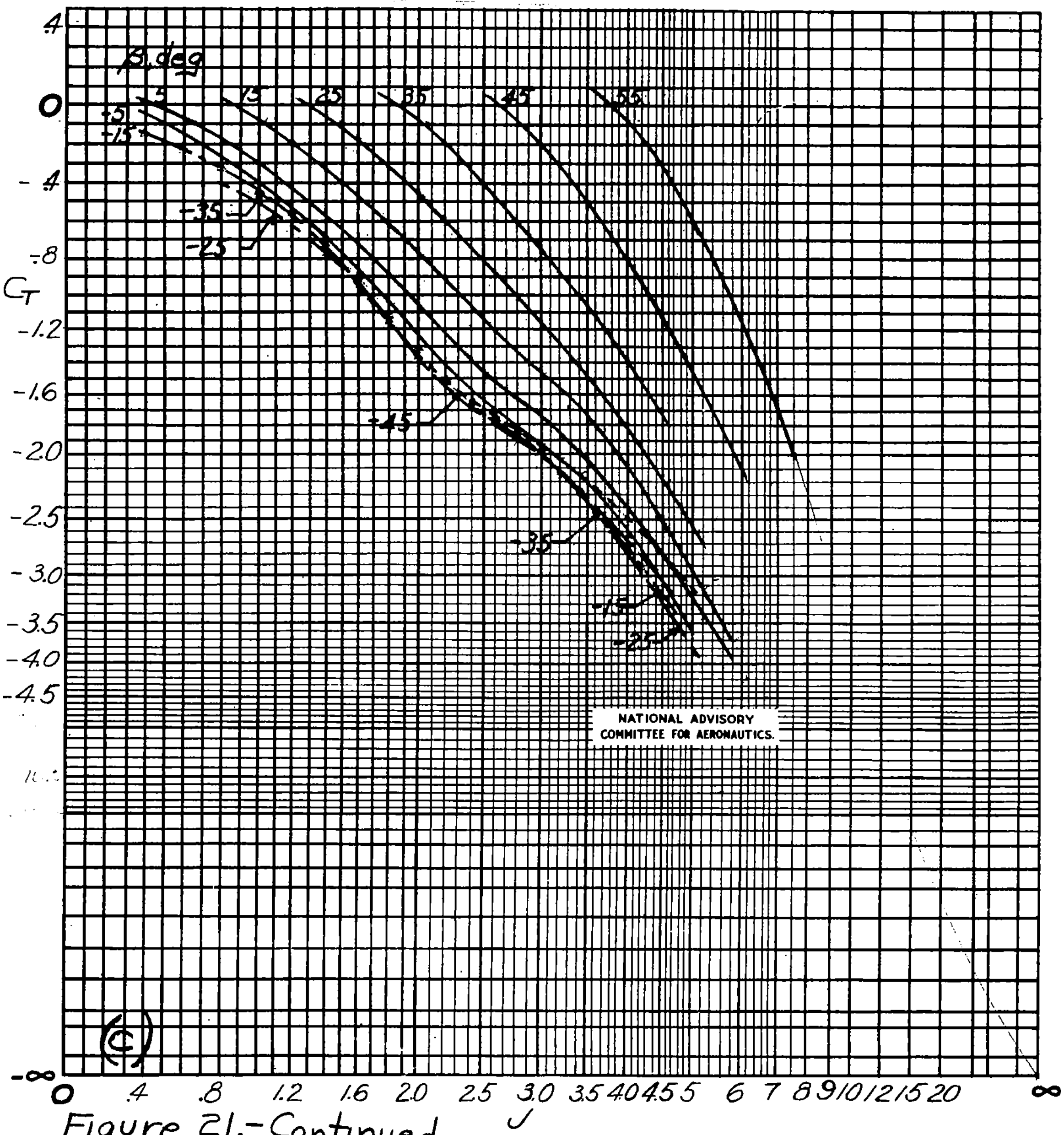

Figure 21.- Continued

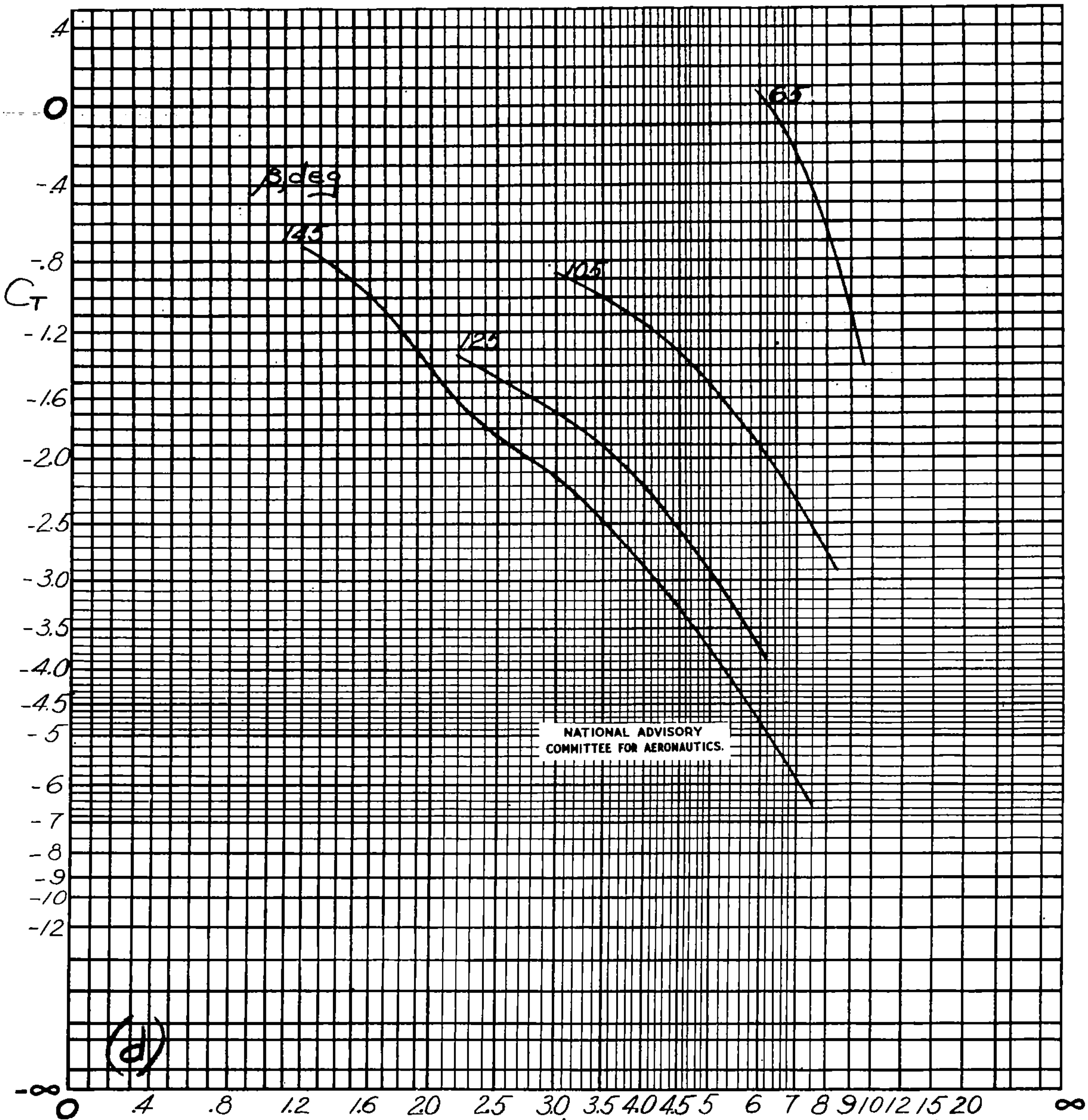

Figure 21.- Concluded

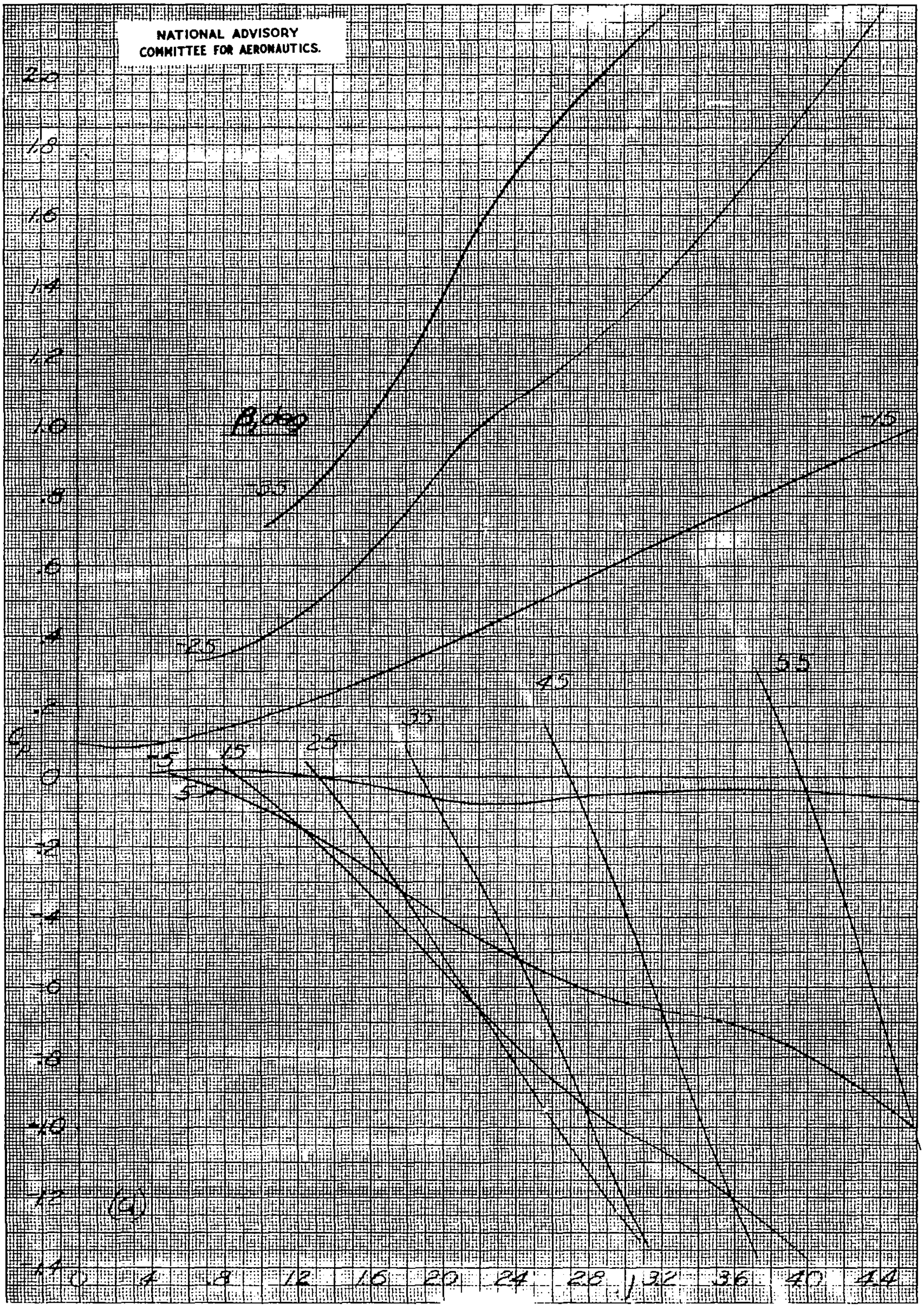

Figure 22.- Variation of power coefficient with advance ratio, six wide blades, dual rotation.

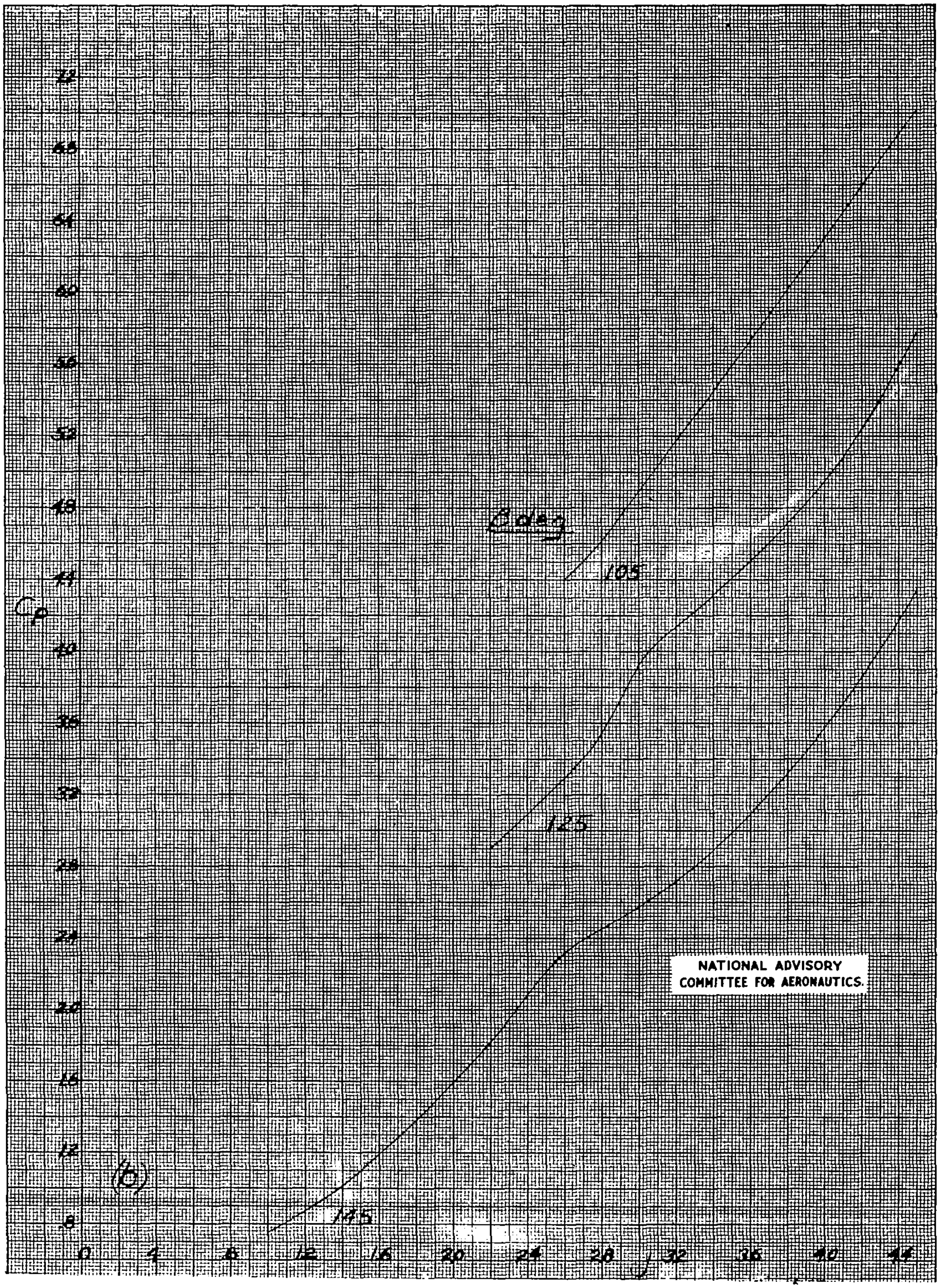

Figure 22.- Continued.

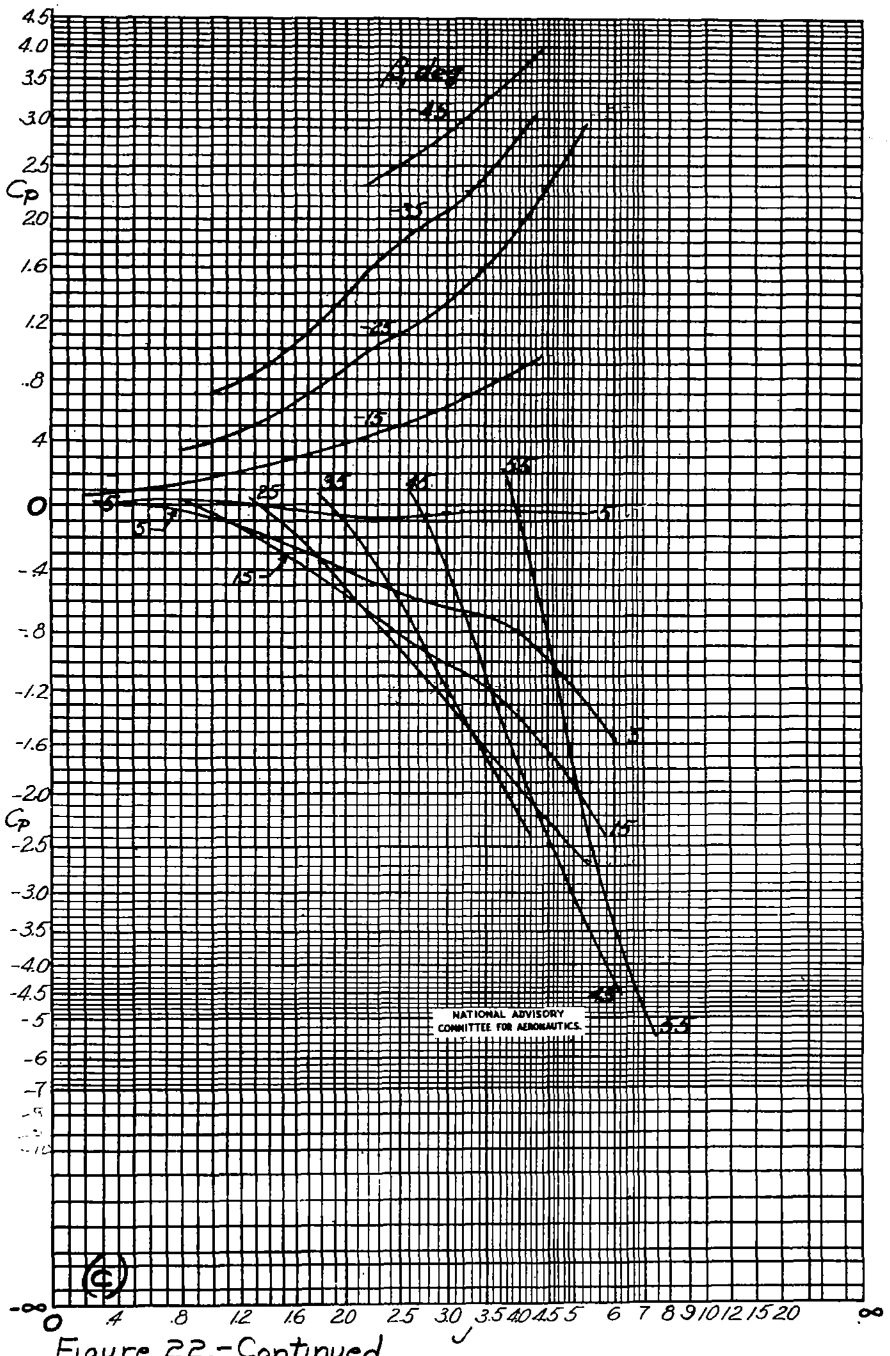

Figure 22.- Continued

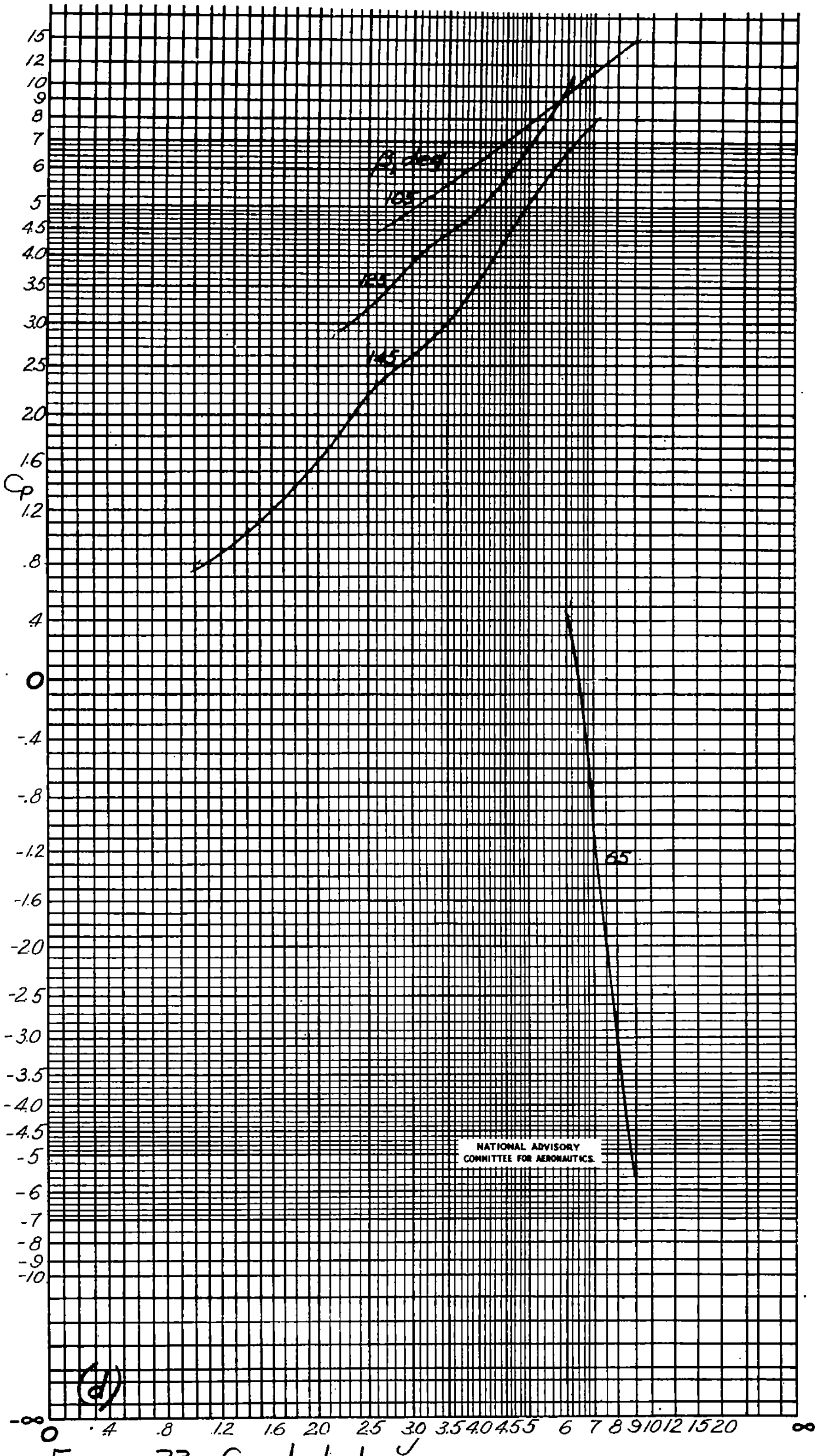

Figure 22.-Concluded

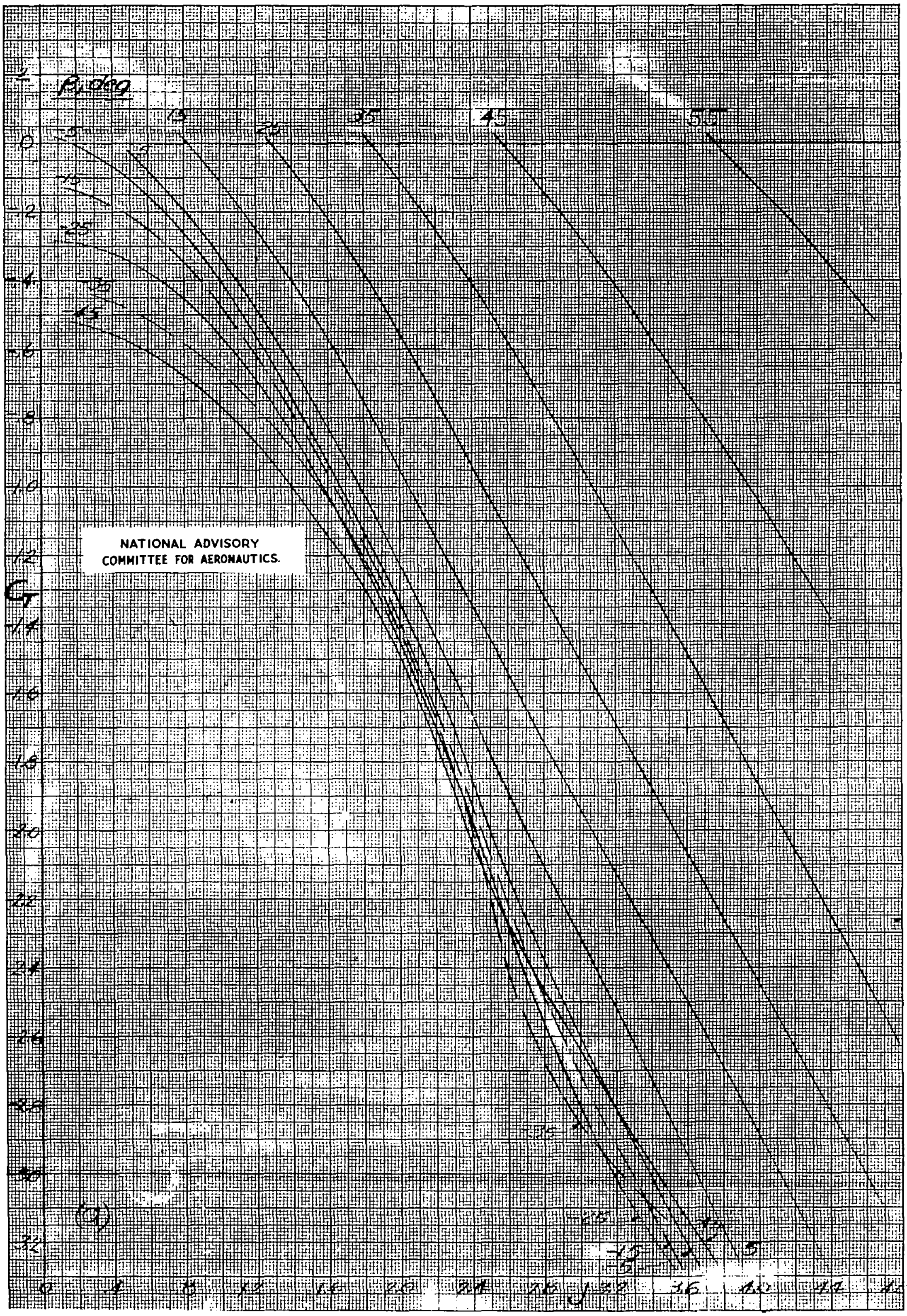

Figure 23.- Variation of thrust coefficient with advance ratio, eight wide blades, dual rotation.

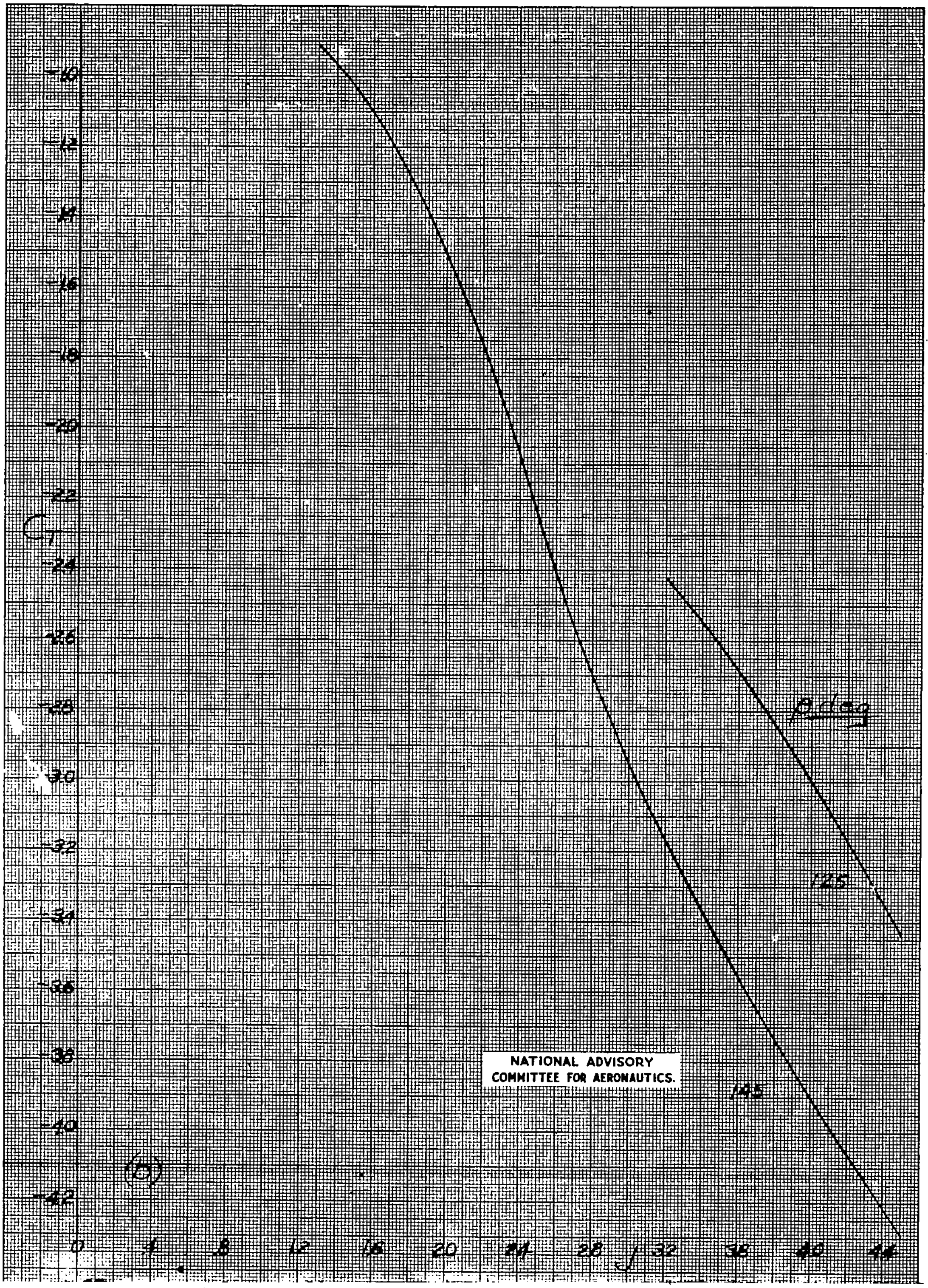

Figure 23.- Continued.

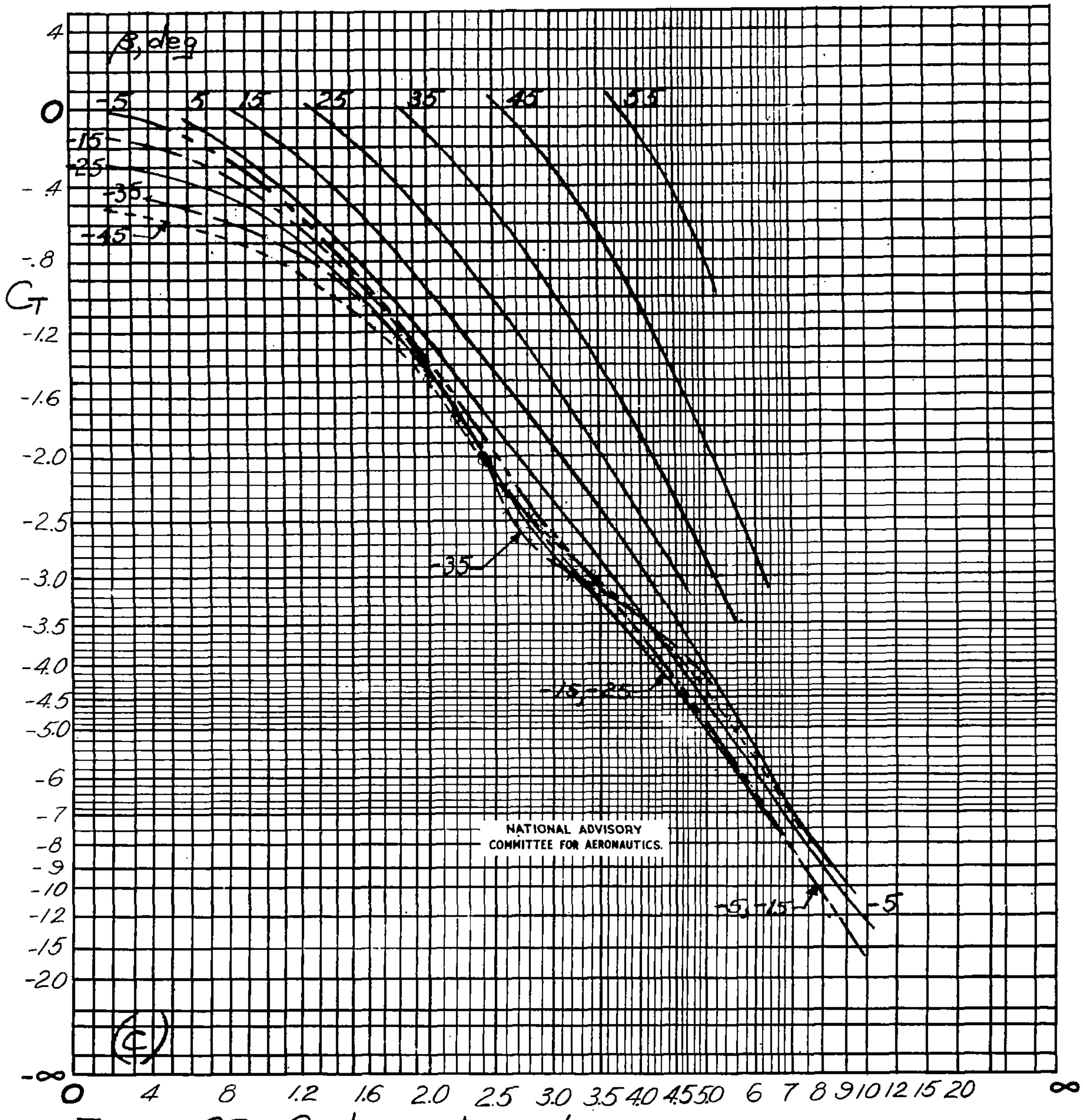

Figure 23.- Continued

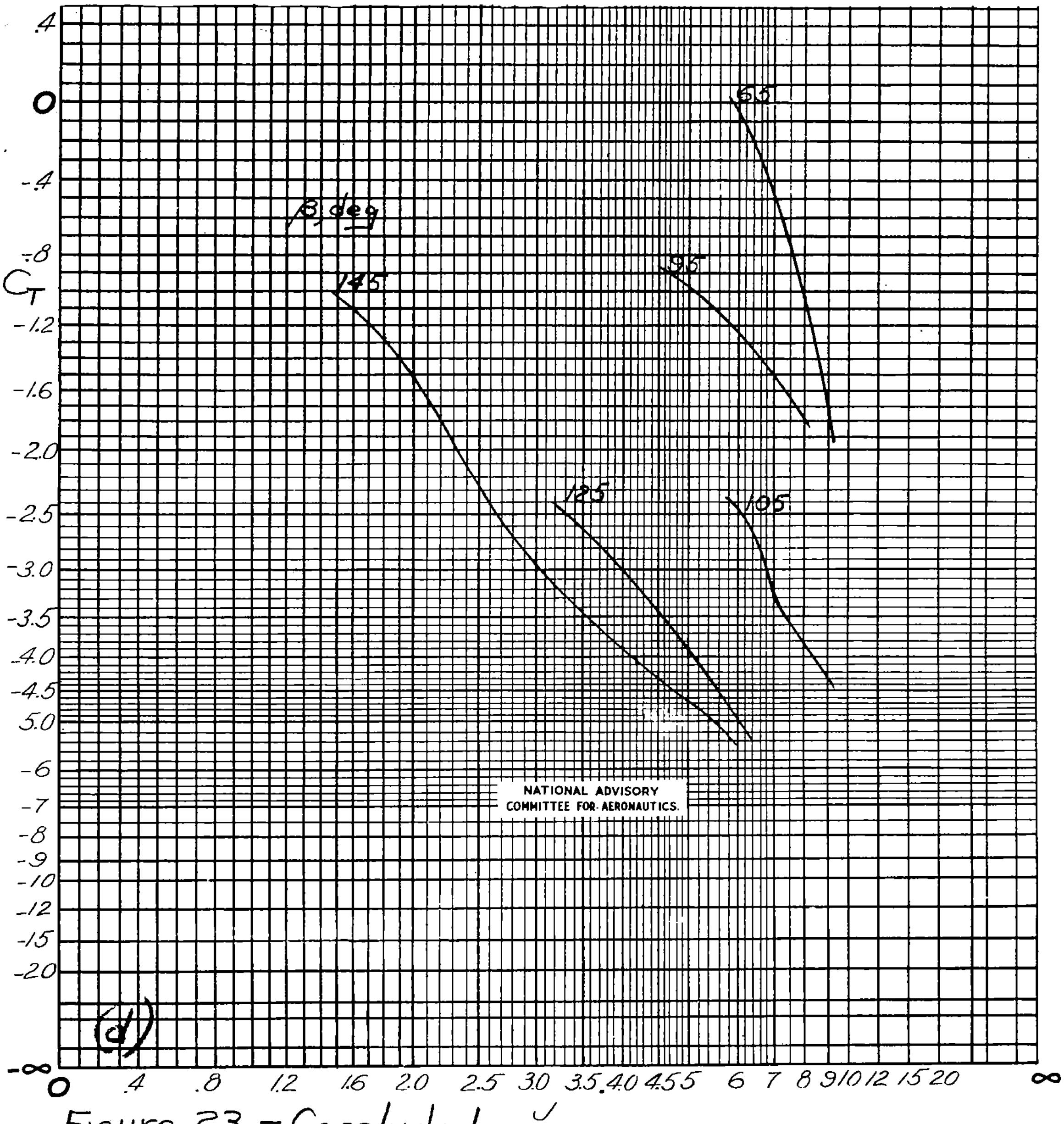

Figure 23.- Concluded

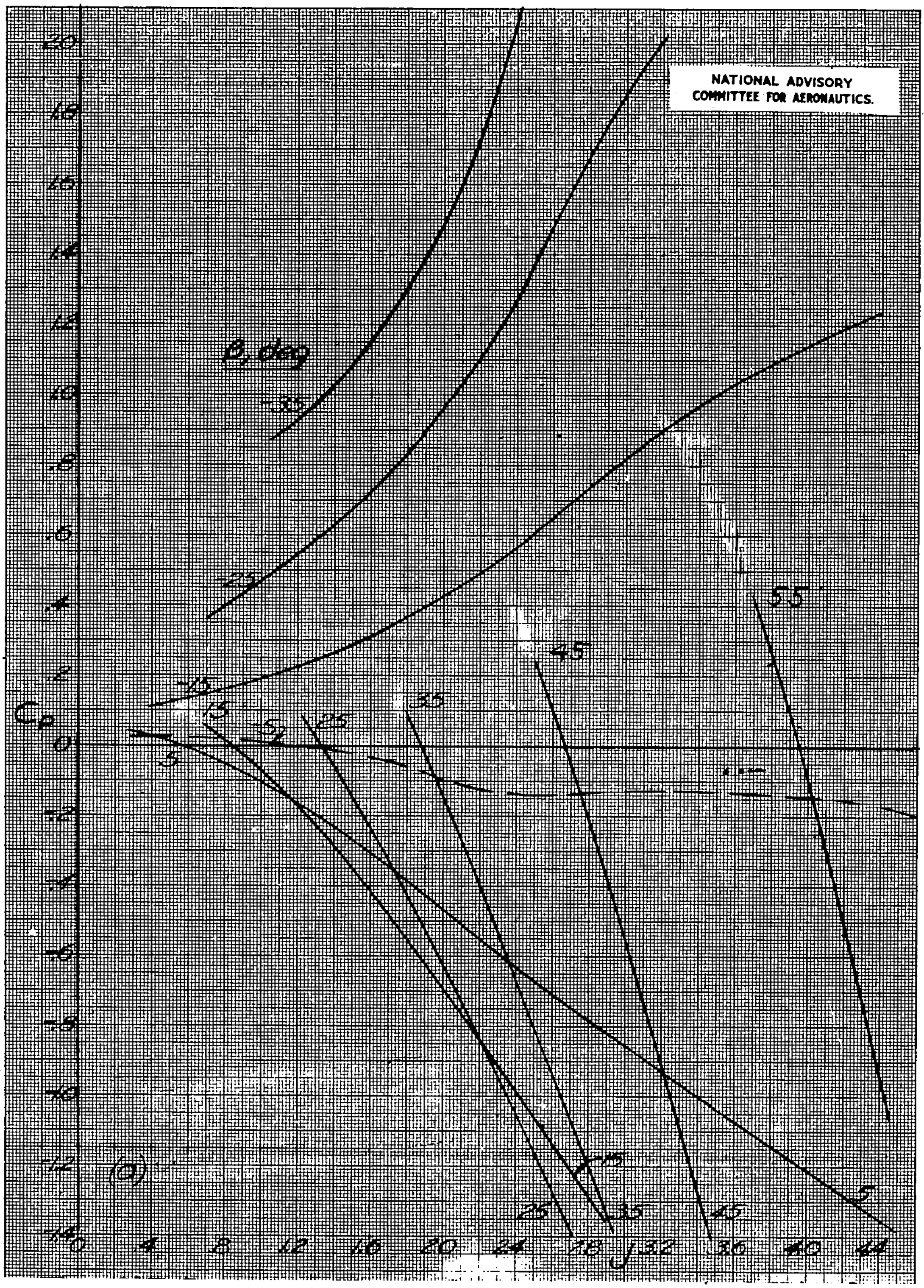

Figure 24.- Variation of power coefficient with advance ratio, eight wide blades, dual rotation.

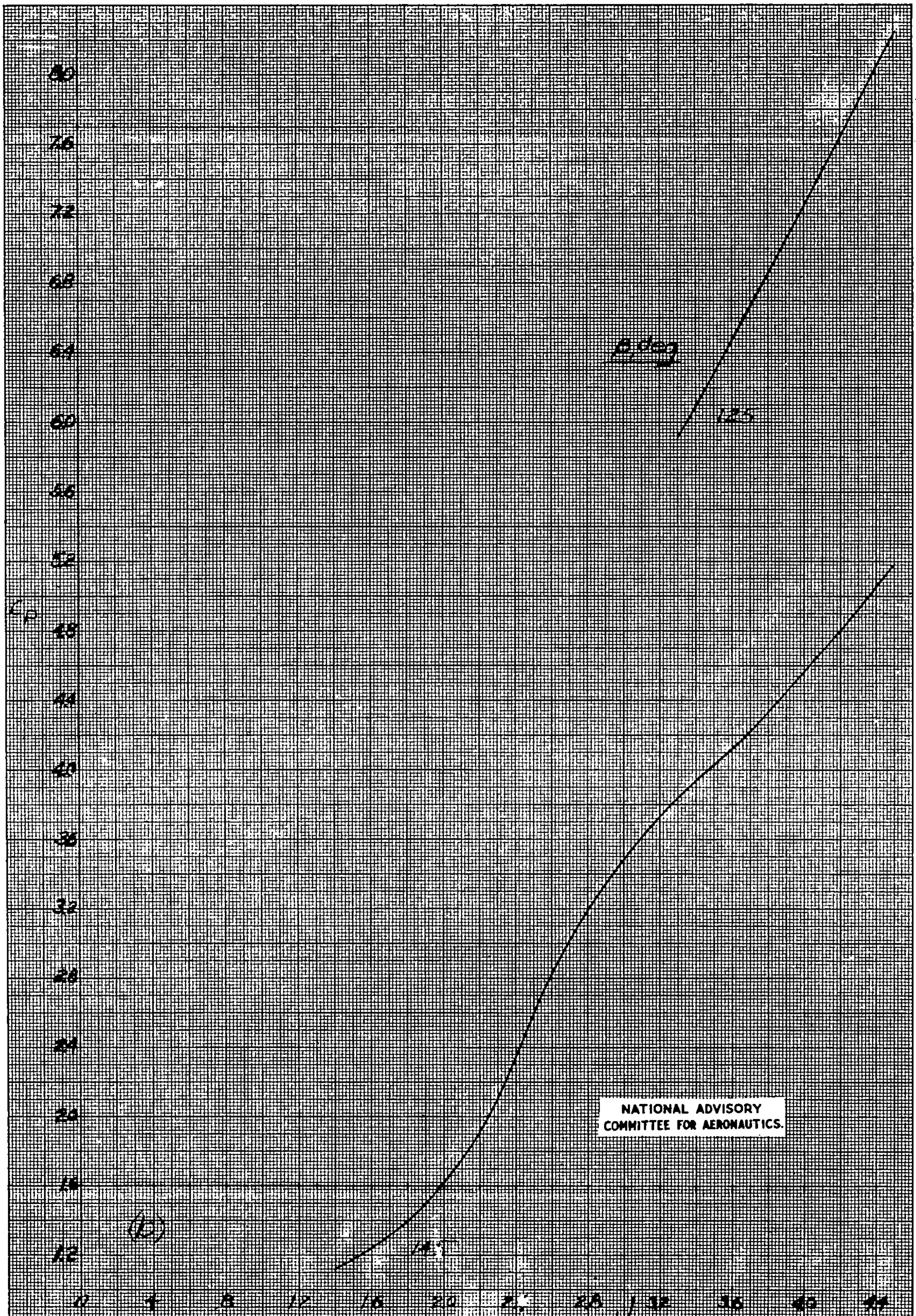

Figure 24.- Continued.

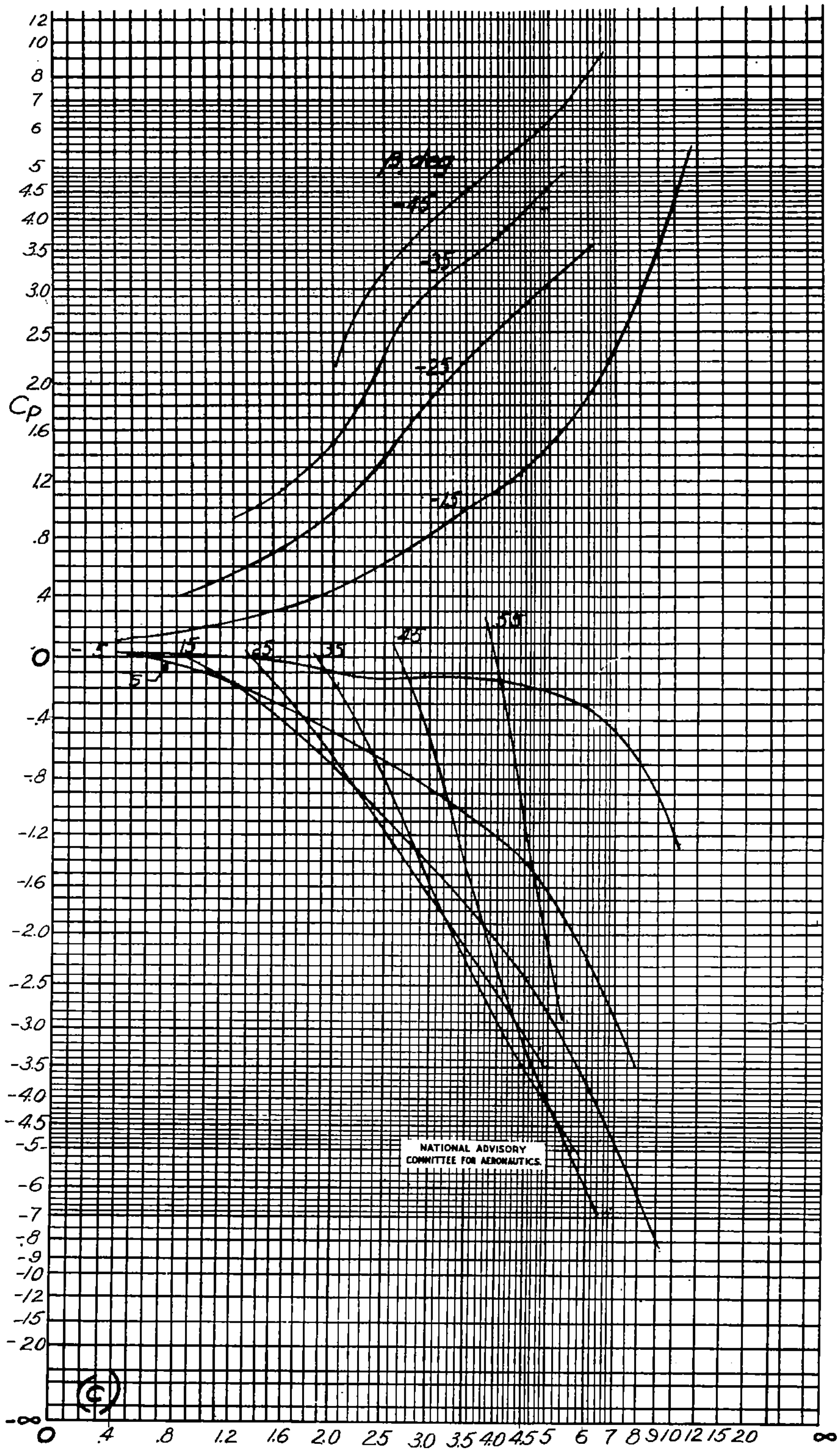

Figure 24.-Continued

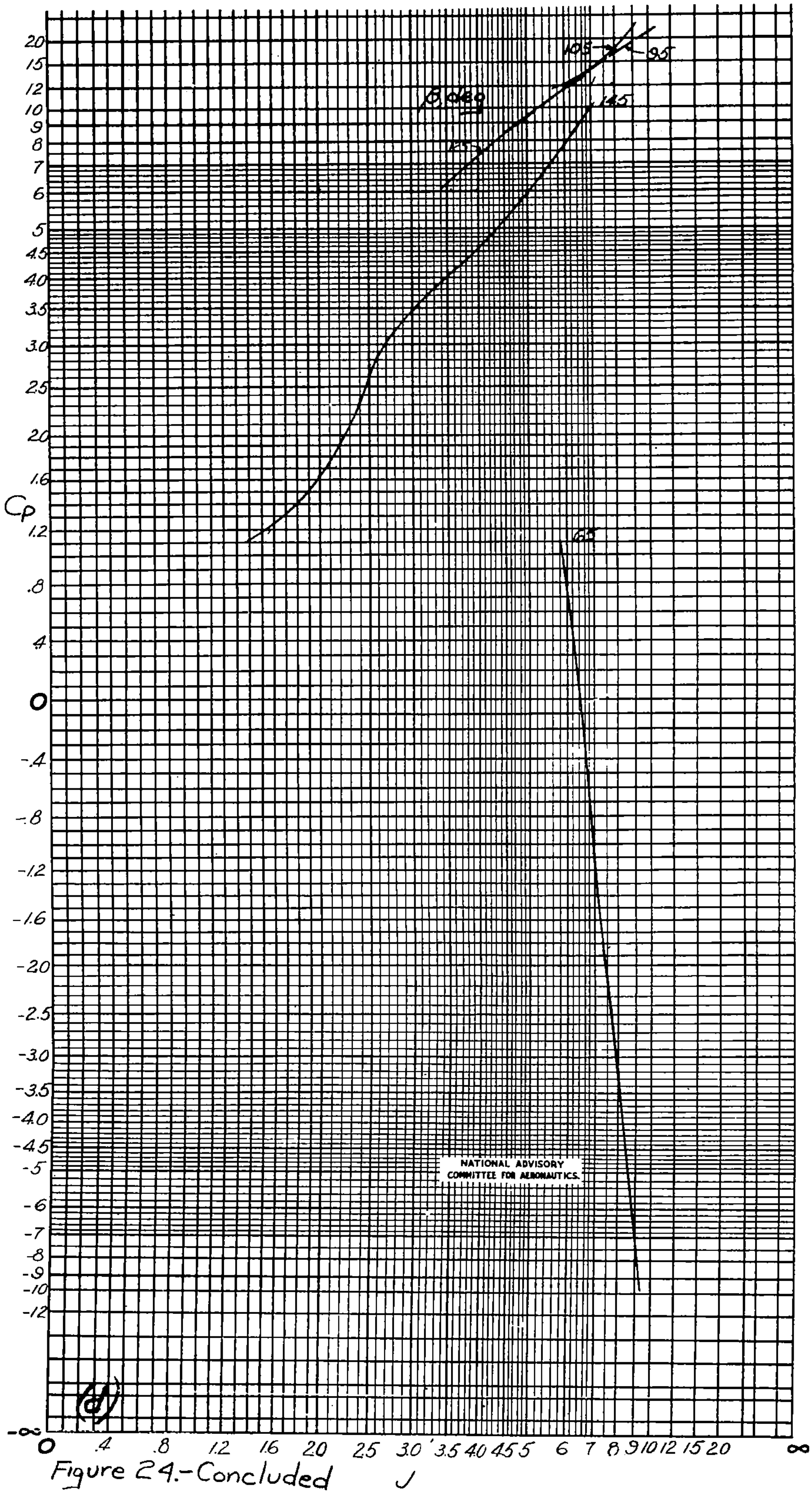

Figure 24.-Concluded

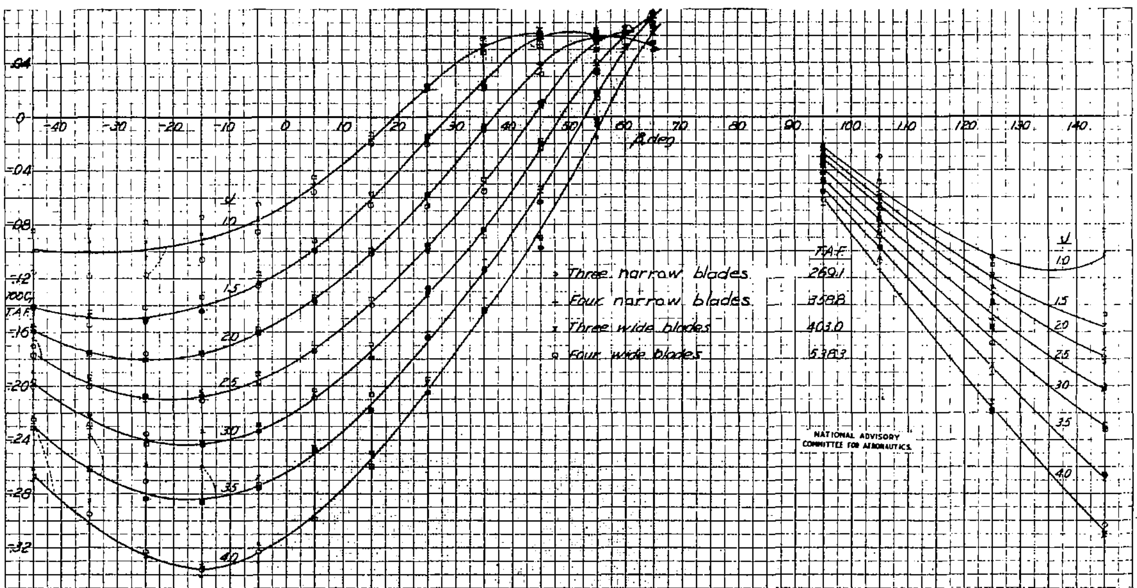

(a) Single rotation, thrust coefficient.

Figure 25.- General propeller chart based on common activity factor.

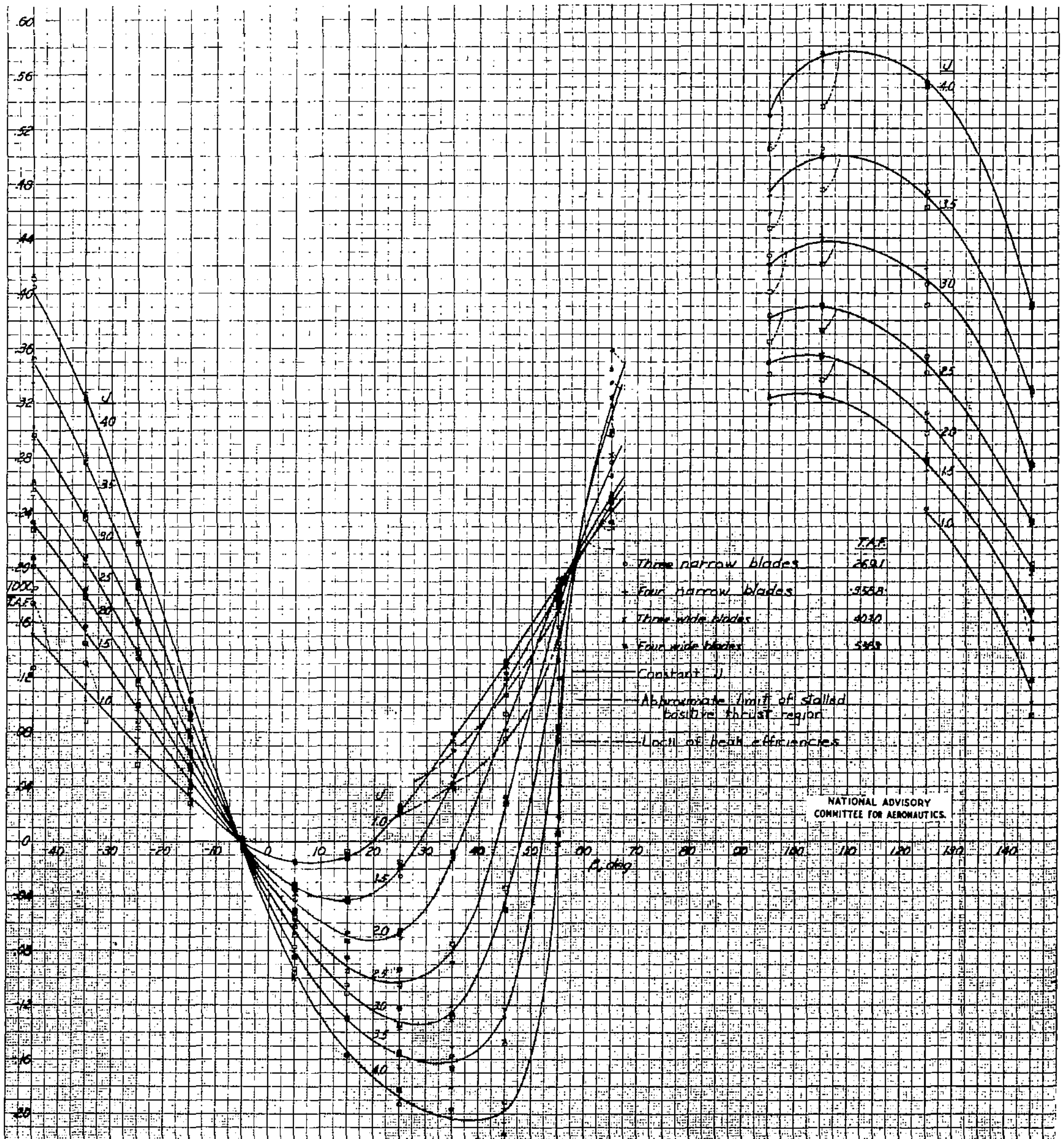

(b) Single rotation, power coefficient.
Figure 25.- Continued.

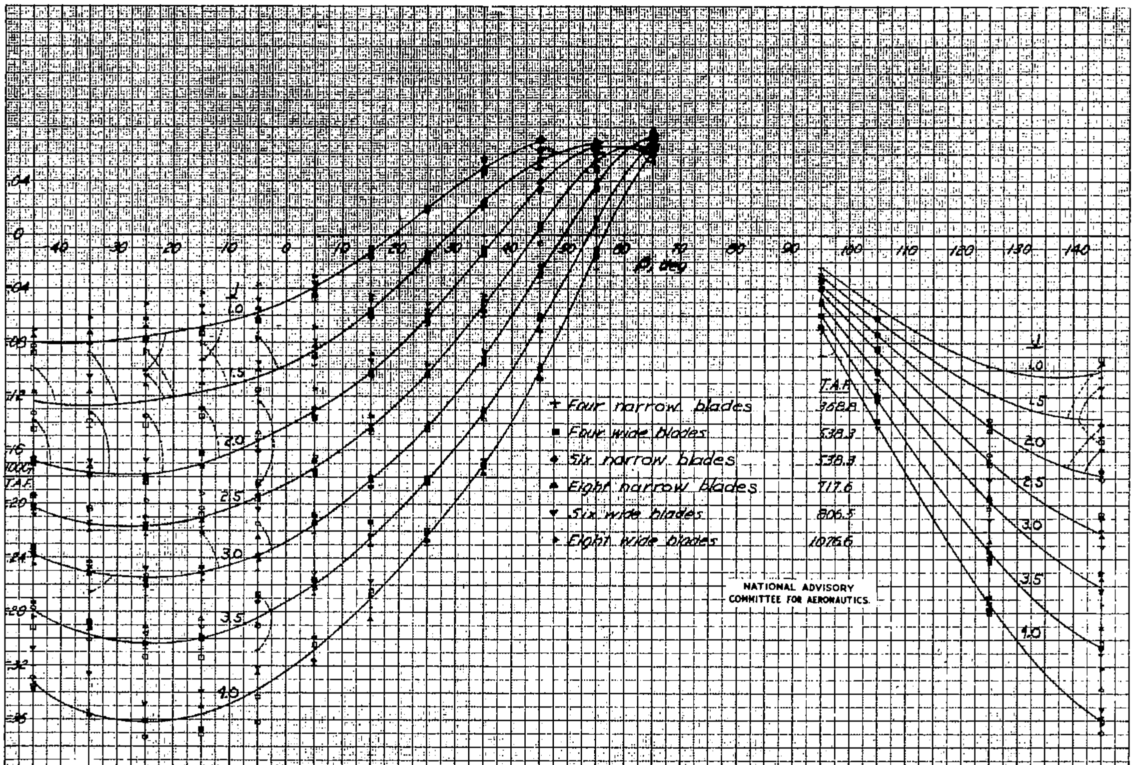

(c) Dual rotation, thrust coefficient.

Figure 25.- Continued.

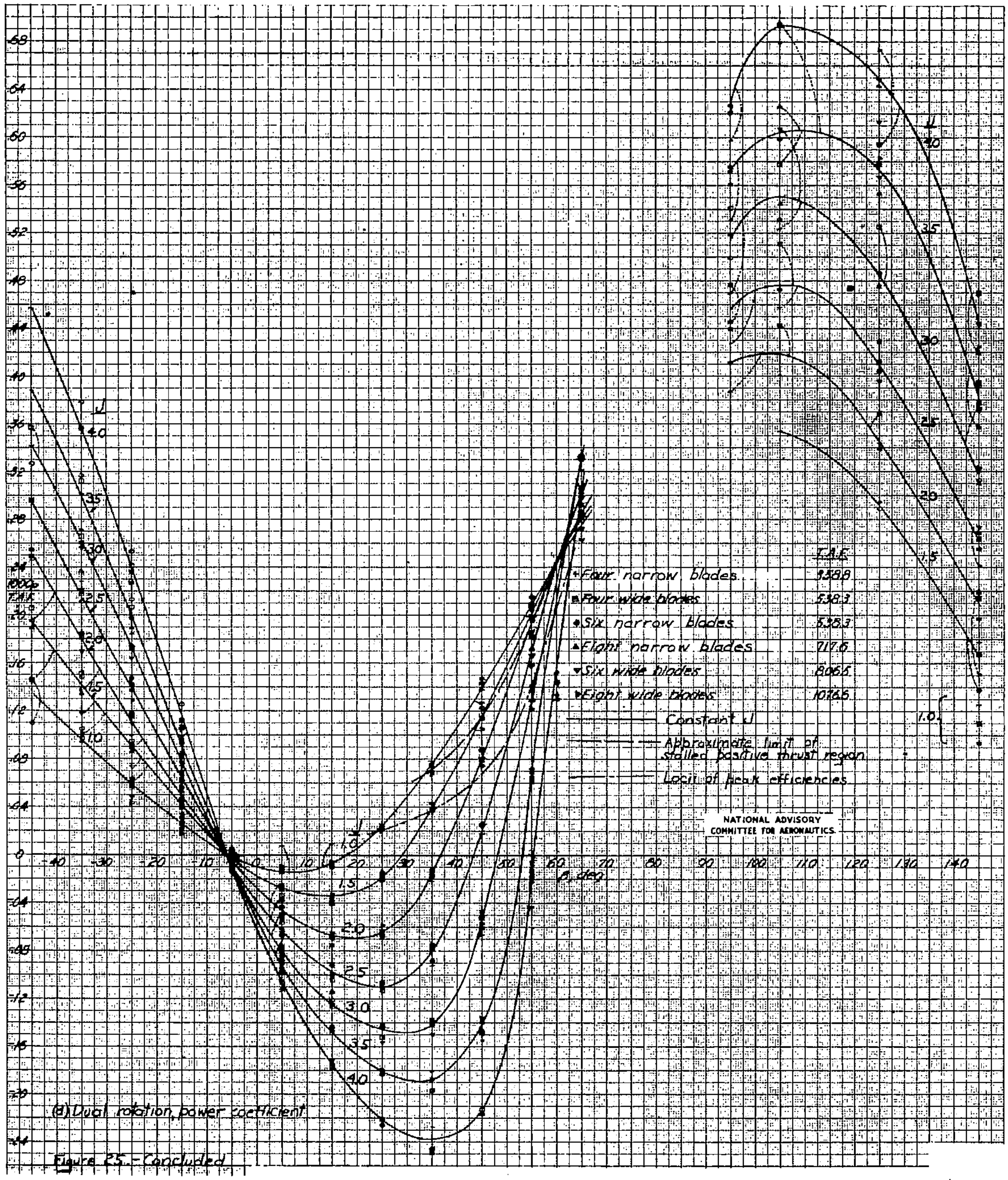

Figure 25. - Concluded.

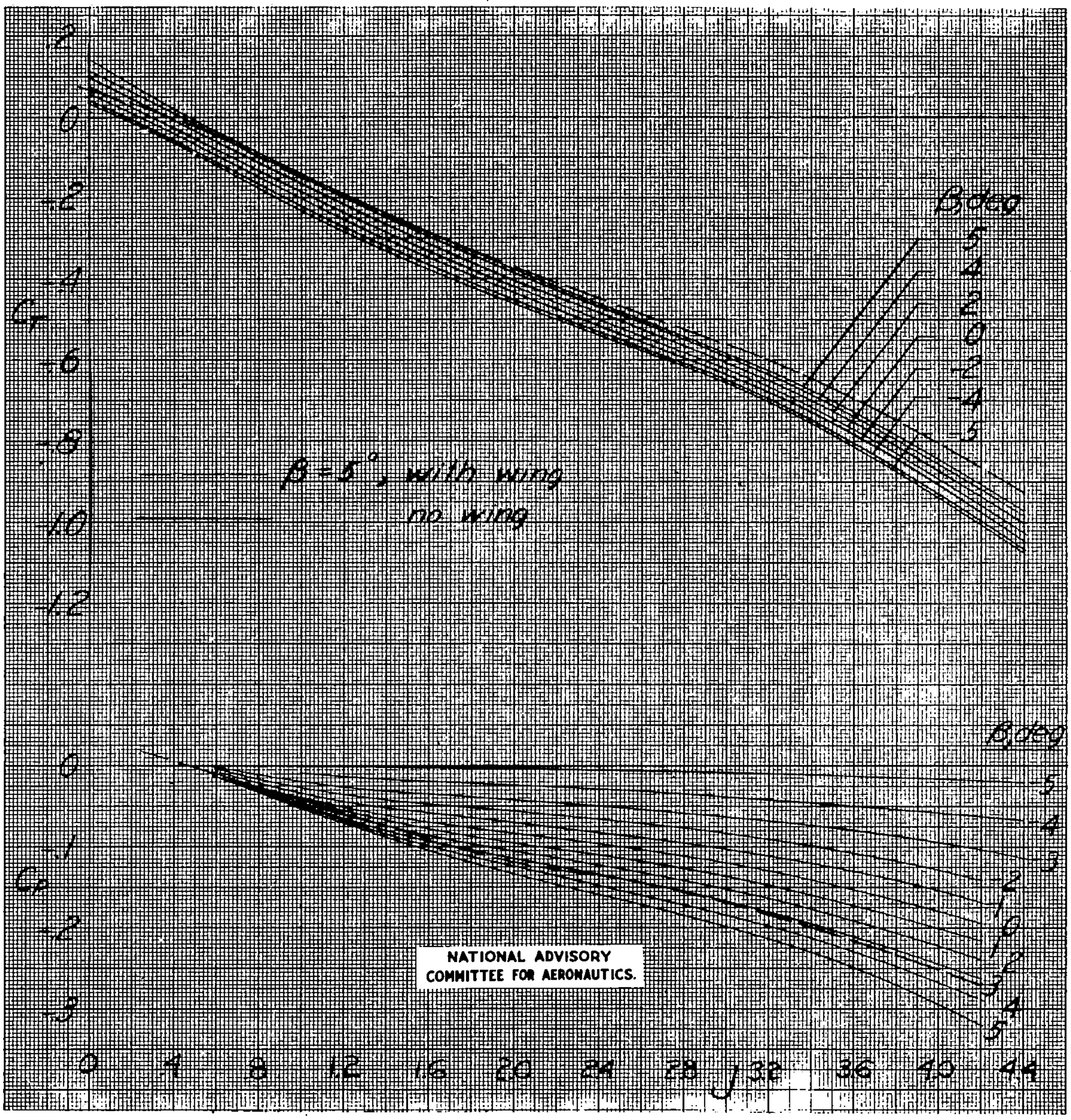

Figure 26.- Variation of thrust and power coefficients with advance ratio for small increments of β, three narrow blades.

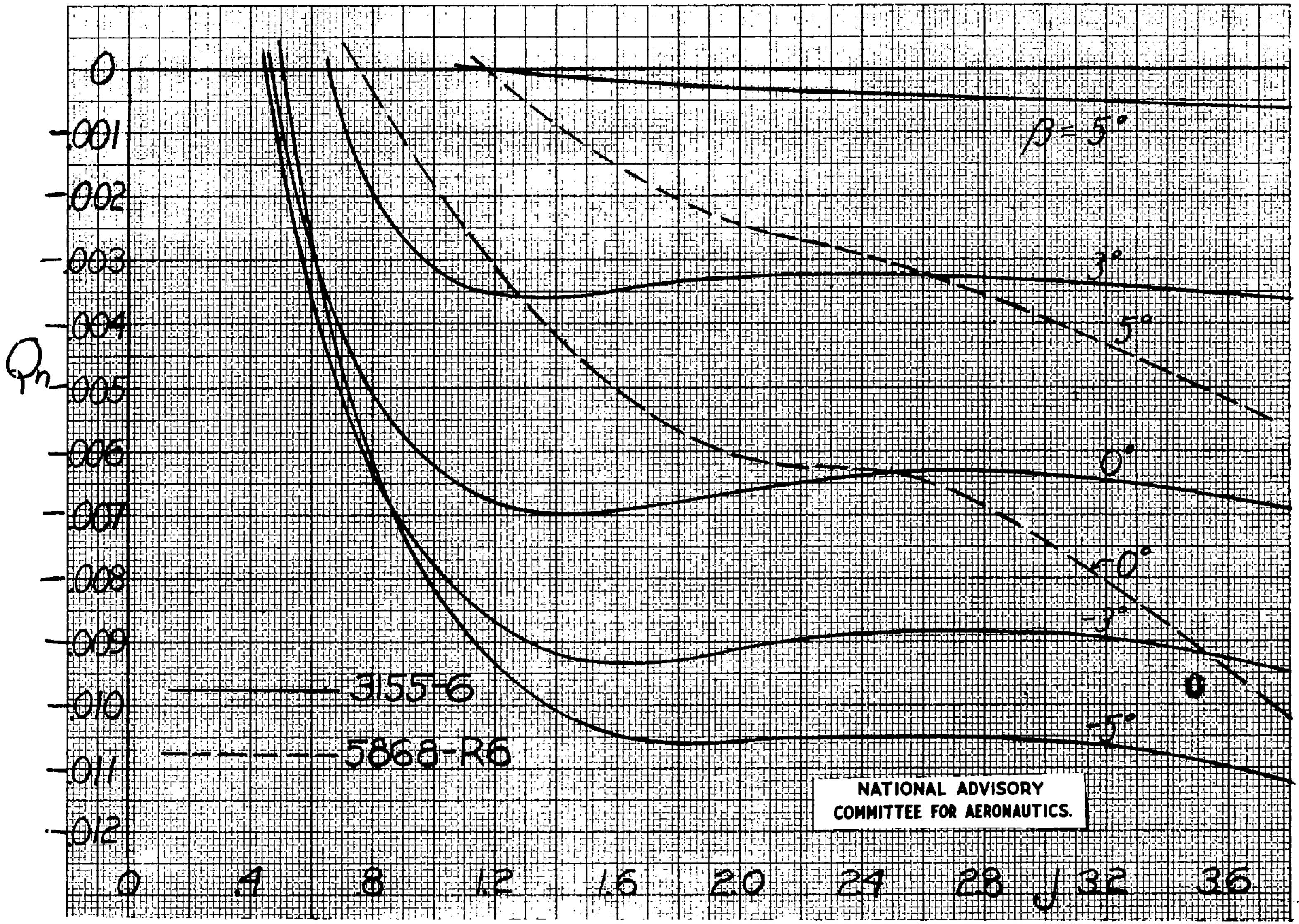

Figure 27.- Variation of torque coefficient with advance ratio at low blade angles.

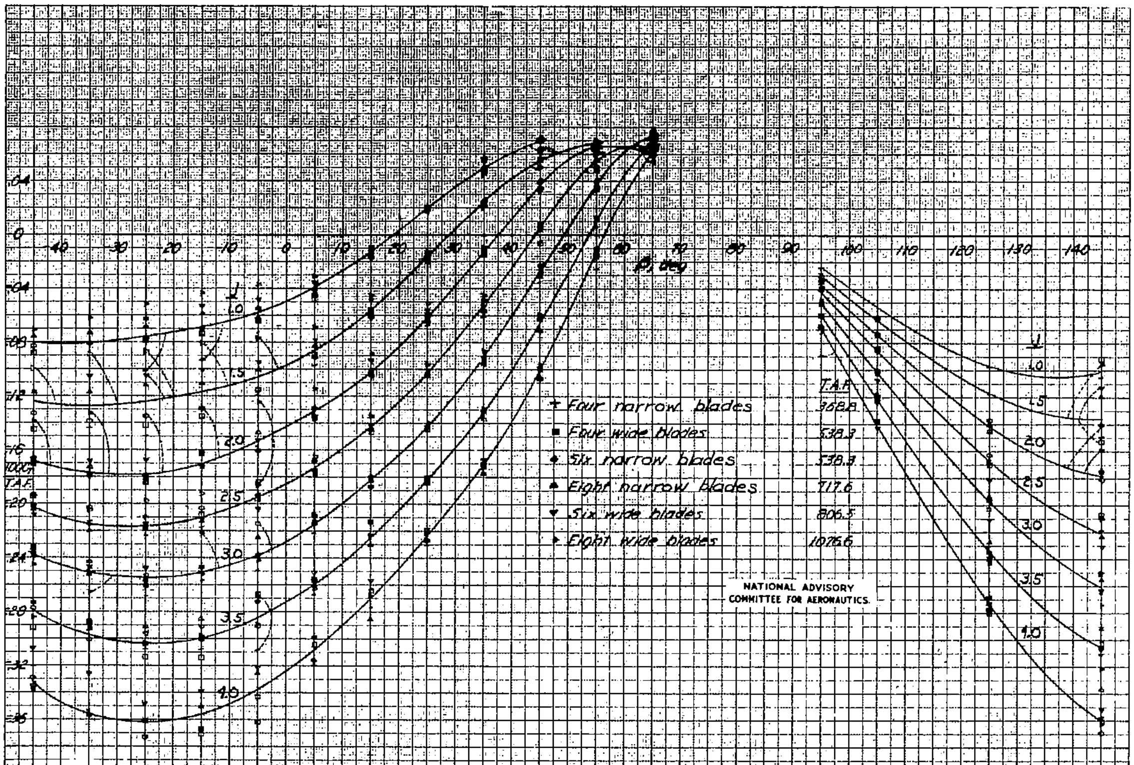

(c) Dual rotation, thrust coefficient.

Figure 25.- Continued.

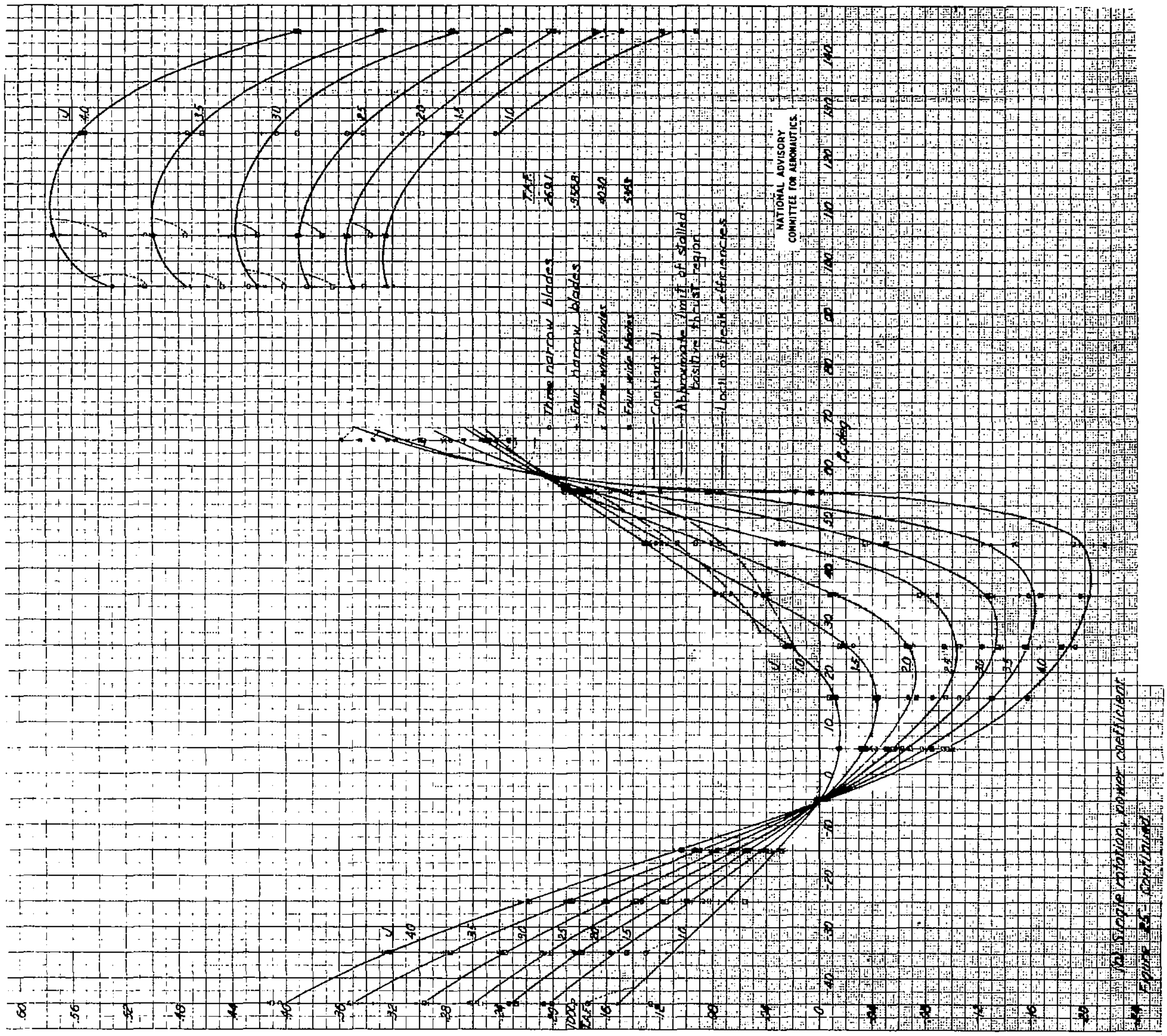

(b) Single rotation power coefficient.

Figure 25.- Continued.

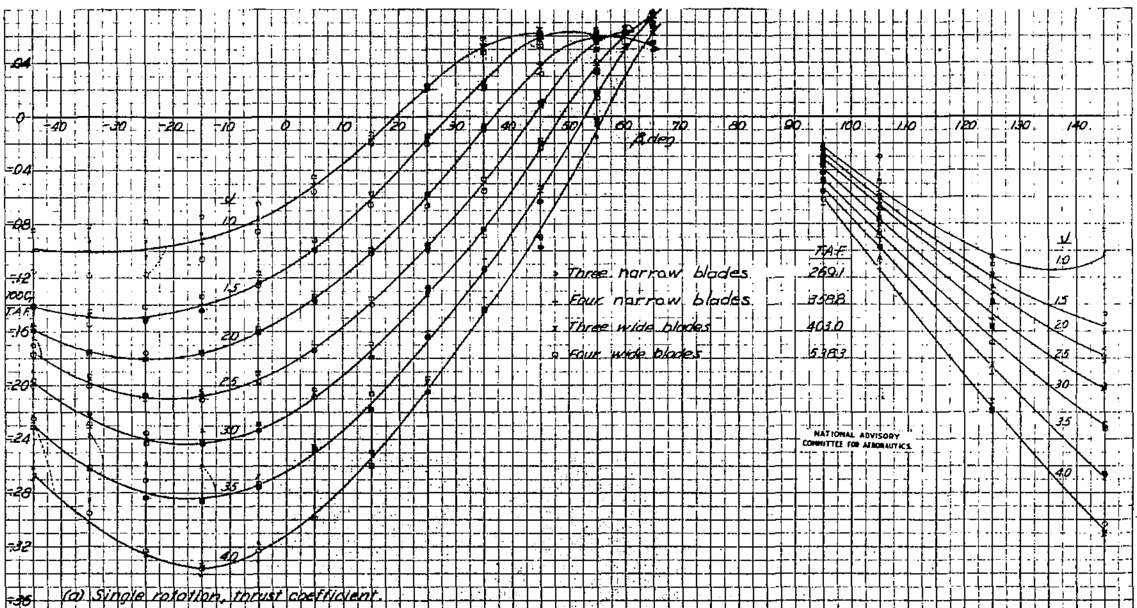

(a) Single rotation, thrust coefficient.

Figure 25.- General propeller chart based on common activity factor.

solution of problems such as determination of the rate of pitch change necessary to limit overspeeding to a reasonable value. The question of overspeeding is of major importance when the blade-angle changes involved are from high positive values to negative angles. Methods of approach to this as well as to other problems employing special coefficients and plotting methods are outlined in reference 7.

Subsequent to the original test program additional tests were run with the three-blade 3155-6 design propeller to obtain characteristics for each degree of blade angle between -5° and 5°. These additional results are presented in figure 26 with the results of the original tests at 5° superimposed. The curves for -5° and 5° were not duplicated within several percent, not only because the original tests included a wing in the propeller wake whereas the tests at 1° increments were made without a wing but also because the magnitudes of the thrust in relation to tare drag and power were extremely small.

The primary reason for the additional program of blade angles was to check results which indicated three equilibrium rotational speeds (and consequently three thrusts) at a given forward velocity in the blade angle region between 3° and -4°.

Figure 27, which is a plot showing the variation of Q_n with J of the three-blade 3155-6 propeller at several blade angles, illustrates the characteristics in this doubtful range. For a given value of Q_n, V, and D, it would be reasonable to expect a unique value of J, and consequently, n. The results presented in figure 27, however, indicate as many as three possible values of J for a given Q_n. Similar curves obtained from 5868-R6 propeller results in reference 3 show only one value of J in the same range of blade angles.

An attempt to explain these peculiar results by theory was not conclusive because of the lack of adequate section data for the high negative angles of attack experienced.

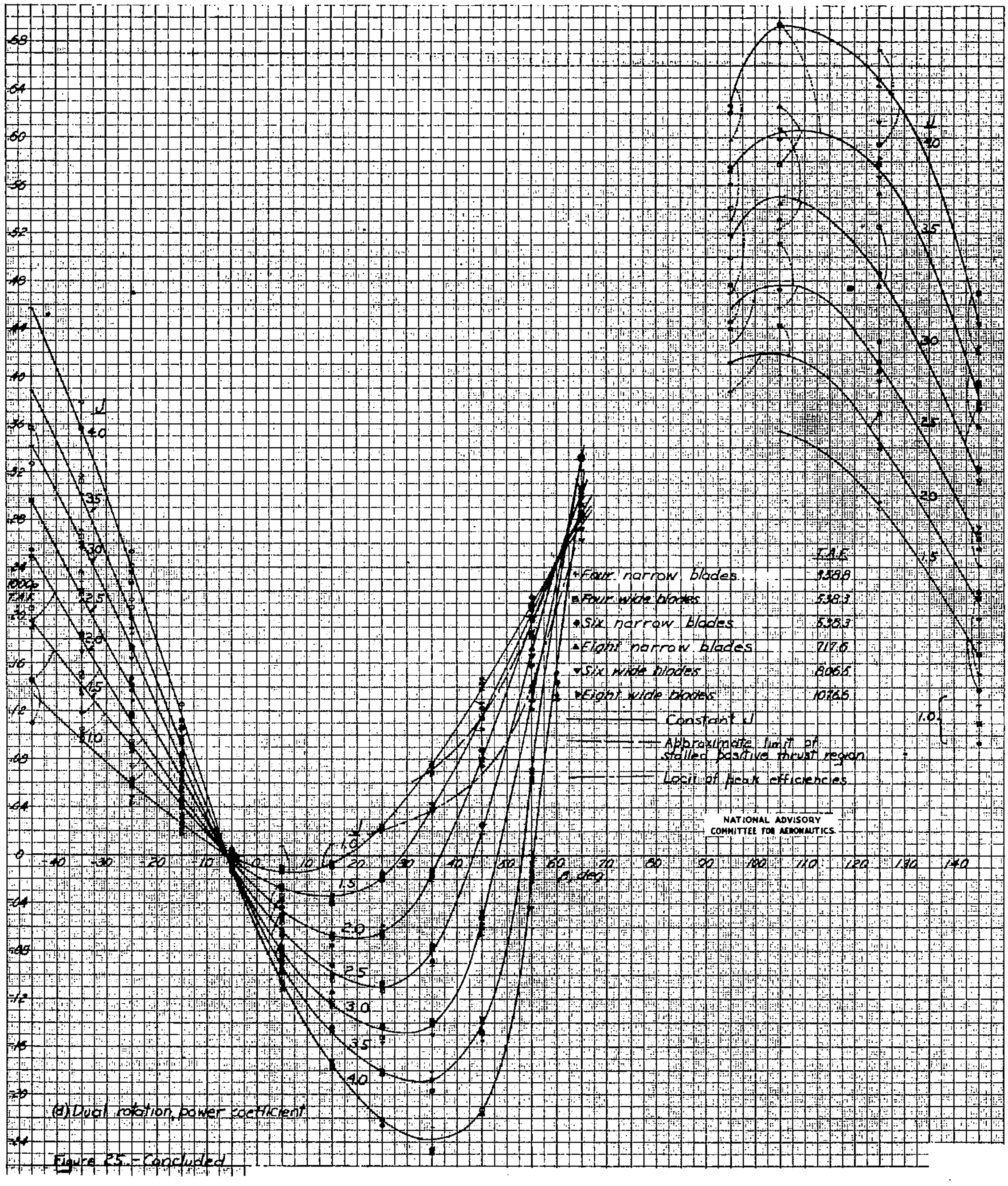

(b) Dual rotation power coefficient

Figure 25.- Concluded